Analysis of Nonlinear Oscillations Using Computer Algebra

Masakazu Yagi

February 2008

Contents

Chapter 1

Introduction

1.1 Background in Nonlinear Oscillations

Many phenomena associated with nonlinear oscillations, such as synchronizations, bifurcation phenomena, almost periodic oscillations, and chaotic oscillations, occur in nonlinear systems. In order to analyze the phenomena, we model the systems that exhibit the oscillations by nonlinear equations. One of the most studied nonlinear systems is the system described by ordinary differential equations, such as Duffing equation [1] and van der Pol equation [2–4] which are typical models of damped oscillators. Despite the simplicity of the models, these equations show complex behaviors, and are difficult to solve analytically in general.

In order to solve the nonlinear equations, we can use computational simulations, e.g., Runge-Kutta method which provides numerical solutions. However, to understand the nonlinear phenomena, it is essential not only to obtain solutions but also to analyze qualitative behavior of the actual nonlinear systems. For the qualitative analysis, various approximations, such as perturbation method which is the most classical technique and harmonic balance (HB) method which is well-known principle in frequency domain [5–8], have been widely applied. With the development of computer technology, those approximations are vital tools in the qualitative analysis of nonlinear oscillations based on numerical approaches. In particular, the HB method clarifies the bifurcation diagram, which represents qualitative behavior corresponding to different values of system parameters, in a global parameter space [9–12].

When we calculate a solution of a nonlinear equation using numerical approaches, we must fix parameters of the nonlinear equation because numerical computation manipulates only numerical values. Thus, if we obtain the bifurcation diagram in the global parameter space by the

numerical approaches, then we have to solve the nonlinear equation for all specified parameters one by one, and the repeated calculation requires a large amount of computational cost. Because the bifurcation diagram is given only by a set of numerical values, we cannot clarify intrinsic algebraic relations between oscillations and parameters by the numerical approaches although the bifurcation diagram constructed by the HB method is represented by algebraic curves.

Because the bifurcation diagram by the approximations has the approximation error, a guaranteed bifurcation diagram is required in some cases. In the HB method, we can guarantee an approximated solution by error bound, which is a boundary of the region containing both the approximated solution and the exact solution [13–15]. If we need to calculate guaranteed bifurcation diagrams evaluated by the error bound of the HB method, we have to express the high dimensional error bound using a set of numerical values. Thus, its computational cost is tremendously large.

In order to overcome the difficulties of the numerical approaches, computer algebra has recently been recognized as an important field. Because the computer algebra manipulates variables and parameters in symbolic form, we can analyze the algebraic structures of equations without fixing the values of parameters and easily represent the high-dimensional objects. In this thesis, we propose algebraic approaches to the analysis of the nonlinear oscillations using the computer algebra.

1.2 Background in Computer Algebra

In the computer algebra, Gröbner base is a very useful tool to deal with polynomials in several variables. Gröbner base was introduced by Hironaka as "standard basis" [16,17] and invented independently by Buchberger [18–20]. The essential observation for applying Gröbner techniques is the fact that solutions of polynomial equations depend not only on the original polynomial equations but on an infinite set of polynomial equations which have the same solutions of the original equations. The infinite set of polynomials is called ideal generated by the original polynomials, and Gröbner base is the base of the ideal [18–22]. A method for calculating Gröbner base is known as Buchberger's algorithm which is implemented in many computer algebra systems, e.g., Mathematica, Maple, Risa/Asir, SINGULAR, Macaulay2, and so on. The properties and applications of Gröbner base are shown as follows;

Elimination: Buchberger's algorithm is based on the elimination of variables in polynomial

equations. We can apply the elimination of variables to the transformation of variables.

Triangular form: The elimination of variables gives us the triangular form corresponding to algebraic solutions of the polynomial equations. Thus, Gröbner base provides a method for solving polynomial equations.

Factorization: The triangular form contains a polynomial with only one variable. Factorizing the polynomial, we can decompose the polynomial systems.

Ideal membership: Because Gröbner base is the standard base of an ideal, it gives a method checking whether a polynomial equation is in the ideal. Using this method, we can classify polynomial equations.

Due to the above properties, there are widespread applications of Gröbner base in various fields. Many applications are based on the triangular form of Gröbner base. That is, the triangular form is applied to the problems such as controls of robots [20,21,23], designs of wavelet [24–26], and calculation of accurate bifurcation points [27]. Even though Gröbner base has many algebraic properties, those applications use Gröbner base only for solving polynomial equations. Meanwhile, some researchers have proposed approaches which utilize the algebraic properties efficiently. For instance, using the "ideal membership," we can classify local bifurcations [28–30] and nonlinear circuits [31], automatically. Moreover, the algorithm for deciding the ideal membership gives optimized solutions in integer programming [32–34]. Using the "factorization," we can decompose bifurcation diagrams in global parameter spaces [35, 36]. Further, some approaches for designing systems are based on the "elimination of variables" [37–40]. Other applications based on the concept of Buchberger's algorithm are algebraic statistics [41, 42] and decoding of algebraic geometric codes [43–45].

Although Gröbner base is applied to many fields as stated above, we do not yet have any applications for the analysis of nonlinear oscillations except for a few examples such as [31]. Moreover, though there are some applications for bifurcations, many of them are analyses of local bifurcations [28–30,35,36]. Meanwhile, the bifurcation analysis in global parameter spaces is realized by a few applications of Gröbner base [35, 36]. In this thesis, we propose a method to clarify the bifurcations of the nonlinear oscillations in the global parameter spaces by extending the method in [35, 36].

However, because Buchberger's algorithm requires high computational cost for the analysis of the nonlinear oscillations, the computational cost significantly limits its practical applications.

In fact, the direct method of [35, 36] can decompose only the bifurcation diagrams of simple maps, but not oscillations due to the computational cost. In order to reduce the computational cost of Buchberger's algorithm, some methods are now being developed. For example, Faugère proposed the algorithms F_4 and F_5 which are efficient methods for calculating Gröbner base in many cases [46, 47]. Moreover, Gröbner walk is a known algorithm for following how Gröbner base changes as we change the monomial order [48, 49]. This technique is helpful to obtain the triangular form. Further, other methods such as optimizations of orders [50] and homogenization of ideals are being proposed. Although those methods are effective, it is not enough to deal with large-scale applications. Even by the above methods, the computational cost of Gröbner base limits its practical applications for the analysis of the nonlinear oscillations. Thus, we propose alternative efficient methods for the analysis of the nonlinear oscillations using features of the nonlinear systems.

1.3 Objectives

The first objective of this thesis is to clarify bifurcations of periodic oscillations in a global parameter space by the computer algebra. That is, we propose an algebraic representation of a bifurcation diagram using Gröbner base. It further includes the mode decomposition of the bifurcation diagram based on the "factorization."

The second objective is the reduction of the bifurcation diagram by invariants. In order to realize the reduction, we use the transformation of variables based on the "elimination of variables." The reduction makes it possible to find out amplitude equations which represents the relation of each frequency component of oscillations. Further, the amplitude relations enable to determine design parameters for electric oscillators.

The third objective is to give a guaranteed bifurcation diagram by an algebraic representation of the high-dimensional error bound. The representation is obtained by the "elimination of variables."

1.4 Overview of the Thesis

This thesis is organized as follows;

In Chapter 2, for the discussion in subsequent chapters, we describe our system which exhibits periodic oscillations. In order to use Gröbner techniques, we apply the HB method to the

system which have polynomial-type nonlinearity, and derive determining equations called HB equations. Then, we introduce the ideal generated by the HB equation and review the computation of the bifurcation diagram constructed by the HB method using Gröbner base.

In Chapter 3, we propose the algebraic representation of the bifurcation diagram of the HB equation, and clarify the decomposition of the bifurcation diagram. Because the previous method for the decomposition using the"factorization" requires a huge computational cost [35, 36], we propose an efficient method to decompose the bifurcation diagram using the ideal quotient based on the symmetry of the system. Then, we confirm the efficiency of the proposed method and clarify the relation between the bifurcation points and the decomposed bifurcation diagrams. Moreover, we propose a systematic procedure to decompose the bifurcation diagram using homogeneous HB equation.

In Chapter 4, we propose an algebraic approach to reduce the bifurcation diagram of the HB equation. The proposed method focuses on invariants with respect to the symmetry of the system. Because the invariants enable to transform different but equivalent solutions into a unique solution, we propose a method to reduce the HB equation using a transformation of variables based on the "elimination of variables" with respect to the invariants. We show that the bifurcation diagram of the reduced HB equation is simpler than the original bifurcation diagram, and that its computational cost is considerably reduced. Further, we obtain the relations among the amplitudes at each frequency component using the invariants. Additionally, we propose a method for determining circuit parameters using those relations.

In order to obtain the guaranteed bifurcation diagram, Chapter 5 gives the algebraic representation of the high-dimensional error bound of the HB method. We propose an efficient method to obtain the representation using the "elimination of variables." Using the representation, we propose a method for very fast computation of a quadratic approximation of the error bound. In addition, we propose a method to obtain accurate break points of the error bound using the singular points of the algebraic representation.

Finally, Chapter 6 concludes this thesis by summarizing major results obtained by the research.

Chapter 2

Fundamental Formulation of Periodic Oscillation

2.1 Introduction

This chapter derives polynomial determining equations of periodic oscillations by harmonic balance (HB) method and describes fundamental application of the ideal and Gröbner base to bifurcation analysis in global parameter spaces.

The HB method is well known principle for analyzing periodic oscillations on nonlinear networks and systems which are described by a set of nonlinear differential equations [5–8]. From these equations, in sinusoidal steady states, we obtain a simultaneous algebraic equations called the HB equations due to a periodic solution approximated by a truncated Fourier series with several harmonics. Although the HB method is an approximated one in frequency-domain, it is conceptually simpler than the time-domain techniques, and clarifies the essential relations among the system parameters for bifurcations [9–12].

In order to obtain the bifurcation diagram of the HB equation, we introduce the ideal generated by the HB equation. This extension enables to transform the HB equation to a triangular form by elimination ideal. Further, we review the relation between the ideal and the bifurcation diagram, and present a fundamental approach to the mode decomposition of the bifurcation diagram reported in [35, 36].

2.2 State Equation with Sinusoidal Inputs

We consider the following system described by n ordinary differential equations of the first order which are forced only by sinusoidal functions of period $2\pi/\omega_s$;

$$\frac{\mathrm{d}\boldsymbol{u}(t)}{\mathrm{d}t} = \boldsymbol{h}(\boldsymbol{u};\boldsymbol{\lambda}) + \boldsymbol{s}(t), \tag{2.1}$$

$$\begin{array}{rcll}
\boldsymbol{u}(t) & = & (u_1,\ldots,u_n)^{\mathrm{T}} \in \mathbb{R}^n & \text{A vector of state variables,} \\
\boldsymbol{\lambda} & = & (\lambda_1,\ldots,\lambda_l) \in \mathbb{R}^l & \text{A set of system parameters,} \\
\boldsymbol{h}(\boldsymbol{u};\boldsymbol{\lambda}) & = & (h_1,\ldots,h_n)^{\mathrm{T}} \in \mathbb{R}^n & \text{A vector of nonlinear functions of } u_1,\ldots,u_n \\
 & & & \qquad \text{with coefficients in function of } \lambda_1,\ldots,\lambda_l, \\
\boldsymbol{s}(t) & = & (s_1,\ldots,s_n)^{\mathrm{T}} \in \mathbb{R}^n & \text{A vector of sinusoidal forcing functions} \\
 & & & \qquad \text{with the period } 2\pi/\omega_s,
\end{array}$$

where $\boldsymbol{h} : \mathbb{R}^n \times \mathbb{R}^l \to \mathbb{R}^n$, $(\cdot)^{\mathrm{T}}$ denotes the transposition, and $\mathbb{R}$ is the set of real numbers. In order to derive polynomial HB equations, we restrict the function $\boldsymbol{h}$ to polynomial-type nonlinearity of $u_1, \cdots u_n$ with coefficients in a rational function field $\mathbb{Q}(\boldsymbol{\lambda})$ of $\lambda_1,\ldots,\lambda_l$. When we consider autonomous systems, we fix $\boldsymbol{s}(t) = \boldsymbol{0}$.

Let us consider the periodic solution $\boldsymbol{u}(t)$ with period $2\pi/\omega$ of Eq.(2.1) as follows;

$$\boldsymbol{u}(t) = \sum_{k=0}^{\infty} \Re\left[\boldsymbol{X}_k e^{\mathrm{j}k\omega t}\right], \tag{2.2}$$

where $\boldsymbol{X}_k = (X_{k1},\ldots,X_{kn})^{\mathrm{T}} \in \mathbb{C}^n$, and $\Re[\cdot]$ denotes the real part. Now, we assume that ω satisfies $m\omega = \omega_s$ where m is a positive integer. The forced periodic oscillations are divided into three sorts; subharmonic, fundamental harmonic and higher harmonic oscillations. That is, in the case $m = 1$, the periodic solution $\boldsymbol{u}(t)$ consists of fundamental and higher harmonic oscillations. In the case $m = 2, 3, \ldots$, when the $k\omega_s/m$ frequency components become dominant in the periodic solution, we call the oscillations k/m subharmonic oscillations for $k = 1, 2, \ldots$. Thus, if we consider the fundamental and the higher harmonic oscillations, we set $m = 1$. If we consider the k/M subharmonic oscillations, we set $m = M$.

2.3 HB Equation

In order to derive the HB equations, we define a projection operator K^* that expresses the truncation of the Fourier series with $p + 1$ frequency components with $p \geq m$. The operator K^*

approximates the periodic solution $\boldsymbol{u}$ in (2.2) by

$$\boldsymbol{u}^*(t) = (u_1^*, \ldots, u_n^*)^{\mathrm{T}} = K^*\boldsymbol{u}(t) = \sum_{k=0}^{p} \Re\left[\boldsymbol{X}_k e^{\mathrm{j}k\omega t}\right]. \tag{2.3}$$

Substituting the approximated solutions $\boldsymbol{u}^*$ into Eq.(2.1) and applying the operator K^* to Eq.(2.1), we obtain

$$\sum_{k=0}^{p} \Re\left[\{-\mathrm{j}k\omega\boldsymbol{X}_k + \boldsymbol{Y}_k(\boldsymbol{X}) + \boldsymbol{E}_k\} e^{\mathrm{j}k\omega t}\right] = \boldsymbol{0}, \tag{2.4}$$

where

$$\begin{aligned}
K^*\boldsymbol{h}(\boldsymbol{u}^*;\boldsymbol{\lambda}) &= \sum_{k=0}^{p} \boldsymbol{Y}_k(\boldsymbol{X}) e^{\mathrm{j}k\omega t}, & K^*\boldsymbol{s}(t) &= \sum_{k=0}^{p} \boldsymbol{E}_k e^{\mathrm{j}k\omega t}, \\
\boldsymbol{Y}_k(\boldsymbol{X}) &\equiv (Y_{k1}(\boldsymbol{X}), \ldots, Y_{kn}(\boldsymbol{X}))^{\mathrm{T}} \in \mathbb{C}^n, & \boldsymbol{E}_k &\equiv (E_{k1}, \ldots, E_{kn})^{\mathrm{T}} \in \mathbb{C}^n, \\
\boldsymbol{X} &\equiv \begin{bmatrix} \boldsymbol{X}_0 \\ \vdots \\ \boldsymbol{X}_p \end{bmatrix} \in \mathbb{C}^{n(p+1)}, & \boldsymbol{E} &\equiv \begin{bmatrix} \boldsymbol{E}_0 \\ \vdots \\ \boldsymbol{E}_p \end{bmatrix} \in \mathbb{C}^{n(p+1)}.
\end{aligned}$$

Because the sinusoidal forcing functions have only the frequency components of $\omega_s = m\omega$, the vector of the forcing terms $\boldsymbol{E}$ satisfies

$$\begin{cases} \boldsymbol{E}_k = \boldsymbol{0} \ \text{ for } \ k = 0, \ldots, p, \ k \neq m & \text{(for periodically forcing system)} \\ \boldsymbol{E} = \boldsymbol{0} & \text{(for autonomous system)} \end{cases}. \tag{2.5}$$

Equating the coefficients of Eq.(2.4) to zero, we obtain the following simultaneous equation.

$$\begin{aligned}
\boldsymbol{F}(\boldsymbol{X}) &\equiv \boldsymbol{F}(\boldsymbol{X};\omega,\boldsymbol{\lambda},\boldsymbol{E}) \equiv \begin{bmatrix} \boldsymbol{F}_0 \\ \vdots \\ \boldsymbol{F}_p \end{bmatrix} = \boldsymbol{0}, \\
\boldsymbol{F}_k &\equiv (F_{k1}, \ldots, F_{kn})^{\mathrm{T}} \in \mathbb{C}^n \\
&\equiv -\mathrm{j}k\omega\boldsymbol{X}_k + \boldsymbol{Y}_k(\boldsymbol{X}) + \boldsymbol{E}_k, \\
k &= 0, \ldots, p.
\end{aligned} \tag{2.6}$$

We call Eq.(2.6) complex HB equation.

In order to consider the real polynomial equation, we transform the variables $\boldsymbol{X},\ \boldsymbol{E} \in \mathbb{C}^{n(p+1)}$ into $\boldsymbol{x},\ \boldsymbol{e} \in \mathbb{R}^N$ with $N = n(2p+1)$ using the relations

$$X_{ki} = x_{\mathrm{r}ki} + \mathrm{j}x_{\mathrm{s}ki}, \quad X_{0i} = x_{\mathrm{r}0i}, \tag{2.7}$$

$$E_{ki} = e_{\mathrm{r}ki} + \mathrm{j}e_{\mathrm{s}ki}, \quad E_{0i} = e_{\mathrm{r}0i}, \tag{2.8}$$

$$
\begin{array}{rclrcl}
\boldsymbol{x} & \equiv & \left[\begin{array}{c} \boldsymbol{x}_0 \\ \vdots \\ \boldsymbol{x}_p \end{array}\right], & \boldsymbol{e} & \equiv & \left[\begin{array}{c} \boldsymbol{e}_0 \\ \vdots \\ \boldsymbol{e}_p \end{array}\right], \\
\boldsymbol{x}_0 & \equiv & (x_{\mathrm{r}01}, \ldots, x_{\mathrm{r}0n})^{\mathrm{T}} \in \mathbb{R}^n, & \boldsymbol{e}_0 & \equiv & (e_{\mathrm{r}01}, \ldots, e_{\mathrm{r}0n})^{\mathrm{T}} \in \mathbb{R}^n, \\
\boldsymbol{x}_k & \equiv & (x_{\mathrm{r}k1}, x_{\mathrm{s}k1}, \ldots, x_{\mathrm{r}kn}, x_{\mathrm{s}kn})^{\mathrm{T}} \in \mathbb{R}^{2n}, & \boldsymbol{e}_k & \equiv & (e_{\mathrm{r}k1}, e_{\mathrm{s}k1}, \ldots, e_{\mathrm{r}kn}, e_{\mathrm{s}kn})^{\mathrm{T}} \in \mathbb{R}^{2n}, \\
 & & k = 1, \ldots, p. & & &
\end{array}
$$

From Eq.(2.5), the real forcing terms $\boldsymbol{e}$ satisfies

$$
\begin{cases} \boldsymbol{e}_k = \boldsymbol{0} \ \text{ for } \ k = 0, \ldots, p, \ k \neq m & \text{(for periodically forcing system)} \\ \boldsymbol{e} = \boldsymbol{0} & \text{(for autonomous system)} \end{cases} . \tag{2.9}
$$

Using the real variables $\boldsymbol{x}$ and $\boldsymbol{e}$, we define the HB equation expressed as real polynomial equations

$$
\begin{aligned}
\boldsymbol{f}(\boldsymbol{x}) &\equiv \boldsymbol{f}(\boldsymbol{x}; \omega, \boldsymbol{\lambda}, \boldsymbol{e}) \equiv \left[\begin{array}{c} \boldsymbol{f}_0 \\ \vdots \\ \boldsymbol{f}_p \end{array}\right] = \boldsymbol{0} \in \mathbb{R}^N, \qquad (2.10) \\
\boldsymbol{f}_0 &\equiv (f_{\mathrm{r}01}, \ldots, f_{\mathrm{r}0n})^{\mathrm{T}} \\
&\equiv (\Re[F_{01}], \ldots, \Re[F_{0n}])^{\mathrm{T}} \in \mathbb{R}^n, \\
\boldsymbol{f}_k &\equiv (f_{\mathrm{r}k1}, f_{\mathrm{s}k1}, \ldots, f_{\mathrm{r}kn}, f_{\mathrm{s}kn})^{\mathrm{T}} \\
&\equiv (\Re[F_{k1}], \Im[F_{k1}], \ldots, \Re[F_{kn}], \Im[F_{kn}])^{\mathrm{T}} \in \mathbb{R}^{2n}, \\
k &= 1, \ldots, p,
\end{aligned}
$$

where $\Im[\cdot]$ denotes the imaginary part. The HB equation is polynomial equations with the coefficients in a rational function field $\mathbb{Q}(\omega, \boldsymbol{\lambda}, \boldsymbol{e})$ of $\omega, \boldsymbol{\lambda}$, and $\boldsymbol{e}$.

The HB equation (2.10) has the symmetry derived by the symmetry of the system equation (2.1). We will show the detail of the symmetry in Chapter 3 because this property is a key relation for the decomposition of bifurcation diagrams.

2.4 Example – Duffing Equation

2.4.1 Circuit Equation

We consider the RLC nonlinear circuit shown in Figure 2.1 because the system exhibits bifurcation phenomena despite the simplicity. Now, we assume that the magnetizing characteristics of

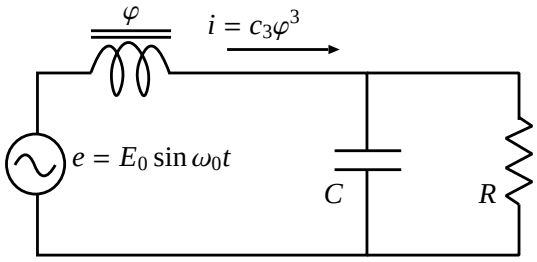

Figure 2.1: Periodically Forced Circuit.

the nonlinear inductor is approximated by cubic-polynomial, i.e., the current i satisfies $i = c_3\varphi^3$, where φ is a magnetic flux. The scaled differential equation of φ is

$$\frac{\mathrm{d}^2u(t)}{\mathrm{d}t^2} + \mu\frac{\mathrm{d}u(t)}{\mathrm{d}t} + u(t)^3 = E\cos\omega_s t, \tag{2.11}$$

where

$$u = \frac{\varphi}{\Phi_\mathrm{n}},\ \ \omega_s t = m\omega t = \omega_0 t - \tan^{-1}\frac{\mu}{m},\ \ \mu = \frac{1}{\omega_0 RC},\ \ E = \frac{E_0}{\omega_0\Phi_\mathrm{n}}\sqrt{\mu^2+m^2},$$

and Φ_n is a value for the normalized magnetic flux determined by $\Phi_\mathrm{n} = \sqrt{\frac{\omega_0^2 C}{c_3}}$. This equation is well known as Duffing equation [1]. We transform Eq.(2.11) into the formulation of Eq.(2.1);

$$\frac{\mathrm{d}}{\mathrm{d}t}\begin{bmatrix} u_1 \\ u_2 \end{bmatrix} = \begin{bmatrix} u_2 \\ -\mu u_2 - {u_1}^3 \end{bmatrix} + \begin{bmatrix} 0 \\ E\cos\omega_s t \end{bmatrix}, \tag{2.12}$$
$$u_1 = u,\ u_2 = \frac{\mathrm{d}u}{\mathrm{d}t}.$$

2.4.2 HB Equation

Let us consider the case of $m = 1$, i.e., fundamental harmonic oscillations. We apply the HB method with $p = 3$ to Eq.(2.12). For simplicity, we assume that the direct current components equal zero, i.e., $X_{01} = X_{02} = 0$, since the HB equation is complicated by the direct current even though it is not important in the bifurcation analysis. Thus, we approximate the $u_1(t)$ and $u_2(t)$ by

$$\begin{aligned} u_1^*(t) &= \Re\left[X_{11}e^{\mathrm{j}\omega t} + X_{21}e^{\mathrm{j}2\omega t} + X_{31}e^{\mathrm{j}3\omega t}\right] \\ &= \Re\left[(x_{\mathrm{r}11} + \mathrm{j}x_{\mathrm{s}11})e^{\mathrm{j}\omega t} + (x_{\mathrm{r}21} + \mathrm{j}x_{\mathrm{s}21})e^{\mathrm{j}2\omega t} + (x_{\mathrm{r}31} + \mathrm{j}x_{\mathrm{s}31})e^{\mathrm{j}3\omega t}\right], \end{aligned} \tag{2.13}$$

$$
\begin{aligned}
u_2^*(t) &= \Re\left[X_{12}e^{\mathrm{j}\omega t} + X_{22}e^{\mathrm{j}2\omega t} + X_{32}e^{\mathrm{j}3\omega t}\right] \\
&= \Re\left[(x_{\mathrm{r}12} + \mathrm{j}x_{\mathrm{s}12})e^{\mathrm{j}\omega t} + (x_{\mathrm{r}22} + \mathrm{j}x_{\mathrm{s}22})e^{\mathrm{j}2\omega t} + (x_{\mathrm{r}32} + \mathrm{j}x_{\mathrm{s}32})e^{\mathrm{j}3\omega t}\right]. \qquad (2.14)
\end{aligned}
$$

Then, the HB equation is described by

$$
\begin{aligned}
\boldsymbol{f}(\boldsymbol{x}) &= \boldsymbol{f}(\boldsymbol{x}; \omega, \mu, E) \\
&= \begin{bmatrix} \boldsymbol{f}_1 \\ \boldsymbol{f}_2 \\ \boldsymbol{f}_3 \end{bmatrix} = \boldsymbol{0}, \qquad (2.15) \\
\boldsymbol{f}_k &\equiv (f_{\mathrm{r}k1}, f_{\mathrm{s}k1}, f_{\mathrm{r}k2}, f_{\mathrm{s}k2})^{\mathrm{T}}, \\
\boldsymbol{x} &= \begin{bmatrix} \boldsymbol{x}_1 \\ \boldsymbol{x}_2 \\ \boldsymbol{x}_3 \end{bmatrix}, \\
\boldsymbol{x}_k &\equiv (x_{\mathrm{r}k1}, x_{\mathrm{s}k1}, x_{\mathrm{r}k2}, x_{\mathrm{s}k2})^{\mathrm{T}}, \\
k &= 1, 2, 3.
\end{aligned}
$$

Though the derivation of the HB equation is complicated for many frequency components, the HB equation can be automatically calculated using symbolic computation. In fact, the calculated polynomials are as follows;

$$
\begin{aligned}
f_{\mathrm{r}11} &= \omega x_{\mathrm{s}11} - x_{\mathrm{r}12}, \\
f_{\mathrm{s}11} &= -x_{\mathrm{s}12} - \omega x_{\mathrm{r}11}, \\
f_{\mathrm{r}12} &= x_{\mathrm{r}11}\left(\frac{3x_{\mathrm{s}31}^2}{2} + \frac{3x_{\mathrm{s}21}^2}{2} + \frac{3x_{\mathrm{r}31}^2}{2} + \frac{3x_{\mathrm{r}21}^2}{2}\right) + \frac{3x_{\mathrm{r}21}x_{\mathrm{s}21}x_{\mathrm{s}31}}{2} + \frac{3x_{\mathrm{r}11}x_{\mathrm{s}11}x_{\mathrm{s}31}}{2} - \frac{3x_{\mathrm{r}31}x_{\mathrm{s}21}^2}{4} \\
&\quad + \omega x_{\mathrm{s}12} + \left(\frac{3x_{\mathrm{r}11}}{4} - \frac{3x_{\mathrm{r}31}}{4}\right)x_{\mathrm{s}11}^2 + \frac{3x_{\mathrm{r}21}^2 x_{\mathrm{r}31}}{4} + \frac{3x_{\mathrm{r}11}^2 x_{\mathrm{r}31}}{4} + \mu x_{\mathrm{r}12} + \frac{3x_{\mathrm{r}11}^3}{4} - E, \\
f_{\mathrm{s}12} &= x_{\mathrm{s}11}\left(\frac{3x_{\mathrm{s}31}^2}{2} + \frac{3x_{\mathrm{s}21}^2}{2} + \frac{3x_{\mathrm{r}31}^2}{2} - \frac{3x_{\mathrm{r}11}x_{\mathrm{r}31}}{2} + \frac{3x_{\mathrm{r}21}^2}{2} + \frac{3x_{\mathrm{r}11}^2}{4}\right) + \left(\frac{3x_{\mathrm{s}21}^2}{4} - \frac{3x_{\mathrm{r}21}^2}{4}\right)x_{\mathrm{s}31} \\
&\quad - \frac{3x_{\mathrm{s}11}^2 x_{\mathrm{s}31}}{4} + \frac{3x_{\mathrm{r}11}^2 x_{\mathrm{s}31}}{4} + \frac{3x_{\mathrm{r}21}x_{\mathrm{r}31}x_{\mathrm{s}21}}{2} + \mu x_{\mathrm{s}12} + \frac{3x_{\mathrm{s}11}^3}{4} - \omega x_{\mathrm{r}12}, \\
f_{\mathrm{r}21} &= 2\omega x_{\mathrm{s}21} - x_{\mathrm{r}22}, \\
f_{\mathrm{s}21} &= -x_{\mathrm{s}22} - 2\omega x_{\mathrm{r}21}, \\
f_{\mathrm{r}22} &= \frac{3x_{\mathrm{r}21}x_{\mathrm{s}31}^2}{2} + x_{\mathrm{r}11}\left(\frac{3x_{\mathrm{s}21}x_{\mathrm{s}31}}{2} + \frac{3x_{\mathrm{r}21}x_{\mathrm{r}31}}{2}\right) + x_{\mathrm{s}11}\left(\frac{3x_{\mathrm{r}31}x_{\mathrm{s}21}}{2} - \frac{3x_{\mathrm{r}21}x_{\mathrm{s}31}}{2}\right) \\
&\quad + 2\omega x_{\mathrm{s}22} + x_{\mathrm{r}21}\left(\frac{3x_{\mathrm{s}21}^2}{4} + \frac{3x_{\mathrm{r}31}^2}{2}\right) + \frac{3x_{\mathrm{r}21}x_{\mathrm{s}11}^2}{2} + \mu x_{\mathrm{r}22} + \frac{3x_{\mathrm{r}21}^3}{4} + \frac{3x_{\mathrm{r}11}^2 x_{\mathrm{r}21}}{2},
\end{aligned}
$$

$$
\begin{aligned}
f_{\mathrm{s22}} &= \frac{3x_{\mathrm{s21}}x_{\mathrm{s31}}^2}{2} + x_{\mathrm{s11}}\left(\frac{3x_{\mathrm{s21}}x_{\mathrm{s31}}}{2} + \frac{3x_{\mathrm{r21}}x_{\mathrm{r31}}}{2}\right) + x_{\mathrm{r11}}\left(\frac{3x_{\mathrm{r21}}x_{\mathrm{s31}}}{2} - \frac{3x_{\mathrm{r31}}x_{\mathrm{s21}}}{2}\right) \\
&\quad + \mu x_{\mathrm{s22}} + \frac{3x_{\mathrm{s21}}^3}{4} + \frac{3x_{\mathrm{s11}}^2x_{\mathrm{s21}}}{2} + \frac{3x_{\mathrm{r31}}^2x_{\mathrm{s21}}}{2} + \frac{3x_{\mathrm{r21}}^2x_{\mathrm{s21}}}{4} + \frac{3x_{\mathrm{r11}}^2x_{\mathrm{s21}}}{2} - 2\omega x_{\mathrm{r22}}, \\
f_{\mathrm{r31}} &= 3\omega x_{\mathrm{s31}} - x_{\mathrm{r32}}, \\
f_{\mathrm{s31}} &= -x_{\mathrm{s32}} - 3\omega x_{\mathrm{r31}}, \\
f_{\mathrm{r32}} &= 3\omega x_{\mathrm{s32}} + \frac{3x_{\mathrm{r31}}x_{\mathrm{s31}}^2}{4} + \frac{3x_{\mathrm{r31}}x_{\mathrm{s21}}^2}{2} + x_{\mathrm{r11}}\left(\frac{3x_{\mathrm{r21}}^2}{4} - \frac{3x_{\mathrm{s21}}^2}{4}\right) + \frac{3x_{\mathrm{r21}}x_{\mathrm{s11}}x_{\mathrm{s21}}}{2} \\
&\quad + \left(\frac{3x_{\mathrm{r31}}}{2} - \frac{3x_{\mathrm{r11}}}{4}\right)x_{\mathrm{s11}}^2 + \mu x_{\mathrm{r32}} + \frac{3x_{\mathrm{r31}}^3}{4} + \frac{3x_{\mathrm{r21}}^2x_{\mathrm{r31}}}{2} + \frac{3x_{\mathrm{r11}}^2x_{\mathrm{r31}}}{2} + \frac{x_{\mathrm{r11}}^3}{4}, \\
f_{\mathrm{s32}} &= \mu x_{\mathrm{s32}} + \frac{3x_{\mathrm{s31}}^3}{4} + \left(\frac{3x_{\mathrm{s21}}^2}{2} + \frac{3x_{\mathrm{r31}}^2}{4} + \frac{3x_{\mathrm{r21}}^2}{2}\right)x_{\mathrm{s31}} + \frac{3x_{\mathrm{s11}}^2x_{\mathrm{s31}}}{2} + \frac{3x_{\mathrm{r11}}^2x_{\mathrm{s31}}}{2} \\
&\quad + x_{\mathrm{s11}}\left(\frac{3x_{\mathrm{s21}}^2}{4} - \frac{3x_{\mathrm{r21}}^2}{4} + \frac{3x_{\mathrm{r11}}^2}{4}\right) + \frac{3x_{\mathrm{r11}}x_{\mathrm{r21}}x_{\mathrm{s21}}}{2} - \frac{x_{\mathrm{s11}}^3}{4} - 3\omega x_{\mathrm{r32}}.
\end{aligned}
$$

We can confirm that the forcing term E is contained only in f_{r12}.

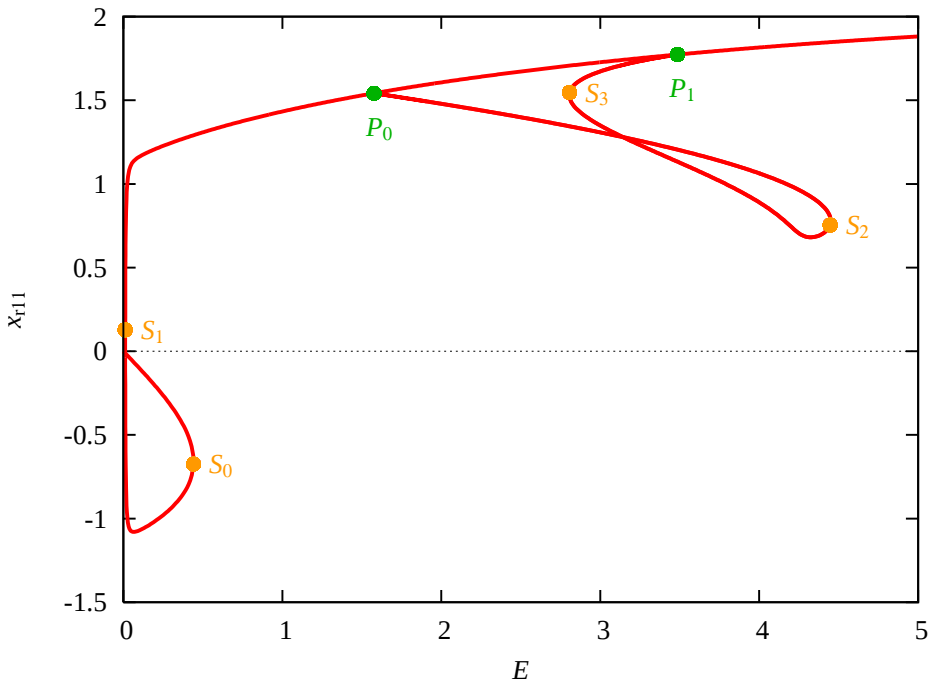

Figure 2.2: Bifurcation diagram (E - x_{r11}), the parameter E versus the real part of the fundamental oscillation x_{r11} ($m = 1, \omega = 1, \mu = 0.01$).

2.4.3 Bifurcation Diagram

In numerical approaches, we calculate the bifurcation diagram by solving the HB equation (2.15) for all specified parameters one by one. Namely, the bifurcation diagram is represented by a set of numerical solutions of the HB equation. The bifurcation diagram calculated by the numerical approach is shown in Figure 2.2 which represents the relation between the parameter E and the real part of the fundamental oscillation $x_{\mathrm{r}11}$ with $\omega = 1$ and $\mu = 0.01$. Now, we denotes the relation between E and $x_{\mathrm{r}11}$ by (E - $x_{\mathrm{r}11}$). In this figure, S_0, S_1, S_2, S_3, P_0, and P_1 denote bifurcation points defined by the Jacobian of $\boldsymbol{f}(\boldsymbol{x})$. Namely, if the Jacobian $\left.\dfrac{\partial \boldsymbol{f}(\boldsymbol{x})}{\partial \boldsymbol{x}}\right|_{\boldsymbol{x}=\boldsymbol{x}_0, E=E_0}$ has a zero eigenvalue for a point $(\boldsymbol{x}; E) = (\boldsymbol{x}_0; E_0)$, then $(\boldsymbol{x}_0; E_0)$ is a bifurcation point, and can be classified by Lyapunov-Schmidt decomposition [51, 52]. In fact, as Figure 2.2 shows, S_0, S_1, S_2, and S_3 are called saddle node bifurcation points corresponding to turning points in the bifurcation diagram. Moreover, P_0 and P_1 are branch points called pitchfork bifurcation points due to symmetry breaking. Thus, we can find out the local bifurcations using only the numerical approach.

Nevertheless, it is important to view the bifurcations from algebraic aspects. Since the HB equation is described as polynomial equations such as Eq.(2.15), the bifurcation diagram of the HB equation is expected to be represented by algebraic curves described by an algebraic equation of $x_{\mathrm{r}11}$ and E. Then, what kind of singularity are the pitchfork bifurcation points? It is, however, difficult to clarify such algebraic structure of the bifurcation diagram only by the numerical approaches. In order to calculate the bifurcation diagram algebraically, we have to introduce the concept of the ideal generated by the HB equation.

2.5 Fundamental Approach by Ideal

2.5.1 Ideal Generated by HB Equation

In order to introduce the concept of the ideal generated by the HB equation, we recall a universal definition of ideals [21, 22].

Definition 1 (Ideal)**.** *Let $\mathbb{Q}(\boldsymbol{\lambda})[\boldsymbol{x}]$ be a polynomial ring with coefficients in rational function field $\mathbb{Q}(\boldsymbol{\lambda})$. A subset $I \subset \mathbb{Q}(\boldsymbol{\lambda})[\boldsymbol{x}]$ is an ideal if it satisfies;*

(i) $0 \in I$.

(ii) *If $f, g \in I$, then $f + g \in I$.*

(iii) *If* $f \in I$ *and* $a \in \mathbb{Q}(\boldsymbol{\lambda})[\boldsymbol{x}]$*, then* $af \in I$*.*

The definition indicates that the ideal I is an infinite set of polynomials. In addition, if a set of polynomials $f_1, \cdots, f_s \in \mathbb{Q}(\boldsymbol{\lambda})[\boldsymbol{x}]$ is given, the following set satisfies the conditions of the ideal;

$$\langle f_1, \ldots, f_s \rangle = \{a_1 f_1 + \cdots + a_s f_s \mid a_1, \ldots, a_s \in \mathbb{Q}(\boldsymbol{\lambda})[\boldsymbol{x}]\}. \tag{2.16}$$

We call it the ideal generated by $f_1, \cdots f_s$, which is denoted by $\langle f_1, \ldots, f_s \rangle$. Similarly, the ideal generated by the polynomial HB equation $\boldsymbol{f}(\boldsymbol{x}) = \boldsymbol{0}$ is defined by

$$\begin{aligned} \langle \boldsymbol{f}(\boldsymbol{x}) \rangle &\equiv \langle \boldsymbol{f}_0, \ldots, \boldsymbol{f}_p \rangle \\ &\equiv \left\{ \sum_{i=1}^{n} a_{\mathrm{r}0i} f_{\mathrm{r}0i} + \sum_{k=1}^{p} \sum_{i=1}^{n} (a_{\mathrm{r}ki} f_{\mathrm{r}ki} + a_{\mathrm{s}ki} f_{\mathrm{s}ki}) \right. \\ &\qquad \left. \Big| \; a_{\mathrm{r}0i}, a_{\mathrm{r}ki}, a_{\mathrm{s}ki} \in \mathbb{Q}(\omega, \boldsymbol{\lambda}, \boldsymbol{e})[\boldsymbol{x}] \text{ for } k = 1, \ldots, p, i = 1, \ldots, n \right\}. \end{aligned} \tag{2.17}$$

It is noted that we use also the notation $\boldsymbol{I}[\boldsymbol{f}(\boldsymbol{x})] \equiv \langle \boldsymbol{f}(\boldsymbol{x}) \rangle$ for the ideal generated by $\boldsymbol{f}(\boldsymbol{x})$ in contrast to the variety introduced in the next section.

2.5.2 Variety Generated by HB Equation

In order to clarify the meaning of the ideal, we introduce the concept of variety. The real variety $\boldsymbol{V}$ generated by the polynomial HB equation $\boldsymbol{f}(\boldsymbol{x}) = \boldsymbol{0}$ is defined by

$$\boldsymbol{V}[\boldsymbol{f}(\boldsymbol{x})] \equiv \left\{ \boldsymbol{x} \in \mathbb{R}^N \mid \boldsymbol{f}(\boldsymbol{x}) = \boldsymbol{0} \right\}. \tag{2.18}$$

The definition indicates that the real variety $\boldsymbol{V}[\boldsymbol{f}(\boldsymbol{x})]$ is a set of solutions of $\boldsymbol{f}(\boldsymbol{x}) = \boldsymbol{0}$. That is, the real variety $\boldsymbol{V}[\boldsymbol{f}(\boldsymbol{x})]$ corresponds to the bifurcation diagram of $\boldsymbol{f}(\boldsymbol{x}) = \boldsymbol{0}$.

The essential reason why the ideal is introduced is that the bifurcation diagram $\boldsymbol{V}[\boldsymbol{f}(\boldsymbol{x})]$ is not determined only by the equation $\boldsymbol{f}(\boldsymbol{x}) = \boldsymbol{0}$ but by the ideal $\boldsymbol{I}[\boldsymbol{f}(\boldsymbol{x})]$ generated by the equation because the ideal $\langle \boldsymbol{f}(\boldsymbol{x}) \rangle$ is an infinite set of polynomial equations which have the same solutions of $\boldsymbol{f}(\boldsymbol{x}) = \boldsymbol{0}$. Hence we may take instead of $\boldsymbol{f}(\boldsymbol{x})$ another generating set (an ideal base), say a Gröbner base. For example, Gröbner base with respect to the lexicographic order gives triangular form of the HB equation [21, 22].

2.5.3 Algebraic Representation of Bifurcation Diagram Using Gröbner Base

If a monomial order is given, Buchberger's algorithm provides corresponding Gröbner base by the cancellation of leading terms [18–22]. For example, if we give a lexicographic order $x_{\mathrm{r}01} \succ_{\mathrm{lex}} x_{\mathrm{r}02} \succ_{\mathrm{lex}} \cdots \succ_{\mathrm{lex}} x_{\mathrm{s}p(n-1)} \succ_{\mathrm{lex}} x_{\mathrm{r}pn} \succ_{\mathrm{lex}} x_{\mathrm{s}pn}$ to the HB equation $\boldsymbol{f}(\boldsymbol{x}) = \boldsymbol{0}$, corresponding Gröbner base, which is called an elimination ideal, is represented by the triangular form;

$$\boldsymbol{g}(\boldsymbol{x}) = \begin{bmatrix} g_1(x_{\mathrm{r}01}, x_{\mathrm{r}02}, \ldots, x_{\mathrm{r}pn}, x_{\mathrm{s}pn}; \omega, \boldsymbol{\lambda}, \boldsymbol{e}) \\ g_2(x_{\mathrm{r}02}, \ldots, x_{\mathrm{r}pn}, x_{\mathrm{s}pn}; \omega, \boldsymbol{\lambda}, \boldsymbol{e}) \\ \vdots \\ g_{N-1}(x_{\mathrm{r}pn}, x_{\mathrm{s}pn}; \omega, \boldsymbol{\lambda}, \boldsymbol{e}) \\ g_N(x_{\mathrm{s}pn}; \omega, \boldsymbol{\lambda}, \boldsymbol{e}) \end{bmatrix}. \tag{2.19}$$

The first polynomial g_1 has all variables $x_{\mathrm{r}01}, x_{\mathrm{r}02}, \cdots, x_{\mathrm{s}pn}$, the second polynomial g_2 has variables $x_{\mathrm{r}02}, \cdots x_{\mathrm{s}pn}$, and the last polynomial $g_N(x_{\mathrm{s}pn}; \omega, \boldsymbol{\lambda}, \boldsymbol{e})$ has only one variable $x_{\mathrm{s}pn}$. Thus, Gröbner base with respect to the lexicographic order provides the bifurcation diagram represented by unique algebraic equation

$$g_N(x_{\mathrm{s}pn}; \omega, \boldsymbol{\lambda}, \boldsymbol{e}) = 0. \tag{2.20}$$

2.5.4 Decomposition of Bifurcation Diagram

The algebraic representation of the bifurcation diagram (2.20) indicates an easy way to decompose it. That is, because Eq.(2.20) has only one variable, we can easily factorize the equation. The factorization corresponds to the mode decomposition of the diagram [35, 36].

The concept of the above factorization leads to ideal decomposition [21, 22]. Let us consider the decomposition of the bifurcation diagram based on the ideal decomposition. If the ideal I is decomposed as $I_1, \ldots, I_r$;

$$I = I_1 \cap I_2 \cap \cdots \cap I_r, \tag{2.21}$$

the corresponding variety $\boldsymbol{V}(I)$ is described as

$$\boldsymbol{V}(I) = \boldsymbol{V}(I_1) \cup \boldsymbol{V}(I_2) \cup \cdots \cup \boldsymbol{V}(I_r), \tag{2.22}$$

due to the ideal-variety correspondence shown in Appendix A. The equation (2.22) shows that the bifurcation diagram is algebraically decomposed by the ideal decomposition.

2.5.5 Decomposition Based on Symmetry

We consider the reason why the bifurcation diagram is decomposed. As one example of the ideal decompositions, when polynomial equations has a symmetry, the ideal generated by the equations can be decomposed [35, 36]. We show the decomposition of the bifurcation diagram based on the symmetry. Let $\boldsymbol{\theta}(\gamma) \in \mathbb{R}^{N\times N}$ be a linear representation of a finite group Γ with $\gamma \in \Gamma$. If the equation $\boldsymbol{f}(\boldsymbol{x})$ has symmetry which corresponds to Γ, then $\boldsymbol{f}(\boldsymbol{x})$ satisfies

$$\boldsymbol{f}(\boldsymbol{\theta}(\gamma)\boldsymbol{x}) = \boldsymbol{\theta}(\gamma)\boldsymbol{f}(\boldsymbol{x}), \tag{2.23}$$

for all $\gamma \in \Gamma$ [53]. If $\boldsymbol{x}$ is a solution of $\boldsymbol{f}(\boldsymbol{x}) = \boldsymbol{0}$, then $\boldsymbol{\theta}(\gamma)\boldsymbol{x}$ is also a solution. Let us consider the symmetric solutions, which satisfy

$$\boldsymbol{x} = \boldsymbol{\theta}(\gamma)\boldsymbol{x} \ \text{ for all } \ \gamma \in \Gamma. \tag{2.24}$$

The ideal which corresponds to the constraint of the symmetry is written by the sum of the ideal

$$\sum_{\gamma\in\Gamma} \langle \boldsymbol{x} - \boldsymbol{\theta}(\gamma)\boldsymbol{x}\rangle \equiv \left\{ \sum_{\gamma\in\Gamma} f_\gamma \;\middle|\; f_\gamma \in \langle \boldsymbol{x} - \boldsymbol{\theta}(\gamma)\boldsymbol{x}\rangle \right\}. \tag{2.25}$$

Since the symmetric solutions are determined by both the original equation $\boldsymbol{f}(\boldsymbol{x}) = \boldsymbol{0}$ and the constraint of the symmetry $\boldsymbol{x} - \boldsymbol{\theta}(\gamma)\boldsymbol{x} = \boldsymbol{0}$, the ideal $\langle \boldsymbol{f}_\Gamma(\boldsymbol{x})\rangle$ which corresponds to the symmetric solutions of $\boldsymbol{f}(\boldsymbol{x}) = \boldsymbol{0}$ is described by the sum of ideals

$$\langle \boldsymbol{f}_\Gamma(\boldsymbol{x})\rangle \equiv \langle \boldsymbol{f}(\boldsymbol{x})\rangle + \sum_{\gamma\in\Gamma} \langle \boldsymbol{x} - \boldsymbol{\theta}(\gamma)\boldsymbol{x}\rangle. \tag{2.26}$$

Because the ideal relation $\langle \boldsymbol{f}_\Gamma(\boldsymbol{x})\rangle \supset \langle \boldsymbol{f}(\boldsymbol{x})\rangle$ is held, the ideal quotient (cf.Appendix.A.4) provides the ideal $\langle \overline{\boldsymbol{f}_\Gamma}(\boldsymbol{x})\rangle$ which corresponds to the asymmetric solutions as follows;

$$\langle \overline{\boldsymbol{f}_\Gamma}(\boldsymbol{x})\rangle \quad \equiv \quad \langle \boldsymbol{f}(\boldsymbol{x})\rangle : \langle \boldsymbol{f}_\Gamma(\boldsymbol{x})\rangle. \tag{2.27}$$

Now, if $\langle \boldsymbol{f}(\boldsymbol{x})\rangle$ is a radical ideal (cf.Appendix.A.4), then the ideal $\langle \boldsymbol{f}(\boldsymbol{x})\rangle$ is decomposed into two ideals corresponding to the symmetric and asymmetric solutions as follows;

$$\langle \boldsymbol{f}(\boldsymbol{x})\rangle \quad = \quad \langle \boldsymbol{f}_\Gamma(\boldsymbol{x})\rangle \cap \langle \overline{\boldsymbol{f}_\Gamma}(\boldsymbol{x})\rangle. \tag{2.28}$$

This relation of the ideal derives the decomposition of the bifurcation diagram into sub-diagrams;

$$\boldsymbol{V}[\boldsymbol{f}(\boldsymbol{x})] \quad = \quad \boldsymbol{V}[\boldsymbol{f}_\Gamma(\boldsymbol{x})] \cup \boldsymbol{V}[\overline{\boldsymbol{f}_\Gamma}(\boldsymbol{x})]. \tag{2.29}$$

Thus, the symmetry leads to the decomposition of the bifurcation diagram.

In fact, because the pitchfork bifurcation is characterized by the breaking of the symmetry, P_0, P_1 in Figure 2.2 correspond to intersection points of the sub-diagrams $\boldsymbol{V}[\boldsymbol{f}_\Gamma(\boldsymbol{x})]$ and $\boldsymbol{V}[\overline{\boldsymbol{f}_\Gamma}(\boldsymbol{x})]$ as is shown in Chapter 3. Although this algebraic approach gives a novel aspect of the local pitchfork bifurcation, this simple approach by Gröbner base with respect to the lexicographic order requires tremendously huge computational cost and we cannot apply the method to the analysis of periodic oscillations.

2.6 Concluding Remarks

We derived determining polynomial equation of periodic oscillations using the HB method and presented an example of bifurcation diagrams. Then, in order to introduce an algebraic approach, we presented fundamentals of the ideal and the variety. Further, we reviewed a simple algebraic approach to the bifurcation diagram and revealed an algebraic aspect of the pitchfork bifurcation based on the decomposition of the bifurcation diagrams.

Chapter 3

Decomposition of Bifurcation Diagram

3.1 Introduction

This chapter proposes an algebraic approach to decompose a bifurcation diagram of periodic oscillations in a global parameter space. The proposed method is based on the research presented in the previous chapter [35, 36]. Although the decomposition of the bifurcation diagram in [35, 36] is very powerful to clarify the bifurcations in the global parameter space based on Gröbner base, the computational cost of calculating Gröbner base prevents its practical applications such as the bifurcation of the periodic oscillations.

In order to overcome the difficulty, we propose an efficient method to decompose the bifurcation diagram using the ideal quotient based on the symmetry of the HB equation. Further, this chapter reveals the symmetry of the homogeneous HB equation that has no terms corresponding to sinusoidal forcing functions. The homogeneous HB equation has the highest symmetries and the nonhomogeneous HB equations are generated by the break of the symmetries. We demonstrate that this property enables a systematic analysis of the HB equations using the ideal quotient.

3.2 Ideal Decomposition by Ideal Quotient

Although the bifurcation diagram can be decomposed when the HB equation has a symmetry such as the previous chapter, the previous method in [35, 36] based on the factorization of the lexicographic order Gröbner base requires a high computational cost. To overcome the difficulty of this problem, we obtain the decomposition of the bifurcation diagram for the HB equation using the ideal quotient. If the ideal I is represented by $I = J \cap K$ and if J is coprime to K, then

the ideal K is calculated by the ideal quotient

$$K = I : J. \tag{3.1}$$

The computational cost of the ideal quotient is considerably less than that of the lexicographic order Gröbner base. In order to find out the ideal J, we use a symmetry of the HB equation (2.10) since the ideals corresponding to the symmetric and asymmetric solutions are obviously coprime. Namely, we obtain the ideal $\langle \boldsymbol{f}_\Gamma(\boldsymbol{x}) \rangle$ which corresponds to the symmetric solutions given by Eq.(2.26) using the symmetry in advance. Then, we calculate the ideal $\langle \overline{\boldsymbol{f}_\Gamma}(\boldsymbol{x}) \rangle$ which corresponds to the asymmetric solutions by the ideal quotient $\langle \boldsymbol{f}(\boldsymbol{x}) \rangle : \langle \boldsymbol{f}_\Gamma(\boldsymbol{x}) \rangle$ shown in Eq.(2.27).

3.3 Symmetry of HB Equation

For the decomposition of the bifurcation diagram, we begin with finding the symmetry of the HB equation derived by the symmetry of the system. Let us rewrite the system equation (2.1) to

$$\boldsymbol{H}[\boldsymbol{u}(t); \boldsymbol{\lambda}, \boldsymbol{s}(t)] \equiv -\frac{\mathrm{d}\boldsymbol{u}}{\mathrm{d}t} + \boldsymbol{h}(\boldsymbol{u}; \boldsymbol{\lambda}) + \boldsymbol{s}(t) \equiv -\frac{\mathrm{d}\boldsymbol{u}}{\mathrm{d}t} + \boldsymbol{L}[\boldsymbol{u}] + \boldsymbol{N}[\boldsymbol{u}] + \boldsymbol{s}(t) = \boldsymbol{0}, \tag{3.2}$$

where $\boldsymbol{h}$ is divided into a linear part $\boldsymbol{L}$ and a nonlinear part $\boldsymbol{N}$. We assume that the $\boldsymbol{N}$ has an odd symmetry; $\boldsymbol{N}[-\boldsymbol{u}] = -\boldsymbol{N}[\boldsymbol{u}]$.

We consider the symmetry of the HB equation from the symmetry of the equation $\boldsymbol{H}[\boldsymbol{u}(t); \boldsymbol{\lambda}, \boldsymbol{s}(t)] = \boldsymbol{0}$, and lead to the constraints (2.24) of the symmetric solutions.

3.3.1 Periodically Forced System

First, we consider the symmetry of a periodically forced system. The system has the odd symmetry $\boldsymbol{N}[-\boldsymbol{u}] = -\boldsymbol{N}[\boldsymbol{u}]$ and the symmetry based on the time shift $2\pi/\omega_s$ which is the period of the fundamental oscillations, i.e., $\boldsymbol{s}(t + 2\pi/\omega_s) = \boldsymbol{s}(t)$.

Odd Symmetry

Let us consider π/ω time shift based on the odd symmetry; $\boldsymbol{N}[-\boldsymbol{u}] = -\boldsymbol{N}[\boldsymbol{u}]$. We define an operator $\mathcal{T}_{\mathrm{odd}}$

$$\mathcal{T}_{\mathrm{odd}}\boldsymbol{u}(t) = -\boldsymbol{u}(t + \pi/\omega). \tag{3.3}$$

Now, we assume that the forcing functions have the odd symmetry $\mathcal{T}_{\rm odd}\boldsymbol{s}(t) = -\boldsymbol{s}(t+\pi/\omega) = \boldsymbol{s}(t)$, that is, m is odd number. $\boldsymbol{H}$ satisfies the relation as follows;

$$\begin{aligned}\boldsymbol{H}[\mathcal{T}_{\rm odd}\boldsymbol{u}(t);\boldsymbol{\lambda},\boldsymbol{s}(t)] &= \frac{{\rm d}\boldsymbol{u}(t+\pi/\omega)}{{\rm d}t} + \boldsymbol{L}[-\boldsymbol{u}(t+\pi/\omega)] + \boldsymbol{N}[-\boldsymbol{u}(t+\pi/\omega)] + \boldsymbol{s}(t) \\ &= -\left\{-\frac{{\rm d}\boldsymbol{u}(t+\pi/\omega)}{{\rm d}t} + \boldsymbol{L}[\boldsymbol{u}(t+\pi/\omega)] + \boldsymbol{N}[\boldsymbol{u}(t+\pi/\omega)] + \boldsymbol{s}(t+\pi/\omega)\right\} \\ &= \mathcal{T}_{\rm odd}\boldsymbol{H}[\boldsymbol{u}(t);\boldsymbol{\lambda},\boldsymbol{s}(t)]. \end{aligned} \tag{3.4}$$

In particular, if $\boldsymbol{u}(t)$ is a solution of $\boldsymbol{H}[\boldsymbol{u}(t);\boldsymbol{\lambda},\boldsymbol{s}(t)] = \boldsymbol{0}$, then $-\boldsymbol{u}(t+\pi/\omega)$ is also a solution. The same relations are satisfied also by the truncated solutions;

$$\begin{aligned}K^*\boldsymbol{H}[\mathcal{T}_{\rm odd}\boldsymbol{u}^*(t);\boldsymbol{\lambda},\boldsymbol{e}(t)] &= \sum_{k=0}^{p}\Re\left[{\rm j}k\omega\boldsymbol{X}_k e^{{\rm j}k\omega(t+\pi/\omega)}\right] + \sum_{k=0}^{p}\Re\left[\boldsymbol{Y}_k(-\boldsymbol{X})e^{{\rm j}k\omega(t+\pi/\omega)}\right] + \sum_{k=0}^{p}\Re\left[\boldsymbol{E}_k e^{{\rm j}k\omega t}\right] \\ &= -\sum_{k=0}^{p}\Re\left[\{-{\rm j}k\omega\boldsymbol{X}_k + \boldsymbol{Y}_k(\boldsymbol{X}) + \boldsymbol{E}_k\}\, e^{{\rm j}k\omega(t+\pi/\omega)}\right] \\ &= \mathcal{T}_{\rm odd}K^*\boldsymbol{H}[\boldsymbol{u}^*(t);\boldsymbol{\lambda},\boldsymbol{e}(t)], \end{aligned} \tag{3.5}$$

where we use $\boldsymbol{Y}_k(-\boldsymbol{X}) = -\boldsymbol{Y}_k(\boldsymbol{X})$ for $k = 0,\ldots,p$ and $\boldsymbol{E}_k = \boldsymbol{0}$ for $k = 0 \bmod 2$ corresponding to $\boldsymbol{s}(t) = -\boldsymbol{s}(t+\pi/\omega)$.

Based on the symmetry of Eq.(3.5) and the relation $\mathcal{T}_{\rm odd}[e^{{\rm j}k\omega t}] = (-1)^{k+1}e^{{\rm j}k\omega t}$, the complex HB equation $\boldsymbol{F}(\boldsymbol{X}) = \boldsymbol{0}$ satisfies the following relation;

$$\boldsymbol{F}(\boldsymbol{\Theta}_{\rm odd}^{\,i}\boldsymbol{X}) = \boldsymbol{\Theta}_{\rm odd}^{\,i}\boldsymbol{F}(\boldsymbol{X}) \quad \text{for} \quad i = 1,2, \tag{3.6}$$

where

$$\boldsymbol{\Theta}_{\rm odd} = \begin{bmatrix} -\boldsymbol{I}_n & & & \boldsymbol{0} \\ & \boldsymbol{I}_n & & \\ & & \ddots & \\ \boldsymbol{0} & & & (-1)^{p+1}\boldsymbol{I}_n \end{bmatrix},$$

and $\boldsymbol{I}_n$ denotes an identity matrix of $n \times n$. From this symmetry, if $\boldsymbol{X}$ is a solution of $\boldsymbol{F}(\boldsymbol{X}) = \boldsymbol{0}$, then $\boldsymbol{\Theta}_{\rm odd}^{\,i}\boldsymbol{X}$ is also a solution for $i = 1,2$. The symmetry (3.6) of the complex HB equation is transformed to the following symmetry of the real HB equation $\boldsymbol{f}(\boldsymbol{x}) = \boldsymbol{0}$;

$$\boldsymbol{f}(\boldsymbol{\theta}_{\rm odd}^{\,i}\boldsymbol{x}) = \boldsymbol{\theta}_{\rm odd}^{\,i}\boldsymbol{f}(\boldsymbol{x}) \quad \text{for} \quad i = 1,2, \tag{3.7}$$

where

$$\boldsymbol{\theta}_{\rm odd} = \begin{bmatrix} -\boldsymbol{I}_n & & & 0 \\ & \boldsymbol{I}_{2n} & & \\ & & \ddots & \\ 0 & & & (-1)^{p+1}\boldsymbol{I}_{2n} \end{bmatrix} \in \mathbb{R}^{N\times N}.$$

From this symmetry, if $\boldsymbol{x}$ is a solution of $\boldsymbol{f}(\boldsymbol{x}) = \boldsymbol{0}$, then $\boldsymbol{\theta}_{\rm odd}^{\,i}\boldsymbol{x}$ is also a solution for $i = 1, 2$. Here we denote the odd symmetry by $\Gamma_{\rm odd}$.

Thus, the symmetric solutions with respect to $\Gamma_{\rm odd}$ satisfy the constraint

$$\boldsymbol{x} = \boldsymbol{\theta}_{\rm odd}^{\,i}\boldsymbol{x} \ \text{ for } \ i = 1, 2, \tag{3.8}$$

which corresponds to Eq.(2.24).

Symmetry Based on $2\pi/\omega_{\rm s}$ Time Shift

We assume that Eq.(3.2) has the solutions which contain $1/m$ subharmonic oscillations with the period $2\pi/\omega$. We consider the time shift of the fundamental oscillation period $2\pi/\omega_s$ due to $\boldsymbol{s}(t + 2\pi/\omega_s) = \boldsymbol{s}(t)$. We define the $2\pi/\omega_s$ time shift operator $\mathcal{T}_{2\pi/\omega_s}$

$$\mathcal{T}_{2\pi/\omega_s}\boldsymbol{u}(t) = \boldsymbol{u}(t + 2\pi/\omega_s). \tag{3.9}$$

$\boldsymbol{H}$ satisfies the relation as follows;

$$\begin{aligned} \boldsymbol{H}[\mathcal{T}_{2\pi/\omega_s}\boldsymbol{u}(t); \boldsymbol{\lambda}, \boldsymbol{s}(t)] &= -\frac{{\rm d}\boldsymbol{u}(t + 2\pi/\omega_s)}{{\rm d}t} + \boldsymbol{h}(\boldsymbol{u}(t + 2\pi/\omega_s)\,; \boldsymbol{\lambda}) + \boldsymbol{s}(t) \\ &= -\frac{{\rm d}\boldsymbol{u}(t + 2\pi/\omega_s)}{{\rm d}t} + \boldsymbol{h}(\boldsymbol{u}(t + 2\pi/\omega_s)\,; \boldsymbol{\lambda}) + \boldsymbol{s}(t + 2\pi/\omega_s) \\ &= \mathcal{T}_{2\pi/\omega_s}\boldsymbol{H}[\boldsymbol{u}(t); \boldsymbol{\lambda}, \boldsymbol{s}(t)]. \end{aligned} \tag{3.10}$$

In particular, if $\boldsymbol{u}(t)$ is a solution of $\boldsymbol{H}[\boldsymbol{u}(t); \boldsymbol{\lambda}, \boldsymbol{s}(t)] = \boldsymbol{0}$, then $\boldsymbol{u}(t + 2\pi/\omega_s)$ is also a solution. The same relations are satisfied also by the truncated solutions;

$$\begin{aligned} K^*\boldsymbol{H}[\mathcal{T}_{2\pi/\omega_s}\boldsymbol{u}^*(t); \boldsymbol{\lambda}, \boldsymbol{e}(t)] &= \sum_{k=0}^{p} \Re\left[\{-{\rm j}k\omega\boldsymbol{X}_k + \boldsymbol{Y}_k(\boldsymbol{X})\}\, e^{{\rm j}k\omega(t+2\pi/\omega_s)}\right] + \sum_{k=0}^{p} \Re\left[\boldsymbol{E}_k e^{{\rm j}k\omega t}\right] \\ &= \sum_{k=0}^{p} \Re\left[\{-{\rm j}k\omega\boldsymbol{X}_k + \boldsymbol{Y}_k(\boldsymbol{X}) + \boldsymbol{E}_k\}\, e^{{\rm j}k\omega(t+2\pi/\omega_s)}\right] \\ &= \mathcal{T}_{2\pi/\omega_s}K^*\boldsymbol{H}[\boldsymbol{u}^*(t); \boldsymbol{\lambda}, \boldsymbol{e}(t)], \end{aligned} \tag{3.11}$$

where we use $\boldsymbol{E}_k = \boldsymbol{0}$ for $k \neq m$ in Eq.(2.5).

Based on the symmetry of Eq.(3.11) and the relation $\mathcal{T}_{2\pi/\omega_s}[e^{\mathrm{j}k\omega t}] = e^{\mathrm{j}\frac{2\pi k}{m}} e^{\mathrm{j}k\omega t}$, the complex HB equation $\boldsymbol{F}(\boldsymbol{X}) = \boldsymbol{0}$ satisfies the following relation;

$$\boldsymbol{F}(\boldsymbol{\Theta}^{i}_{2\pi/m}\boldsymbol{X}) = \boldsymbol{\Theta}^{i}_{2\pi/m}\boldsymbol{F}(\boldsymbol{X}) \ \text{ for } \ i = 1, \ldots, m, \tag{3.12}$$

where

$$\boldsymbol{\Theta}_{2\pi/m} = \begin{bmatrix} \boldsymbol{I}_n & & & 0 \\ & \boldsymbol{I}_n e^{\mathrm{j}\frac{2\pi}{m}} & & \\ & & \ddots & \\ 0 & & & \boldsymbol{I}_n e^{\mathrm{j}\frac{2\pi p}{m}} \end{bmatrix}.$$

From this symmetry, if $\boldsymbol{X}$ is a solution of $\boldsymbol{F}(\boldsymbol{X}) = \boldsymbol{0}$, then $\boldsymbol{\Theta}^{i}_{2\pi/m}\boldsymbol{X}$ is also a solution for $i = 1, \ldots, m$. The symmetry (3.12) of the complex HB equation is transformed to the following symmetry of the real HB equation $\boldsymbol{f}(\boldsymbol{x}) = \boldsymbol{0}$;

$$\boldsymbol{f}(\boldsymbol{\theta}^{i}_{2\pi/m}\boldsymbol{x}) = \boldsymbol{\theta}^{i}_{2\pi/m}\boldsymbol{f}(\boldsymbol{x}) \ \text{ for } \ i = 1, \ldots, m, \tag{3.13}$$

where

$$\boldsymbol{\theta}_{2\pi/m} = \begin{bmatrix} \boldsymbol{I}_n & & & 0 \\ & \boldsymbol{\theta}_{2\pi/m,1} & & \\ & & \ddots & \\ 0 & & & \boldsymbol{\theta}_{2\pi/m,p} \end{bmatrix} \in \mathbb{R}^{N\times N},$$

$$\boldsymbol{\theta}_{2\pi/m,k} = \begin{bmatrix} \cos\frac{2\pi k}{m} & \sin\frac{2\pi k}{m} & & & 0 \\ -\sin\frac{2\pi k}{m} & \cos\frac{2\pi k}{m} & & & \\ & & \ddots & & \\ & & & \cos\frac{2\pi k}{m} & \sin\frac{2\pi k}{m} \\ 0 & & & -\sin\frac{2\pi k}{m} & \cos\frac{2\pi k}{m} \end{bmatrix} \in \mathbb{R}^{2n\times 2n},$$

$$k = 1, \ldots, p. \tag{3.14}$$

From this symmetry, if $\boldsymbol{x}$ is a solution of $\boldsymbol{f}(\boldsymbol{x}) = \boldsymbol{0}$, then $\boldsymbol{\theta}^{i}_{2\pi/m}\boldsymbol{x}$ is also a solution for $i = 1, \ldots, m$. Here we denote the symmetry based on $2\pi/\omega_s$ time shift by $\Gamma_{2\pi/m}$.

Thus, the symmetric solutions with respect to $\Gamma_{2\pi/m}$ satisfy the constraint

$$\boldsymbol{x} = \boldsymbol{\theta}^{i}_{2\pi/m}\boldsymbol{x} \ \text{ for } \ i = 1, \ldots, m, \tag{3.15}$$

which corresponds to Eq.(2.24).

3.3.2 Autonomous System

Although the bifurcation diagram of an autonomous system cannot be decomposed by its symmetry, we consider the symmetry since it will be used in Chapter 4. Namely, we set $\boldsymbol{s}(t) = \boldsymbol{0}$, and describe Eq.(3.2) as $\boldsymbol{H}[\boldsymbol{u}(t); \boldsymbol{\lambda}, \boldsymbol{0}] = \boldsymbol{0}$. The autonomous system has the odd symmetry, which is considered in the previous subsection, and the symmetry based on an arbitrary time shift.

Arbitrary Time Shift

The equation $\boldsymbol{H}[\boldsymbol{u}(t); \boldsymbol{\lambda}, \boldsymbol{0}] = \boldsymbol{0}$ has the arbitrary time ϕ/ω shift symmetry. Now, a shift operator $\mathcal{T}_{\text{arbitrary}}$ which represents the arbitrary time ϕ/ω shift is defined by

$$\mathcal{T}_{\text{arbitrary}}\boldsymbol{u}(t) = \boldsymbol{u}(t + \phi/\omega). \tag{3.16}$$

$\boldsymbol{H}$ satisfies the relation as follows;

$$\boldsymbol{H}[\mathcal{T}_{\text{arbitrary}}\boldsymbol{u}(t); \boldsymbol{\lambda}, \boldsymbol{0}] = -\frac{\mathrm{d}\boldsymbol{u}(t + \phi/\omega)}{\mathrm{d}t} + \boldsymbol{h}(\boldsymbol{u}(t + \phi/\omega)\,; \boldsymbol{\lambda}) = \mathcal{T}_{\text{arbitrary}}\boldsymbol{H}[\boldsymbol{u}(t); \boldsymbol{\lambda}, \boldsymbol{0}]. \tag{3.17}$$

In particular, if $\boldsymbol{u}(t)$ is a solution of $\boldsymbol{H}[\boldsymbol{u}(t); \boldsymbol{\lambda}, \boldsymbol{0}] = \boldsymbol{0}$, then $\boldsymbol{u}(t + \phi/\omega)$ is also a solution. The same relations are satisfied also by the truncated solutions;

$$K^*\boldsymbol{H}[\mathcal{T}_{\text{arbitrary}}\boldsymbol{u}^*(t); \boldsymbol{\lambda}, \boldsymbol{0}] = \sum_{k=0}^{p} \Re\left[\{-\mathrm{j}k\omega\boldsymbol{X}_k + \boldsymbol{Y}_k(\boldsymbol{X})\}\, e^{\mathrm{j}k\omega(t+\phi/\omega)}\right] = \mathcal{T}_{\text{arbitrary}}K^*\boldsymbol{H}[\boldsymbol{u}^*(t); \boldsymbol{\lambda}, \boldsymbol{0}]. \tag{3.18}$$

Based on the symmetry of Eq.(3.18) and the relation $\mathcal{T}_{\text{arbitrary}}[e^{\mathrm{j}k\omega t}] = e^{\mathrm{j}k\phi}e^{\mathrm{j}k\omega t}$, the complex HB equation $\boldsymbol{F}(\boldsymbol{X}) = \boldsymbol{0}$ satisfies the following relation;

$$\boldsymbol{F}(\boldsymbol{\Theta}_{\text{arbitrary}}(\phi)\boldsymbol{X}) = \boldsymbol{\Theta}_{\text{arbitrary}}(\phi)\boldsymbol{F}(\boldsymbol{X}), \tag{3.19}$$

where

$$\boldsymbol{\Theta}_{\text{arbitrary}}(\phi) = \begin{bmatrix} \boldsymbol{I}_n & & & 0 \\ & \boldsymbol{I}_n e^{\mathrm{j}\phi} & & \\ & & \ddots & \\ 0 & & & \boldsymbol{I}_n e^{\mathrm{j}p\phi} \end{bmatrix}.$$

From this symmetry, if $\boldsymbol{X}$ is a solution of $\boldsymbol{F}(\boldsymbol{X}) = \boldsymbol{0}$, then $\boldsymbol{\Theta}_{\text{arbitrary}}(\phi)\boldsymbol{X}$ is also a solution for all ϕ. The symmetry (3.19) of the complex HB equation is transformed to the following symmetry of the real HB equation $\boldsymbol{f}(\boldsymbol{x}) = \boldsymbol{0}$;

$$\boldsymbol{f}(\boldsymbol{\theta}_{\text{arbitrary}}(\phi)\boldsymbol{x}) = \boldsymbol{\theta}_{\text{arbitrary}}(\phi)\boldsymbol{f}(\boldsymbol{x}), \tag{3.20}$$

where

$$\boldsymbol{\theta}_{\text{arbitrary}}(\phi) = \begin{bmatrix} \boldsymbol{I}_n & & & 0 \\ & \boldsymbol{\theta}_{\text{arbitrary},1} & & \\ & & \ddots & \\ 0 & & & \boldsymbol{\theta}_{\text{arbitrary},p} \end{bmatrix} \in \mathbb{R}^{N\times N},$$

$$\boldsymbol{\theta}_{\text{arbitrary},k} = \begin{bmatrix} \cos k\phi & \sin k\phi & & & 0 \\ -\sin k\phi & \cos k\phi & & & \\ & & \ddots & & \\ & & & \cos k\phi & \sin k\phi \\ 0 & & & -\sin k\phi & \cos k\phi \end{bmatrix} \in \mathbb{R}^{2n\times 2n},$$

$k = 1, \ldots, p.$

From this symmetry, if $\boldsymbol{x}$ is a solution of $\boldsymbol{f}(\boldsymbol{x}) = \boldsymbol{0}$, then $\boldsymbol{\theta}_{\text{arbitrary}}(\phi)\boldsymbol{x}$ is also a solution for all ϕ. Here we denote the symmetry based on the ϕ/ω time shift by $\Gamma_{\text{arbitrary}}$.

Thus, the symmetric solutions with respect to Γ_ϕ satisfy the constraint

$$\boldsymbol{x} = \boldsymbol{\theta}_{\text{arbitrary}}(\phi)\boldsymbol{x} \quad \text{for all} \quad \phi \in \mathbb{R}. \tag{3.21}$$

3.4 Ideal Decomposition of HB Equation

The HB equation has the symmetry derived by the symmetry of the original system such as described in the previous section. Thus, the decomposition of bifurcation diagrams based on the symmetry of the HB equation corresponds to the mode decomposition of the system. In this section, we consider the ideal decompositions based on the symmetries Γ_{odd}, $\Gamma_{2\pi/m}$, and $\Gamma_{\text{arbitrary}}$ of the HB equation.

3.4.1 Decomposition by Ideal Quotient

In the previous section, we derived the constraints (3.8) and (3.15) with respect to the symmetries Γ_{odd}, $\Gamma_{2\pi/m}$, and $\Gamma_{\text{arbitrary}}$ respectively. In order to obtain the ideal quotient using the constraints, let us consider the linear representations $\boldsymbol{\theta}_{\text{odd}}$, $\boldsymbol{\theta}_{2\pi/m}$, and $\boldsymbol{\theta}_{\text{arbitrary}}$ in detail.

In the case of Γ_{odd}, because the matrix $\boldsymbol{\theta}_{\text{odd}}$ is diagonal, the symmetric solutions can be obtained by the set of equations

$$(1+1)x_{\text{r}0i} = 0,$$

$$\left(\begin{bmatrix} 1 & 0 \\ 0 & 1 \end{bmatrix} - \begin{bmatrix} (-1)^{k+1} & 0 \\ 0 & (-1)^{k+1} \end{bmatrix}\right)\begin{bmatrix} x_{\mathrm{r}ki} \\ x_{\mathrm{s}ki} \end{bmatrix} = \begin{bmatrix} 0 \\ 0 \end{bmatrix}, \quad \begin{matrix} k = 1, \ldots, p, \\ i = 1, \ldots, n. \end{matrix} \tag{3.22}$$

The solution $x_{\mathrm{r}ki} = x_{\mathrm{s}ki} = 0$ is obtained when k are odd numbers. That is, the symmetric solutions satisfy

$$\boldsymbol{x}_k = \mathbf{0} \ \text{ for } k = 0 \bmod 2. \tag{3.23}$$

In the case of $\Gamma_{2\pi/m}$, because the matrix $\boldsymbol{\theta}_{2\pi/m}$ is block diagonal, the symmetric solutions satisfies the set of equations

$$\begin{aligned} (1-1)x_{\mathrm{r}0i} &= 0, \\ \left(\begin{bmatrix} 1 & 0 \\ 0 & 1 \end{bmatrix} - \begin{bmatrix} \cos\frac{2\pi k}{m} & \sin\frac{2\pi k}{m} \\ -\sin\frac{2\pi k}{m} & \cos\frac{2\pi k}{m} \end{bmatrix}\right)\begin{bmatrix} x_{\mathrm{r}ki} \\ x_{\mathrm{s}ki} \end{bmatrix} &= \begin{bmatrix} 0 \\ 0 \end{bmatrix}, \quad \begin{matrix} k = 1, \ldots, p, \\ i = 1, \ldots, n. \end{matrix} \end{aligned} \tag{3.24}$$

Specifically, the solution $x_{\mathrm{r}ki} = x_{\mathrm{s}ki} = 0$ is obtained when $\frac{2\pi k}{m} \neq 2\pi, 4\pi, \ldots$. That is, the symmetric solutions satisfy

$$\boldsymbol{x}_k = \mathbf{0} \ \text{ for } k \neq 0 \bmod m. \tag{3.25}$$

In the case of $\Gamma_{\mathrm{arbitrary}}$, because the matrix $\boldsymbol{\theta}_{\mathrm{arbitrary}}$ is block diagonal, the symmetric solutions satisfies the set of equations

$$\begin{aligned} (1-1)x_{\mathrm{r}0i} &= 0, \\ \left(\begin{bmatrix} 1 & 0 \\ 0 & 1 \end{bmatrix} - \begin{bmatrix} \cos k\phi & \sin k\phi \\ -\sin k\phi & \cos k\phi \end{bmatrix}\right)\begin{bmatrix} x_{\mathrm{r}ki} \\ x_{\mathrm{s}ki} \end{bmatrix} &= \begin{bmatrix} 0 \\ 0 \end{bmatrix}, \quad \begin{matrix} k = 1, \ldots, p, \\ i = 1, \ldots, n. \end{matrix} \end{aligned} \tag{3.26}$$

Specifically, the solution $x_{\mathrm{r}ki} = x_{\mathrm{s}ki} = 0$ is obtained when $k\phi \neq 2\pi, 4\pi, \ldots$. That is, the symmetric solutions satisfy

$$\boldsymbol{x}_k = \mathbf{0} \ \text{ for } k \neq 0. \tag{3.27}$$

Because the symmetric solutions with respect to the infinite group $\Gamma_{\mathrm{arbitrary}}$ have no oscillations due to Eq.(3.27), we can not decompose the bifurcation diagram of the autonomous system using the symmetry $\Gamma_{\mathrm{arbitrary}}$. Note that the symmetry with respect to $\Gamma_{\mathrm{arbitrary}}$ leads to invariants in Chapter 4.

Let us consider only the periodically forced system in this chapter. When the periodically forced system has the symmetries Γ_{odd} and $\Gamma_{2\pi/m}$ the ideal $\langle \boldsymbol{f}_\Gamma \rangle$ in Eq.(2.26) which corresponds to the symmetric solutions is represented by

$$\langle \boldsymbol{f}_\Gamma(\boldsymbol{x}) \rangle = \langle \boldsymbol{f}(\boldsymbol{x}) \rangle + \sum_{k \in \kappa} \langle \boldsymbol{x}_k \rangle, \tag{3.28}$$

where κ is defined by

$$\begin{aligned} \kappa &\in \{\kappa_{\text{odd}}, \kappa_{2\pi/m}\}, \\ \kappa_{\text{odd}} &\equiv \{k \in \mathbb{Z}_{\geq 0} \mid 0 \leq k \leq p,\ k = 0 \bmod 2\} \qquad (\text{Symmetry } \Gamma_{\text{odd}}) \\ \kappa_{2\pi/m} &\equiv \{k \in \mathbb{Z}_{\geq 0} \mid 0 \leq k \leq p,\ k \neq 0 \bmod m\} \qquad (\text{Symmetry } \Gamma_{2\pi/m}) \end{aligned} . \tag{3.29}$$

Thus, if solutions of the HB equation are symmetric solutions, the oscillations do not have frequency components in the κ. The number m is not included in the set κ_{odd} because the m is odd number when the system has the symmetry Γ_{odd}. As a result, the number m does not belong to the set κ. Namely, the forcing term $\boldsymbol{e}_k$ in $\boldsymbol{f}(\boldsymbol{x})$ equals $\mathbf{0}$ for $k \in \kappa$ due to Eq.(2.9). This property is used in the systematic procedure for decomposition on Section 3.6.

Using this ideal $\langle \boldsymbol{f}_\Gamma \rangle$, we can calculate the ideal $\langle \overline{\boldsymbol{f}_\Gamma} \rangle$ in Eq.(2.27) which corresponds to the asymmetric solutions by

$$\langle \overline{\boldsymbol{f}_\Gamma}(\boldsymbol{x}) \rangle = \langle \boldsymbol{f}(\boldsymbol{x}) \rangle : \left(\langle \boldsymbol{f}(\boldsymbol{x}) \rangle + \sum_{k \in \kappa} \langle \boldsymbol{x}_k \rangle \right). \tag{3.30}$$

Because the multiplicity of the bifurcation diagram of the HB equation $\boldsymbol{f}(\boldsymbol{x}) = \mathbf{0}$ is one, the ideal $\langle \boldsymbol{f}(\boldsymbol{x}) \rangle$ is a radical ideal. Thus, the ideal decomposition (2.28) is obtained by

$$\begin{aligned} \langle \boldsymbol{f}(\boldsymbol{x}) \rangle &= \langle \boldsymbol{f}_\Gamma(\boldsymbol{x}) \rangle \cap \langle \overline{\boldsymbol{f}_\Gamma}(\boldsymbol{x}) \rangle \\ &= \left\{ \langle \boldsymbol{f}(\boldsymbol{x}) \rangle + \sum_{k \in \kappa} \langle \boldsymbol{x}_k \rangle \right\} \cap \left\{ \langle \boldsymbol{f}(\boldsymbol{x}) \rangle : \left(\langle \boldsymbol{f}(\boldsymbol{x}) \rangle + \sum_{k \in \kappa} \langle \boldsymbol{x}_k \rangle \right) \right\}. \end{aligned} \tag{3.31}$$

However, the computation of this ideal decomposition still requires more than 15 GiB of memory.

3.4.2 Efficient Methods for Ideal Quotient

Using two propositions of the quotient operation shown in Appendix A.5, we propose an efficient method to calculate the ideal quotient (3.31). First, if we assume that an ideal J is represented by $J = \sum_{i=1}^{s} J_i$, the ideal quotient $I : J$ is provided by

$$I : J = I : \left(\sum_{i=1}^{s} J_i \right) = \bigcap_{i=1}^{s} (I : J_i). \tag{3.32}$$

Using this relation (3.32) and $\langle \boldsymbol{f}(\boldsymbol{x}) \rangle : \langle \boldsymbol{f}(\boldsymbol{x}) \rangle = \langle 1 \rangle$, we can represent Eq.(3.30) by

$$\langle \overline{\boldsymbol{f}_\Gamma}(\boldsymbol{x}) \rangle = \langle \boldsymbol{f}(\boldsymbol{x}) \rangle : \sum_{k \in \kappa} \langle \boldsymbol{x}_k \rangle. \tag{3.33}$$

Secondary, when the ideal I is represented by $I = \sum_{i=1}^{r} I_i$ and J is coprime to I_i for $i = 1, \ldots, r$, the ideal quotient $I : J$ is represented by

$$I : J = \left(\sum_{i=1}^{r} I_i \right) : J = \sum_{i=1}^{r} (I_i : J) . \tag{3.34}$$

This relation indicates that the computation of the ideal quotient $I : J$ is equivalent to the sum of the partial ideal quotients $I_i : J$.

We can apply Eq.(3.34) to Eq.(3.33) because the ideals which correspond to symmetric and asymmetric solutions are obviously coprime. Thus, we obtain the ideal $\langle \overline{\boldsymbol{f}_\Gamma}(\boldsymbol{x}) \rangle$ by

$$\langle \overline{\boldsymbol{f}_\Gamma}(\boldsymbol{x}) \rangle = \left(\sum_{k \in \kappa} \langle \boldsymbol{f}_k(\boldsymbol{x}) \rangle : \sum_{k \in \kappa} \langle \boldsymbol{x}_k \rangle \right) + \left(\sum_{k \notin \kappa} \langle \boldsymbol{f}_k(\boldsymbol{x}) \rangle : \sum_{k \in \kappa} \langle \boldsymbol{x}_k \rangle \right), \tag{3.35}$$

where we use the relation $\langle \boldsymbol{f}(\boldsymbol{x}) \rangle = \sum_{k \in \kappa} \langle \boldsymbol{f}_k \rangle + \sum_{k \notin \kappa} \langle \boldsymbol{f}_k \rangle$. Namely, the ideal quotient is divided into the ideals generated by the polynomials corresponding symmetric solutions and asymmetric solutions.

By the relation $\sum_{k \notin \kappa} \langle \boldsymbol{f}_k \rangle \not\subset \sum_{k \in \kappa} \langle \boldsymbol{x}_k \rangle$ shown in Appendix B, the ideal $\langle \overline{\boldsymbol{f}_\Gamma}(\boldsymbol{x}) \rangle$ in Eq.(3.35) is represented by

$$\langle \overline{\boldsymbol{f}_\Gamma}(\boldsymbol{x}) \rangle = \left(\sum_{k \in \kappa} \langle \boldsymbol{f}_k(\boldsymbol{x}) \rangle : \sum_{k \in \kappa} \langle \boldsymbol{x}_k \rangle \right) + \sum_{k \notin \kappa} \langle \boldsymbol{f}_k(\boldsymbol{x}) \rangle. \tag{3.36}$$

Namely, it is calculated only by the ideal quotient corresponding to frequency components in κ

$$\sum_{k \in \kappa} \langle \boldsymbol{f}_k(\boldsymbol{x}) \rangle : \sum_{k \in \kappa} \langle \boldsymbol{x}_k \rangle. \tag{3.37}$$

We call the ideal quotient (3.37) as the partial ideal quotient. Thus, the partial ideal quotient (3.37) enables to calculate the ideal quotient (3.30) using only the components in κ. Moreover, using the relation $\sum_{k \in \kappa} \langle \boldsymbol{f}_k \rangle \subset \sum_{k \in \kappa} \langle \boldsymbol{x}_k \rangle$ shown in Appendix B, we rewrite the ideal $\langle \boldsymbol{f}_\Gamma(\boldsymbol{x}) \rangle$ in Eq.(3.28) to

$$\langle \boldsymbol{f}_\Gamma(\boldsymbol{x}) \rangle = \sum_{k \notin \kappa} \langle \boldsymbol{f}_k(\boldsymbol{x}) \rangle + \sum_{k \in \kappa} \langle \boldsymbol{x}_k \rangle. \tag{3.38}$$

Thus, we can obtain the decomposition of the ideal $\langle \boldsymbol{f}(\boldsymbol{x}) \rangle = \langle \boldsymbol{f}_\Gamma(\boldsymbol{x}) \rangle \cap \langle \overline{\boldsymbol{f}_\Gamma}(\boldsymbol{x}) \rangle$ by Eqs.(3.38) and (3.36).

The algorithm to decompose the bifurcation diagram using the partial ideal quotient is described as follows;

S1. We obtain the HB equation $\boldsymbol{f}(\boldsymbol{x}) = \boldsymbol{0}$ from the system equation (2.1).

S2. The κ in Eq.(3.29) is determined by a symmetry Γ of $\boldsymbol{f}(\boldsymbol{x})$.

S3. Using the partial ideal quotient (3.37), we can obtain the $\langle \overline{\boldsymbol{f}_\Gamma}(\boldsymbol{x})\rangle$ corresponding to asymmetric solutions. Further, Eq.(3.38) gives $\langle \boldsymbol{f}_\Gamma(\boldsymbol{x})\rangle$ corresponding to the symmetric solutions.

3.4.3 Partial Ideal Decomposition

Because the term $\sum_{k\notin\kappa}\langle \boldsymbol{f}_k(\boldsymbol{x})\rangle$ in Eqs.(3.36) and (3.38) can be collected, the ideal decomposition (3.31) is rewritten by

$$\begin{aligned}\langle \boldsymbol{f}(\boldsymbol{x})\rangle &= \langle \boldsymbol{f}_\Gamma(\boldsymbol{x})\rangle \cap \langle \overline{\boldsymbol{f}_\Gamma}(\boldsymbol{x})\rangle \\ &= \left(\sum_{k\in\kappa}\langle \boldsymbol{x}_k\rangle\right) \cap \left(\sum_{k\in\kappa}\langle \boldsymbol{f}_k(\boldsymbol{x})\rangle : \sum_{k\in\kappa}\langle \boldsymbol{x}_k\rangle\right) + \sum_{k\notin\kappa}\langle \boldsymbol{f}_k(\boldsymbol{x})\rangle. \end{aligned} \tag{3.39}$$

Now, we look at the following decomposition in Eq.(3.39)

$$\sum_{k\in\kappa}\langle \boldsymbol{f}_k(\boldsymbol{x})\rangle = \left(\sum_{k\in\kappa}\langle \boldsymbol{x}_k\rangle\right) \cap \left(\sum_{k\in\kappa}\langle \boldsymbol{f}_k(\boldsymbol{x})\rangle : \sum_{k\in\kappa}\langle \boldsymbol{x}_k\rangle\right). \tag{3.40}$$

We call the decomposition a partial ideal decomposition. The decomposition of the ideal $\langle \boldsymbol{f}(\boldsymbol{x})\rangle$ is caused only by this partial ideal decomposition. Because the number m does not belong to the set κ, this partial ideal decomposition does not depend on values of the forcing functions. The ideal decomposition (3.39) is realized by adding the partial ideal decomposition to the ideals $\langle \boldsymbol{f}_k\rangle$ containing the forcing term for $k \notin \kappa$.

Later we will use this partial ideal decomposition for the systematic procedure to decompose the bifurcation diagram.

3.5 Example

We apply the proposed method to the example in Section 2.4. Namely, we consider the fundamental oscillations ($m = 1$), and apply the HB method with 3 frequency components ($p = 3$) to the system shown in Figure 2.1. Now, we use the computer algebra system Risa/Asir in order to obtain the algebraic representation of the bifurcation diagram. In this example, we cannot calculate the decomposition of the bifurcation diagram by using the method in [35, 36] because the computation of Gröbner base of the lexicographic order requires more than 15 GiB of memory.

Let us consider the symmetry of the HB equation $\boldsymbol{f}(\boldsymbol{x}) = \boldsymbol{0}$. The system has only the symmetry $\Gamma_{\rm odd}$ on the target oscillations, and the linear representation $\boldsymbol{\theta}_{\rm odd}$ is written by

$$\boldsymbol{\theta}_{\rm odd} = \begin{bmatrix} \boldsymbol{I}_4 & & 0 \\ & -\boldsymbol{I}_4 & \\ 0 & & \boldsymbol{I}_4 \end{bmatrix}. \tag{3.41}$$

Because the symmetric solutions satisfy $\boldsymbol{x} = \boldsymbol{\theta}_{\rm odd}\boldsymbol{x}$, i.e., $\boldsymbol{x}_2 = \boldsymbol{0}$, the representation $\boldsymbol{\theta}_{\rm odd}$ gives the $\kappa_{\rm odd} = \{2\}$ in Eq.(3.29). Thus, using the symmetry with respect to $\Gamma_{\rm odd}$, we can decompose the ideal $I \equiv \langle \boldsymbol{f}(\boldsymbol{x})\rangle$ generated by the HB equation $\boldsymbol{f}(\boldsymbol{x}) = \boldsymbol{0}$ as follows;

$$I = I_{13} \cap I_{123} = \langle \boldsymbol{f}_{\Gamma_{\rm odd}}(\boldsymbol{x})\rangle \cap \langle \overline{\boldsymbol{f}_{\Gamma_{\rm odd}}}(\boldsymbol{x})\rangle, \tag{3.42}$$

where $I_{13} = \langle \boldsymbol{f}_{\Gamma_{\rm odd}}\rangle$ corresponds to the solutions which contain only the fundamental and the 3rd harmonic oscillations, i.e., the symmetric solutions with respect to $\Gamma_{\rm odd}$, and $I_{123} = \langle \overline{\boldsymbol{f}_{\Gamma_{\rm odd}}}\rangle$ corresponds to the solutions which contain the 2nd harmonic oscillations, that is, the asymmetric solutions with respect to $\Gamma_{\rm odd}$.

Using the partial ideal quotient (3.37), we can obtain the ideal I_{123};

$$I_{123} = \langle \overline{\boldsymbol{f}_{\Gamma_{\rm odd}}}\rangle = \langle \boldsymbol{f}_2\rangle : \langle \boldsymbol{x}_2\rangle + \langle \boldsymbol{f}_1, \boldsymbol{f}_3\rangle. \tag{3.43}$$

Its computational time is 1.112 sec and the required memory is 9.16MB. Thus, the partial ideal quotient reduces the computational cost of dramatically. By Eq.(3.38), the ideal I_{13} for the symmetric solutions is obtained by

$$I_{13} = \langle \boldsymbol{f}_{\Gamma_{\rm odd}}\rangle = \langle \boldsymbol{x}_2\rangle + \langle \boldsymbol{f}_1, \boldsymbol{f}_3\rangle. \tag{3.44}$$

Thus, we can decompose the bifurcation diagram as $\boldsymbol{V}(I) = \boldsymbol{V}(I_{13}) \cup \boldsymbol{V}(I_{123})$ based on the ideal decomposition (3.42).

In order to obtain the algebraic representation of the bifurcation diagram, we use Gröbner base of the block order which eliminates target variables efficiently (cf. Appendix.C). Namely, using Gröbner base of the block order $(x_{\rm s11}, x_{\rm r12}, \ldots, x_{\rm s32}) \succ_{\rm block} x_{\rm r11}$, we eliminate $x_{\rm s11}, x_{\rm r12}, \ldots, x_{\rm s32}$, and show the bifurcation diagram (E - $x_{\rm r11}$) which represents the relation between the parameter E and the real part of the fundamental oscillation $x_{\rm r11}$ in Figure 3.1 where $\omega = 1$ and $\mu = 0.01$. The blue line corresponds to the ideal I_{123} and the red line corresponds to the ideal I_{13}. We confirm that the pitchfork bifurcation points correspond to the intersection points of the sub-diagrams $\boldsymbol{V}(I_{13})$ and $\boldsymbol{V}(I_{123})$ such as Figure 3.1.

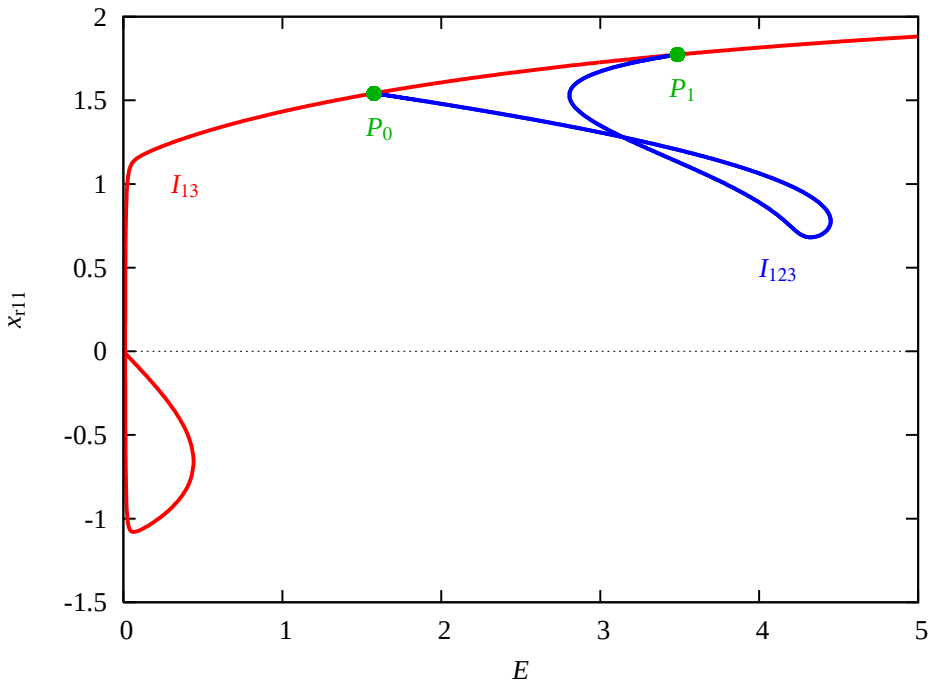

Figure 3.1: Bifurcation diagram (E - x_{r11}) in the case of $m = 1$ (The ideal I_{13} corresponds to the solutions which contain only fundamental and 3rd harmonic oscillations, the ideal I_{123} corresponds to the solutions which contain 2nd harmonic oscillations with $\omega = 1$ and $\mu = 0.01$).

3.6 Systematic Procedure for Decomposition Using Homogeneous HB Equation

Although the proposed method enables to decompose the bifurcation diagram of the HB equation, we have to obtain the symmetry of the HB equation in advance. In order to find out the symmetry without omission, we consider a homogeneous HB equation which is obtained by removing the forcing term from a nonhomogeneous HB equation because the equation has the highest symmetry. Using the symmetry of the homogeneous HB equation, we propose a systematic procedure for the decomposition of corresponding nonhomogeneous HB equations. The symmetry of the nonhomogeneous HB equation are generated by the break of the symmetry of the homogeneous HB equation. Thus, the partial ideal decomposition (3.40) of the homogeneous HB equation enables the systematic procedure to decompose the bifurcation diagrams of the nonhomogeneous HB equation.

3.6.1 Homogeneous HB Equation

Let us consider the following homogeneous HB equation $\hat{\boldsymbol{f}}(\boldsymbol{x}) = \boldsymbol{0}$ is defined by

$$
\begin{aligned}
\hat{\boldsymbol{f}}(\boldsymbol{x}) &\equiv \hat{\boldsymbol{f}}(\boldsymbol{x};\omega,\boldsymbol{\lambda}) \equiv \begin{bmatrix} \hat{\boldsymbol{f}}_0 \\ \vdots \\ \hat{\boldsymbol{f}}_p \end{bmatrix} = \boldsymbol{0} \in \mathbb{R}^N, \qquad (3.45)\\
\hat{\boldsymbol{f}}_0 &\equiv (f_{\mathrm{r}01},\ldots,f_{\mathrm{r}0n})^{\mathrm{T}} \\
&\equiv (\Re[Y_{01}],\ldots,\Re[Y_{0n}])^{\mathrm{T}} \in \mathbb{R}^n, \\
\hat{\boldsymbol{f}}_k &\equiv (f_{\mathrm{r}k1},f_{\mathrm{s}k1},\ldots,f_{\mathrm{r}kn},f_{\mathrm{s}kn})^{\mathrm{T}} \\
&\equiv (\Re[-\mathrm{j}k\omega X_{k1}+Y_{k1}],\Im[-\mathrm{j}k\omega X_{k1}+Y_{k1}], \\
&\qquad \ldots,\Re[-\mathrm{j}k\omega X_{kn}+Y_{kn}],\Im[-\mathrm{j}k\omega X_{kn}+Y_{kn}])^{\mathrm{T}} \in \mathbb{R}^{2n}, \\
k &= 1,\ldots,p.
\end{aligned}
$$

Because the HB equation (2.10) can be written by $\boldsymbol{f}(\boldsymbol{x};\omega,\boldsymbol{\lambda},\boldsymbol{e}) = \hat{\boldsymbol{f}}(\boldsymbol{x};\omega,\boldsymbol{\lambda}) + \boldsymbol{e} = \boldsymbol{0}$, we can describe the HB equation as

$$
\begin{cases} \boldsymbol{f}_m(\boldsymbol{x}) = \hat{\boldsymbol{f}}_m(\boldsymbol{x}) + \boldsymbol{e}_m \\ \boldsymbol{f}_k(\boldsymbol{x}) = \hat{\boldsymbol{f}}_k(\boldsymbol{x}) \qquad \text{for } k \neq m \end{cases}, \qquad (3.46)
$$

from Eq.(2.9).

3.6.2 Symmetry of Homogeneous HB Equation

In order to decompose the bifurcation diagram systematically, let us consider the symmetry of the homogeneous HB equation $\hat{\boldsymbol{f}}(\boldsymbol{x}) = \boldsymbol{0}$. Because the homogeneous HB equation $\hat{\boldsymbol{f}}(\boldsymbol{x}; \omega, \boldsymbol{\lambda}) = \boldsymbol{0}$ equals the HB equation $\boldsymbol{f}(\boldsymbol{x}; \omega, \boldsymbol{\lambda}, \boldsymbol{0}) = \boldsymbol{0}$ for the autonomous system, the equation $\hat{\boldsymbol{f}}(\boldsymbol{x}; \omega, \boldsymbol{\lambda}) = \boldsymbol{0}$ has the arbitrary time ϕ/ω shift symmetry;

$$\hat{\boldsymbol{f}}(\boldsymbol{\theta}_{\text{arbitrary}}(\phi)\boldsymbol{x}) \quad = \quad \boldsymbol{\theta}_{\text{arbitrary}}(\phi)\hat{\boldsymbol{f}}(\boldsymbol{x}) \ \text{ for all } \phi. \tag{3.47}$$

Thus, the symmetric solutions corresponding to $\Gamma_{\text{arbitrary}}$ satisfy the constraint

$$\boldsymbol{x} = \boldsymbol{\theta}_{\text{arbitrary}}(\phi)\boldsymbol{x}. \tag{3.48}$$

The homogeneous HB equation has infinite asymmetric solutions with respect to $\Gamma_{\text{arbitrary}}$ since ϕ is arbitrary.

Now, our target is a set of the nonhomogeneous HB equations which correspond to an identical homogeneous HB equation $\hat{\boldsymbol{f}}(\boldsymbol{x}) = \boldsymbol{0}$ when we fix the number p of the specific frequency components. Because the nonhomogeneous HB equations with the forcing functions of the period $2\pi/\omega_s = 2\pi/m\omega$ have the symmetry $\Gamma_{2\pi/m}$, which corresponds to $\phi = 2\pi/m$ in the symmetry $\Gamma_{\text{arbitrary}}$, we can obtain the symmetry of the nonhomogeneous HB equation from the symmetry of the homogeneous HB equation when we set m. That is, we can say that the homogeneous HB equation has the highest symmetry in the corresponding nonhomogeneous HB equations for $m \leq p$ when we fix p. In order to decompose the bifurcation diagrams of the nonhomogeneous HB equations based on the symmetry, it is enough to consider only the cases of $\phi = 2\pi/i,\ i = 1, \ldots, p$. Namely, we consider $\boldsymbol{\theta}_{2\pi/1}, \ldots, \boldsymbol{\theta}_{2\pi/p}$ corresponding to the symmetries $\Gamma_{2\pi/1}, \ldots, \Gamma_{2\pi/p}$

$$\boldsymbol{\theta}_{2\pi/q} \quad = \quad \begin{bmatrix} \boldsymbol{I}_n & & & \boldsymbol{0} \\ & \boldsymbol{\theta}_{2\pi/q,1} & & \\ & & \ddots & \\ \boldsymbol{0} & & & \boldsymbol{\theta}_{2\pi/q,p} \end{bmatrix} \in \mathbb{R}^{N\times N}, \tag{3.49}$$

$$\boldsymbol{\theta}_{2\pi/q,k} = \begin{bmatrix} \cos\frac{2\pi k}{q} & \sin\frac{2\pi k}{q} & & & \boldsymbol{0} \\ -\sin\frac{2\pi k}{q} & \cos\frac{2\pi k}{q} & & & \\ & & \ddots & & \\ & & & \cos\frac{2\pi k}{q} & \sin\frac{2\pi k}{q} \\ \boldsymbol{0} & & & -\sin\frac{2\pi k}{q} & \cos\frac{2\pi k}{q} \end{bmatrix} \in \mathbb{R}^{2n\times 2n},$$

$$k = 1, \ldots, p, \quad q = 1, \ldots, p.$$

Further, the homogeneous HB equation has the odd symmetry $\Gamma_{\rm odd}$.

The symmetry of the nonhomogeneous HB equation is generated by a part of the symmetry of the homogeneous HB equation when we set m. Namely, the forcing function breaks the symmetry of the homogeneous HB equation.

3.6.3 Ideal Decomposition of Nonhomogeneous HB Equation

In order to realize the systematic procedure for the decomposition of the nonhomogeneous HB equation, we propose a method based on the break of the symmetry of the homogeneous HB equation. We consider the following set of the partial ideal decompositions of the homogeneous HB equation.

$$\sum_{k\in\hat{\kappa}} \langle \hat{\boldsymbol{f}}_k(\boldsymbol{x})\rangle = \left(\sum_{k\in\hat{\kappa}} \langle \boldsymbol{x}_k\rangle\right) \cap \left(\sum_{k\in\hat{\kappa}} \langle \hat{\boldsymbol{f}}_k(\boldsymbol{x})\rangle : \sum_{k\in\hat{\kappa}} \langle \boldsymbol{x}_k\rangle\right), \tag{3.50}$$

where

$$\begin{aligned} \hat{\kappa} &\in \left\{\kappa_{2\pi/q}, \kappa_{\rm odd}\right\}, \\ \kappa_{2\pi/q} &\equiv \{k \in \mathbb{Z}_{\geq 0} \mid 0 \leq k \leq p,\ k \neq 0 \bmod q\} \qquad (\text{Symmetry } \Gamma_{2\pi/q}) \\ \kappa_{\rm odd} &\equiv \{k \in \mathbb{Z}_{\geq 0} \mid 0 \leq k \leq p,\ k = 0 \bmod 2\} \qquad (\text{Symmetry } \Gamma_{\rm odd}) \\ & q = 1, \ldots, p, \end{aligned} \tag{3.51}$$

which corresponds to the partial ideal decomposition (3.40) of the nonhomogeneous HB equation. Let us compare Eq.(3.50) with Eq.(3.40). Because the difference between $\hat{\boldsymbol{f}}(\boldsymbol{x})$ and $\boldsymbol{f}(\boldsymbol{x})$ is only $\boldsymbol{f}_m \neq \hat{\boldsymbol{f}}_m$ due to Eq.(3.46), the set κ is a subset of $\hat{\kappa}$ which does not contain m. Namely, the addition of the forcing term breaks the symmetry of the homogeneous HB equation. Then, the partial ideal decomposition (3.40) is expressed as a subset of the decompositions which are not broken in the partial ideal decompositions (3.50).

Since the ideal decomposition of the nonhomogeneous HB equation is obtained by the partial ideal decomposition (3.40) and the ideal containing the forcing term, we can use the subset of the partial ideal decompositions (3.50) for the decomposition as follows;

$$\begin{aligned} \langle \boldsymbol{f}(\boldsymbol{x})\rangle &= \langle \boldsymbol{f}_\Gamma(\boldsymbol{x})\rangle \cap \langle \overline{\boldsymbol{f}_\Gamma}(\boldsymbol{x})\rangle \\ &= \left(\sum_{k\in\kappa} \langle \boldsymbol{x}_k\rangle\right) \cap \left(\sum_{k\in\kappa} \langle \hat{\boldsymbol{f}}_k(\boldsymbol{x})\rangle : \sum_{k\in\kappa} \langle \boldsymbol{x}_k\rangle\right) + \sum_{k\notin\kappa} \langle \hat{\boldsymbol{f}}_k(\boldsymbol{x}) + \boldsymbol{e}_k\rangle, \\ \kappa &\in \left\{\kappa_{2\pi/q}, \kappa_{\rm odd} \mid\ m \notin \kappa_{2\pi/q},\ m \notin \kappa_{\rm odd},\ q = 1, \ldots, p\right\}, \end{aligned} \tag{3.52}$$

The algorithm for the systematic procedure to decompose the bifurcation diagram using the set of the partial ideal decomposition is written as follows;

S1. We set the homogeneous HB equation $\hat{\boldsymbol{f}}(\boldsymbol{x}) = \boldsymbol{0}$.

S2. We consider the symmetries $\Gamma_{2\pi/1}, \ldots, \Gamma_{2\pi/p}$ and Γ_{odd}, and obtain the set $\hat{\kappa}$ which provides the partial ideal decompositions (3.50).

S3. We set the nonhomogeneous HB equation $\boldsymbol{f}(\boldsymbol{x}) = \hat{\boldsymbol{f}}(\boldsymbol{x}) + \boldsymbol{e} = \boldsymbol{0}$. And we obtain a set κ by selecting the subset of $\hat{\kappa}$ which does not contain m.

S4. Using the set κ and Eq.(3.52), we obtain the decomposition of the ideal $\langle \boldsymbol{f}(\boldsymbol{x}) \rangle$.

S5. We can simultaneously obtain decompositions of other nonhomogeneous HB equations which correspond to the identical homogeneous HB equation.

Thus, the set of the partial ideal decompositions of the homogeneous HB equation enables to decompose the bifurcation diagram of the corresponding nonhomogeneous HB equations systematically.

3.6.4 Example

We consider the homogeneous HB equation with 3 frequency components ($p = 3$) on the RLC circuit shown in Figure 2.1. We assume that the direct current components are equal to zero, similar to Section 2.4. In this case, the symmetries $\Gamma_{2\pi/1}, \Gamma_{2\pi/2}, \Gamma_{2\pi/3}$ and Γ_{odd} of the homogeneous HB equation can be written by

$$\boldsymbol{\theta}_{2\pi/1} = \boldsymbol{I}_{12}, \tag{3.53}$$

$$\boldsymbol{\theta}_{2\pi/2} = \begin{bmatrix} -\boldsymbol{I}_4 & & 0 \\ & \boldsymbol{I}_4 & \\ 0 & & -\boldsymbol{I}_4 \end{bmatrix}, \tag{3.54}$$

$$\boldsymbol{\theta}_{2\pi/3} = \begin{bmatrix} \boldsymbol{\theta}_{2\pi/3,1} & & 0 \\ & \boldsymbol{\theta}_{2\pi/3,2} & \\ 0 & & \boldsymbol{I}_4 \end{bmatrix}, \tag{3.55}$$

$$\boldsymbol{\theta}_{2\pi/3,1} = \begin{bmatrix} \frac{1}{2} & \frac{\sqrt{3}}{2} & & 0 \\ -\frac{\sqrt{3}}{2} & \frac{1}{2} & & \\ & & \frac{1}{2} & \frac{\sqrt{3}}{2} \\ 0 & & -\frac{\sqrt{3}}{2} & \frac{1}{2} \end{bmatrix}, \quad \boldsymbol{\theta}_{2\pi/3,2} = \begin{bmatrix} \frac{1}{2} & -\frac{\sqrt{3}}{2} & & 0 \\ \frac{\sqrt{3}}{2} & \frac{1}{2} & & \\ & & \frac{1}{2} & -\frac{\sqrt{3}}{2} \\ 0 & & \frac{\sqrt{3}}{2} & \frac{1}{2} \end{bmatrix},$$

$$\boldsymbol{\theta}_{\text{odd}} = \begin{bmatrix} \boldsymbol{I}_4 & & 0 \\ & -\boldsymbol{I}_4 & \\ 0 & & \boldsymbol{I}_4 \end{bmatrix}. \tag{3.56}$$

All the solutions of the nonhomogeneous HB equation have symmetry $\Gamma_{2\pi/1}$ because the $\boldsymbol{\theta}_{2\pi/1}$ is an identity matrix. Thus, we cannot decompose the ideal using the symmetry $\Gamma_{2\pi/1}$. By the partial ideal quotient based on the other symmetries $\Gamma_{2\pi/2}$, $\Gamma_{2\pi/3}$, and Γ_{odd}, the partial ideal decompositions (3.50) are represented by

$$\begin{array}{lll} \Gamma_{2\pi/2}; & \kappa_{2\pi/2} = \{1,3\}, & \langle \hat{\boldsymbol{f}}_1, \hat{\boldsymbol{f}}_3 \rangle = \langle \boldsymbol{x}_1, \boldsymbol{x}_3 \rangle \cap (\langle \hat{\boldsymbol{f}}_1, \hat{\boldsymbol{f}}_3 \rangle : \langle \boldsymbol{x}_1, \boldsymbol{x}_3 \rangle), \\ \Gamma_{2\pi/3}; & \kappa_{2\pi/3} = \{1,2\}, & \langle \hat{\boldsymbol{f}}_1, \hat{\boldsymbol{f}}_2 \rangle = \langle \boldsymbol{x}_1, \boldsymbol{x}_2 \rangle \cap (\langle \hat{\boldsymbol{f}}_1, \hat{\boldsymbol{f}}_2 \rangle : \langle \boldsymbol{x}_1, \boldsymbol{x}_2 \rangle), \\ \Gamma_{\text{odd}}; & \kappa_{\text{odd}} = \{2\}, & \langle \hat{\boldsymbol{f}}_2 \rangle = \langle \boldsymbol{x}_2 \rangle \cap (\langle \hat{\boldsymbol{f}}_2 \rangle : \langle \boldsymbol{x}_2 \rangle). \end{array} \tag{3.57}$$

Using the relation (3.57), we can decompose the nonhomogeneous HB equations which are identical except for the forcing term systematically.

For example, we consider the nonhomogeneous HB equations with the forcing function of $m = 1, 2$ and 3 in Eq.(2.11). The HB equations of $m = 1,\ 2$ and 3 correspond to fundamental oscillation, 1/2-subharmonic oscillation and 1/3-subharmonic oscillation, respectively. The each nonhomogeneous HB equation $\boldsymbol{f}(\boldsymbol{x}) = \boldsymbol{0}$ of $m = 1, 2$ and 3 is represented as

$$[m = 1] \qquad \boldsymbol{f}(\boldsymbol{x}) = \begin{bmatrix} \hat{\boldsymbol{f}}_1 + \boldsymbol{e}_1 \\ \hat{\boldsymbol{f}}_2 \\ \hat{\boldsymbol{f}}_3 \end{bmatrix} = \boldsymbol{0}, \tag{3.58}$$

$$[m = 2] \qquad \boldsymbol{f}(\boldsymbol{x}) = \begin{bmatrix} \hat{\boldsymbol{f}}_1 \\ \hat{\boldsymbol{f}}_2 + \boldsymbol{e}_2 \\ \hat{\boldsymbol{f}}_3 \end{bmatrix} = \boldsymbol{0}, \tag{3.59}$$

$$[m = 3] \qquad \boldsymbol{f}(\boldsymbol{x}) = \begin{bmatrix} \hat{\boldsymbol{f}}_1 \\ \hat{\boldsymbol{f}}_2 \\ \hat{\boldsymbol{f}}_3 + \boldsymbol{e}_3 \end{bmatrix} = \boldsymbol{0}. \tag{3.60}$$

The parameter E of frequency component m effects only the constant term of corresponding frequencies.

In the case of $m = 1$ which corresponds to the example in Section 3.5, the symmetries $\Gamma_{2\pi/2}$ and $\Gamma_{2\pi/3}$ are broken because $m = 1$ belongs to $\kappa_{2\pi/2}$ and $\kappa_{2\pi/3}$. As a result, the HB equation has only the symmetry Γ_{odd} and $\kappa = \kappa_{\text{odd}}$. Thus, the ideal decomposition of $I = \langle \boldsymbol{f}(\boldsymbol{x}) \rangle$ is obtained by

$$I = I_{13} \cap I_{123} = \langle \boldsymbol{f}_{\Gamma_{\text{odd}}} \rangle \cap \langle \overline{\boldsymbol{f}_{\Gamma_{\text{odd}}}} \rangle, \tag{3.61}$$

$$I_{13} = \langle \boldsymbol{f}_{\Gamma_{\text{odd}}} \rangle = \langle \boldsymbol{x}_2 \rangle + \langle \hat{\boldsymbol{f}}_1, \hat{\boldsymbol{f}}_3 + \boldsymbol{e}_3 \rangle, \tag{3.62}$$

$$I_{123} = \langle \overline{\boldsymbol{f}_{\Gamma_{\text{odd}}}} \rangle = \langle \hat{\boldsymbol{f}}_2 \rangle : \langle \boldsymbol{x}_2 \rangle + \langle \hat{\boldsymbol{f}}_1 + \boldsymbol{e}_1, \hat{\boldsymbol{f}}_3 \rangle. \tag{3.63}$$

This decomposition agrees with the decomposition in Section 3.5.

In the case of $m = 2$, the symmetries $\Gamma_{2\pi/3}$ and $\Gamma_{\rm odd}$ are broken because $m = 2$ belongs to $\kappa_{2\pi/3}$ and $\kappa_{\rm odd}$. As a result, the HB equation has only the symmetry $\Gamma_{2\pi/2}$ and $\kappa = \kappa_{2\pi/2}$. Thus, the ideal decomposition is obtained by

$$
\begin{aligned}
I &= I_2 \cap I_{123} = \langle \boldsymbol{f}_{\Gamma_{2\pi/2}} \rangle \cap \langle \overline{\boldsymbol{f}_{\Gamma_{2\pi/2}}} \rangle, && (3.64)\\
I_2 &= \langle \boldsymbol{f}_{\Gamma_{2\pi/2}} \rangle = \langle \boldsymbol{x}_1, \boldsymbol{x}_3 \rangle + \langle \hat{\boldsymbol{f}}_2 + \boldsymbol{e}_2 \rangle, && (3.65)\\
I_{123} &= \langle \overline{\boldsymbol{f}_{\Gamma_{2\pi/2}}} \rangle = \langle \hat{\boldsymbol{f}}_1, \hat{\boldsymbol{f}}_3 \rangle : \langle \boldsymbol{x}_1, \boldsymbol{x}_3 \rangle + \langle \hat{\boldsymbol{f}}_2 + \boldsymbol{e}_2 \rangle. && (3.66)
\end{aligned}
$$

The ideal I_2 corresponds to the solutions which contain only fundamental oscillations, and I_{123} corresponds to the solutions which contain 1/2 subharmonic oscillations. We can decompose the bifurcation diagram $\boldsymbol{V}(I_2) \cup \boldsymbol{V}(I_{123})$. The decomposition of the bifurcation diagram is shown in Figure 3.2 which represents the relation between the parameter E and the real part of the fundamental oscillation $x_{\rm r21}$ with $\omega = 1$ and $\mu = 0.01$. The green line corresponds to the ideal I_{123} and the red line corresponds to the ideal I_2.

In the case of $m = 3$, only the symmetry $\Gamma_{2\pi/2}$ is broken because $m = 3$ belongs to only $\kappa_{2\pi/3}$. As a result, the HB equation has both the symmetry $\Gamma_{2\pi/3}$ and $\Gamma_{\rm odd}$, i.e., $\kappa = \{\kappa_{2\pi/3}, \kappa_{\rm odd}\}$. Thus, the ideal decomposition is obtained by

$$
\begin{aligned}
I &= I_3 \cap I_{13} \cap I_{123} = \langle \boldsymbol{f}_{\Gamma_{\rm odd}} \rangle \cap \langle \overline{\boldsymbol{f}_{\Gamma_{\rm odd}}} \rangle \\
&= \left(\langle \boldsymbol{f}_{\Gamma_{2\pi/3}} \rangle \cap \langle \overline{\boldsymbol{f}_{\Gamma_{2\pi/3}}} \rangle \right) \cap \langle \overline{\boldsymbol{f}_{\Gamma_{\rm odd}}} \rangle, && (3.67)\\
I_3 &= \langle \boldsymbol{f}_{\Gamma_{2\pi/3}} \rangle = \langle \boldsymbol{x}_1, \boldsymbol{x}_2 \rangle + \langle \hat{\boldsymbol{f}}_3 + \boldsymbol{e}_3 \rangle, && (3.68)\\
I_{13} &= \langle \boldsymbol{f}_{\Gamma_{\rm odd}} \rangle : \langle \overline{\boldsymbol{f}_{\Gamma_{2\pi/3}}} \rangle = \langle \hat{\boldsymbol{f}}_1 \rangle : \langle \boldsymbol{x}_1 \rangle + \langle \boldsymbol{x}_2 \rangle + \langle \hat{\boldsymbol{f}}_3 + \boldsymbol{e}_3 \rangle, && (3.69)\\
I_{123} &= \langle \overline{\boldsymbol{f}_{\Gamma_{\rm odd}}} \rangle = \langle \hat{\boldsymbol{f}}_2 \rangle : \langle \boldsymbol{x}_2 \rangle + \langle \hat{\boldsymbol{f}}_1, \hat{\boldsymbol{f}}_3 + \boldsymbol{e}_3 \rangle. && (3.70)
\end{aligned}
$$

The ideal I_3, I_{13} and I_{123} correspond to the solutions which contain fundamental, 1/3 subharmonic and 2/3 subharmonic oscillations, respectively. We can decompose the bifurcation diagram $\boldsymbol{V}(I_3) \cup \boldsymbol{V}(I_{13}) \cup \boldsymbol{V}(I_{123})$. The decomposition of the bifurcation diagram is shown in Figure 3.3 which represents the relation between the parameter E and the real part of the fundamental oscillation $x_{\rm r31}$ with $\omega = 1$ and $\mu = 0.01$. The orange line corresponds to the ideal I_{123}, the green line corresponds to the ideal I_{13} and the red line corresponds to the ideal I_3.

We show the summary of these ideal decomposition in Table.3.1. Thus, the ideal decomposition of the each nonhomogeneous HB equation can be systematically obtained using the partial

ideal decomposition of the homogeneous HB equation. Further, the symmetries of the each non-homogeneous HB equation are clarified by the break of the symmetries of the homogeneous HB equation.

3.7 Concluding Remarks

We proposed a method to decompose bifurcation diagrams of periodic oscillations described by the HB equation based on the ideal decomposition using the symmetry of the system. In order to realize the ideal decomposition, we proposed an efficient decomposition using a partial ideal quotient. Moreover, we clarified the symmetry of nonhomogeneous HB equations by the break of the symmetry of the corresponding homogeneous HB equation. Finally, we decomposed the bifurcation diagrams of HB equations which are identical except for the forcing terms by using the symmetry of the homogeneous HB equation systematically.

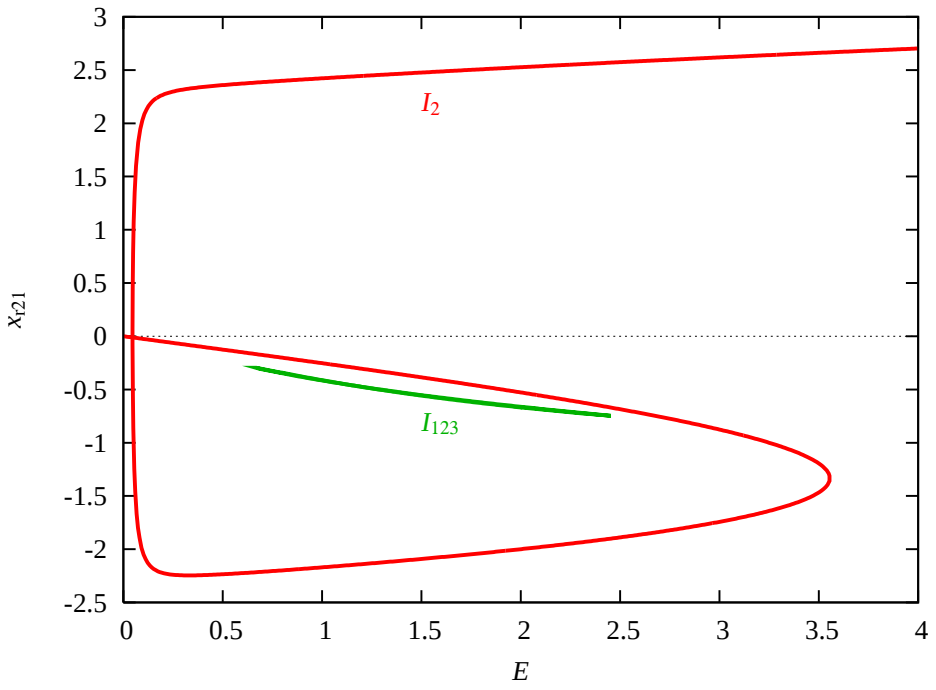

Figure 3.2: Bifurcation diagram (E - x_{r21}) in the case of $m = 2$, the parameter E versus the real part of the fundamental oscillation x_{r21} (The ideal I_2 corresponds to the solutions which contain only fundamental harmonic oscillations, and the ideal I_{123} corresponds to the solutions which contain 1/2 subharmonic oscillations with $\omega = 1$ and $\mu = 0.01$).

Table 3.1: Ideal decomposition of nonhomogeneous HB equations using partial ideal decomposition of homogeneous HB equation

Symmetry	$m = 1$	$m = 2$	$m = 3$
$\Gamma_{2\pi/2}$	-	$I_2 \cap I_{123}$	-
$\Gamma_{2\pi/3}$	-	-	$I_3 \cap I_{13}$
Γ_{odd}	$I_{13} \cap I_{123}$	-	$I_{123} \cap \overline{I_{123}}$

$\overline{I_{123}}$ is represented by $I_3 \cap I_{13}$.

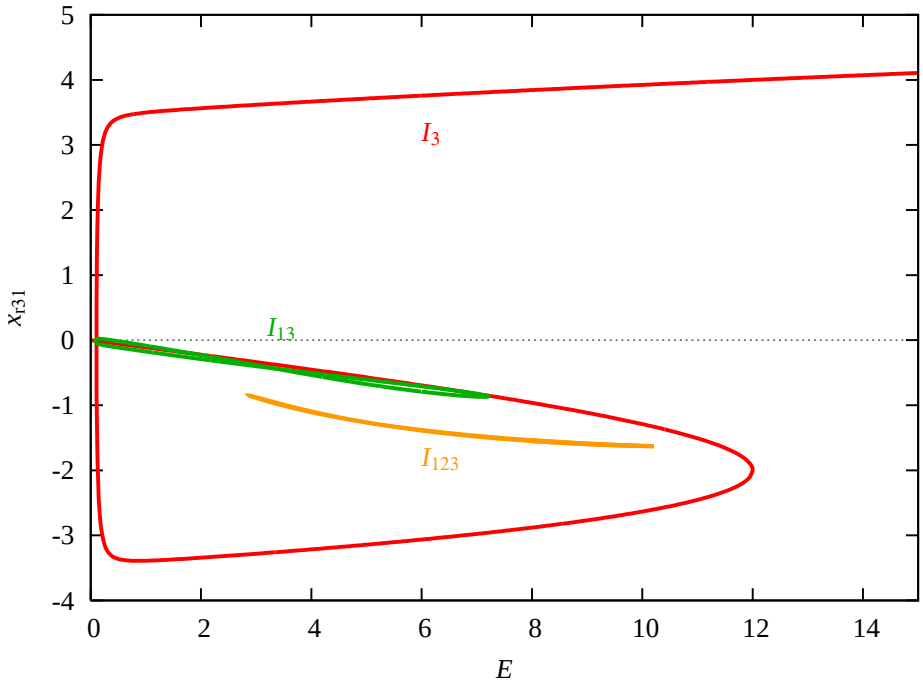

Figure 3.3: Bifurcation diagram (E - x_{r31}) in the case of $m = 3$, the parameter E versus the real part of the fundamental oscillation x_{r31} (The ideal I_3, I_{13} and I_{123} correspond to the solutions which contain fundamental, 1/3 subharmonic and 2/3 subharmonic oscillations, respectively, $\omega = 1$ and $\mu = 0.01$).

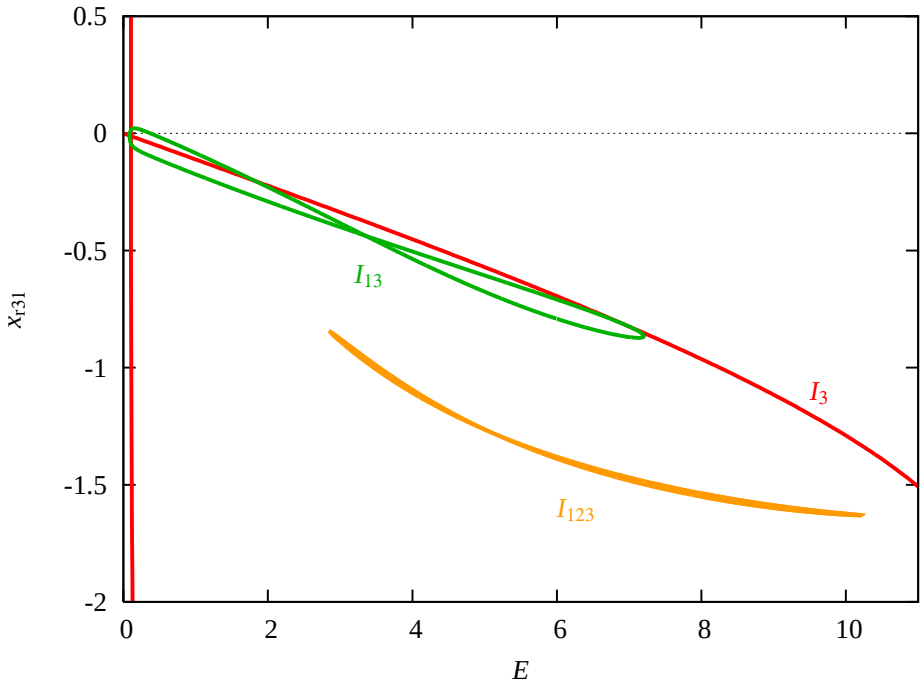

Figure 3.4: Bifurcation diagram (enlargement of Figure 3.3).

Chapter 4

Invariants with Respect to Symmetry and its Applications

4.1 Introduction

As shown in Chapter 3, the bifurcation diagram of the periodic oscillation is calculated by Gröbner base. However, the computational cost of Gröbner base is highly dependent on the complexity of the HB equation, and increases exponentially according to the expansion of considered frequency components. Further, when the system has symmetry, the HB equation has different but equivalent solutions which make the degree of the polynomials in the HB equation high. Hence, the computational cost of obtaining the bifurcation diagram becomes very large by the different but equivalent solutions based on the symmetry.

In order to resolve this problem, we propose a method to reduce the degree of the HB equation using invariants which transform the different but equivalent solutions into a unique solution. Since the degree of the HB equation is reduced by using the invariants, the bifurcation diagram of the reduced HB equation is simpler than the original bifurcation diagram. Additionally, we present that the relations among the amplitudes at each frequency component are easily calculated by the invariants since the information of phases is removed. Further, we propose a method for finding the design parameters of oscillators using the relations among the amplitudes.

4.2 Invariants with Respect to Symmetry

In this chapter, we focus on invariants with respect to the symmetry of the HB equation. The invariants enable to transform different but equivalent solutions based on the symmetry, i.e., asymmetric solutions, into a unique solution. Thus, using the invariants, we can remove the redundancy based on the symmetry. This section describe the number of the different but equivalent solutions with respect to the symmetries of the HB equation shown in Section 3.3, and leads to the invariants with respect to the symmetries.

4.2.1 Asymmetric Solutions of HB Equation

Odd Symmetry

From Eq.(3.8), the symmetric solutions with respect to Γ_{odd} satisfy $\boldsymbol{x} = \boldsymbol{\theta}_{\text{odd}}^{\,i}\boldsymbol{x}$ for $i = 1, 2$, whereas the asymmetric solutions do not satisfy the relation and have different but equivalent solutions $\boldsymbol{x}$ and $\boldsymbol{\theta}_{\text{odd}}\boldsymbol{x}$. The number of the different but equivalent solutions with respect to Γ_{odd} is 2.

Symmetry Based on $2\pi/\omega_{\text{s}}$ Time Shift

From Eq.(3.15), the symmetric solutions with respect to $\Gamma_{2\pi/m}$ satisfy $\boldsymbol{x} = \boldsymbol{\theta}_{2\pi/m}^{\,i}\boldsymbol{x}$ for $i = 1, \ldots, m$, whereas the asymmetric solutions do not satisfy the relation and have different but equivalent solutions $\boldsymbol{\theta}_{2\pi/m}^{\,i}\boldsymbol{x},\ i = 1, \ldots, m$. The number of the different but equivalent solutions with respect to $\Gamma_{2\pi/m}$ is m.

Thus, in the case of the periodically forced system, the oscillation which is asymmetric with respect to Γ_{odd} and $\Gamma_{2\pi/m}$ has $2m$ different but equivalent solutions when m is odd number. Those equivalent solutions of the HB equation on the periodically forced system make the degree of the polynomials in the HB equation high.

Symmetry Based on Arbitrary Time Shift

From Eq.(3.21), the symmetric solutions with respect to $\Gamma_{\text{arbitrary}}$ satisfy $\boldsymbol{x} = \boldsymbol{\theta}_{\text{arbitrary}}(\phi)\boldsymbol{x}$ for all arbitrary, whereas the asymmetric solutions do not satisfy the relation and have infinite different but equivalent solutions $\boldsymbol{\theta}_{\text{arbitrary}}(\phi)\boldsymbol{x}$. A set of the equivalent solutions $\boldsymbol{\theta}_{\text{arbitrary}}(\phi)\boldsymbol{x}$ forms a circle on the complex plane.

In case of the autonomous system, the oscillation which is asymmetric with respect to Γ_{odd} and $\Gamma_{\text{arbitrary}}$ has the infinite different but equivalent solutions.

4.2.2 Fundamental Invariants with Respect to Symmetry

Let us consider invariants which enable to transform a set of different but equivalent solutions into a unique solution. The invariants $g(\boldsymbol{x})$ with respect to the symmetries Γ_{odd}, $\Gamma_{2\pi/m}$, and $\Gamma_{\text{arbitrary}}$ are respectively defined by polynomials which satisfy the following relations;

$$\begin{array}{lll} g(\boldsymbol{x}) = g(\boldsymbol{\theta}_{\text{odd}}^{\,i}\boldsymbol{x}) & \text{for } i = 1,2 & (\text{Symmetry } \Gamma_{\text{odd}}), \\ g(\boldsymbol{x}) = g(\boldsymbol{\theta}_{2\pi/m}^{\,i}\boldsymbol{x}) & \text{for } i = 1,\ldots,m & (\text{Symmetry } \Gamma_{2\pi/m}), \\ g(\boldsymbol{x}) = g(\boldsymbol{\theta}_{\text{arbitrary}}(\phi)\boldsymbol{x}) & \text{for all } \phi & (\text{Symmetry } \Gamma_{\text{arbitrary}}). \end{array} \tag{4.1}$$

From the relations, these invariants transform the equivalent solutions into a unique solution. That is, if we represent the different but equivalent solutions by the invariants $g(\boldsymbol{x})$ instead of $\boldsymbol{x}$, we can remove the redundancy generated by the symmetries. In order to treat the invariants systematically, we consider the sets of the invariants as follows;

$$\begin{aligned} \mathbb{Q}(\boldsymbol{\lambda})[\boldsymbol{x}]^{\Gamma_{\text{odd}}} &\equiv \left\{ \boldsymbol{g} \in \mathbb{Q}(\boldsymbol{\lambda})[\boldsymbol{x}] \mid \boldsymbol{g}(\boldsymbol{x}) = \boldsymbol{g}(\boldsymbol{\theta}_{\text{odd}}^{\,i}\boldsymbol{x}), \text{for } i = 1,2 \right\}, \\ \mathbb{Q}(\boldsymbol{\lambda})[\boldsymbol{x}]^{\Gamma_{2\pi/m}} &\equiv \left\{ \boldsymbol{g} \in \mathbb{Q}(\boldsymbol{\lambda})[\boldsymbol{x}] \mid \boldsymbol{g}(\boldsymbol{x}) = \boldsymbol{g}(\boldsymbol{\theta}_{2\pi/m}^{\,i}\boldsymbol{x}), \text{for } i = 1,\ldots,m \right\}, \\ \mathbb{Q}(\boldsymbol{\lambda})[\boldsymbol{x}]^{\Gamma_{\text{arbitrary}}} &\equiv \left\{ \boldsymbol{g} \in \mathbb{Q}(\boldsymbol{\lambda})[\boldsymbol{x}] \mid \boldsymbol{g}(\boldsymbol{x}) = \boldsymbol{g}(\boldsymbol{\theta}_{\text{arbitrary}}(\phi)\boldsymbol{x}),\ \forall\phi \right\}. \end{aligned} \tag{4.2}$$

Because these sets are closed under addition and multiplication, these are sub-rings of $\mathbb{Q}(\boldsymbol{\lambda})[\boldsymbol{x}]$. The $\mathbb{Q}(\boldsymbol{\lambda})[\boldsymbol{x}]^{\Gamma_{\text{odd}}}$, $\mathbb{Q}(\boldsymbol{\lambda})[\boldsymbol{x}]^{\Gamma_{2\pi/m}}$, and $\mathbb{Q}(\boldsymbol{\lambda})[\boldsymbol{x}]^{\Gamma_{\text{arbitrary}}}$ are called the invariant sub-rings with respect to Γ_{odd}, $\Gamma_{2\pi/m}$, and $\Gamma_{\text{arbitrary}}$, respectively. An arbitrary invariant $g \in \mathbb{Q}(\boldsymbol{\lambda})[\boldsymbol{x}]^{\Gamma}$ with $\Gamma = \{\Gamma_{\text{odd}}, \Gamma_{2\pi/m}, \Gamma_{\text{arbitrary}}\}$ can be generated by finite invariants which is called fundamental invariants [54]. The fundamental invariants are calculated by Reynolds operator [21, 22], and are represented by

$$\boldsymbol{g}_{\text{F}}(\boldsymbol{x}) = (g_{\text{F}1}(\boldsymbol{x}), \ldots, g_{\text{F}s}(\boldsymbol{x}))^{\text{T}}, \tag{4.3}$$

where s denotes the number of the fundamental invariants. A tool for finding the fundamental invariants is provided in SINGULAR [55]. Thus, we can express the all invariants with respect to the symmetry Γ by the addition and multiplication of the fundamental invariants $g_{\text{F}1}(\boldsymbol{x}), \ldots, g_{\text{F}s}(\boldsymbol{x})$.

4.2.3 Squared Amplitudes Associated with Invariants

Let us consider special invariants with respect to Γ_{odd}, $\Gamma_{2\pi/m}$, and $\Gamma_{\text{arbitrary}}$. Because the linear representations $\boldsymbol{\theta}_{\text{odd}}$, $\boldsymbol{\theta}_{2\pi/m}$, and $\boldsymbol{\theta}_{\text{arbitrary}}$ are rotation matrices, the amplitudes at each frequency component of the oscillations are obviously invariants with respect to the symmetries. Thus, we

consider the following polynomials which are correspond to the amplitudes at each frequency component;

$$\begin{aligned}
\boldsymbol{g}_A(\boldsymbol{x}) &\equiv \begin{bmatrix} \boldsymbol{g}_{A0}(\boldsymbol{x}) \\ \vdots \\ \boldsymbol{g}_{Ap}(\boldsymbol{x}) \end{bmatrix}, \qquad (4.4)\\
\boldsymbol{g}_{A0}(\boldsymbol{x}) &= (g_{A01}(\boldsymbol{x}), \ldots, g_{A0n}(\boldsymbol{x}))^{\mathrm{T}} \\
&= ({x_{\mathrm{r}01}}^2, \ldots, {x_{\mathrm{r}0n}}^2)^{\mathrm{T}}, \\
\boldsymbol{g}_{Ak}(\boldsymbol{x}) &= (g_{Ak1}(\boldsymbol{x}), \ldots, g_{Akn}(\boldsymbol{x}))^{\mathrm{T}} \\
&= ({x_{\mathrm{r}k1}}^2 + {x_{\mathrm{s}k1}}^2, \ldots, {x_{\mathrm{r}kn}}^2 + {x_{\mathrm{s}kn}}^2)^{\mathrm{T}}, \\
k &= 1, \ldots, p.
\end{aligned}$$

In order to consider the behavior of this invariant $\boldsymbol{g}_A(\boldsymbol{x})$ instead of $\boldsymbol{x}$, we define the invariant as a new variable $\boldsymbol{A}$;

$$\begin{aligned}
\boldsymbol{A} &\equiv \begin{bmatrix} \boldsymbol{A}_0 \\ \vdots \\ \boldsymbol{A}_p \end{bmatrix} \equiv \boldsymbol{g}_A(\boldsymbol{x}), \qquad (4.5)\\
\boldsymbol{A}_k &= (A_{k1}, \ldots, A_{kn})^{\mathrm{T}}, \\
k &= 0, \ldots, p.
\end{aligned}$$

We call this variable $\boldsymbol{A}$ the squared amplitude. Namely, $\sqrt{A_{ki}}$ correspond to the amplitudes of the k/m th frequency components for $k = 1, \ldots, p,\ i = 1, \ldots, n$.

4.3 Reduction of Bifurcation Diagram Using Invariants

The algebraic representation of the bifurcation diagram is obtained using Gröbner base such as Chapter 3. However, if the HB equation has different but equivalent solutions, the complexity of the bifurcation diagram increases, and its computation is generally time and memory consuming. In order to overcome the difficulty, we propose to reduce the degree of the bifurcation diagram using the invariants such as the squared amplitude $\boldsymbol{A} = \boldsymbol{g}_A(\boldsymbol{x})$ which enable to transform the different but equivalent solutions into a unique solution.

4.3.1 Bifurcation Diagram of Squared Amplitude

Let us consider to obtain the bifurcation diagram with respect to the squared amplitude $\boldsymbol{A} = \boldsymbol{g}_A(\boldsymbol{x})$, which we call bifurcation diagram of squared amplitude. In order to calculate the bifurcation diagram of the squared amplitude, first we eliminate $\boldsymbol{x}$ from the ideal $\langle \boldsymbol{f}(\boldsymbol{x}) \rangle + \langle \boldsymbol{A} - \boldsymbol{g}_A(\boldsymbol{x}) \rangle$ using Gröbner base of the block order $\boldsymbol{x} \succ_{\text{block}} \boldsymbol{A}$. This order Gröbner base transposes

$$\begin{bmatrix} \boldsymbol{f}(\boldsymbol{x}; \omega, \boldsymbol{\lambda}, \boldsymbol{e}) \\ \boldsymbol{A} - \boldsymbol{g}_A(\boldsymbol{x}) \end{bmatrix} = \boldsymbol{0} \quad \text{to} \quad \begin{bmatrix} \boldsymbol{f}_{xA}(\boldsymbol{x}, \boldsymbol{A}; \omega, \boldsymbol{\lambda}, \boldsymbol{e}) \\ \boldsymbol{f}_A(\boldsymbol{A}; \omega, \boldsymbol{\lambda}, \boldsymbol{e}) \end{bmatrix} = \boldsymbol{0}.$$

Thus, we obtain the equation $\boldsymbol{f}_A(\boldsymbol{A}; \omega, \boldsymbol{\lambda}, \boldsymbol{e}) = \boldsymbol{0}$ which contains only $\boldsymbol{A}$ as variables. Next, using Gröbner base of the ideal $\langle \boldsymbol{f}_A(\boldsymbol{A}; \omega, \boldsymbol{\lambda}, \boldsymbol{e}) \rangle$, we calculate the bifurcation diagram of the squared amplitude. The procedure for calculating the bifurcation diagram of the squared amplitude are summarized as follows;

S1. We give the squared amplitude $\boldsymbol{A} = \boldsymbol{g}_A(\boldsymbol{x})$ which is the invariant generated by $\boldsymbol{g}_{\text{F}}(\boldsymbol{x})$.

S2. We obtain $\boldsymbol{f}_A(\boldsymbol{A}; \omega, \boldsymbol{\lambda}, \boldsymbol{e}) = \boldsymbol{0}$ which contains only $\boldsymbol{A}$ by eliminating $\boldsymbol{x}$ from the ideal $\langle \boldsymbol{f}(\boldsymbol{x}) \rangle + \langle \boldsymbol{A} - \boldsymbol{g}_A(\boldsymbol{x}) \rangle$ using Gröbner base of the block order $\boldsymbol{x} \succ_{\text{block}} \boldsymbol{A}$.

S3. If we consider the decomposition of the bifurcation diagram, we apply the proposed method in Chapter 3 to the ideal $\langle \boldsymbol{f}_A(\boldsymbol{A}; \omega, \boldsymbol{\lambda}, \boldsymbol{e}) \rangle$.

S4. We calculate the bifurcation diagram of the squared amplitude using Gröbner base.

The degree of the bifurcation diagram is reduced by the proposed method. The computational time and memory of Gröbner base is also reduced.

In the case of the autonomous system, the solutions of the HB equation are expressed as a circle on the complex plane. However, if we represent the bifurcation diagram by the squared amplitude, we can express the solutions as a unique solution.

4.3.2 Example

HB Equation

Let us consider the RLC circuit shown in Section 2.4. We apply the HB method with 3 frequency components, i.e., $p = 3$. Further, we assume that the direct current components equal zero, i.e.,

$X_{01} = X_{02} = 0$, similar to Section 2.4. Thus, the $u_1(t)$ and $u_2(t)$ are respectively approximated by

$$u_1^*(t) = \Re\left[X_{11}e^{\mathrm{j}\omega t} + X_{21}e^{\mathrm{j}2\omega t} + X_{31}e^{\mathrm{j}3\omega t}\right], \tag{4.6}$$

$$u_2^*(t) = \Re\left[X_{12}e^{\mathrm{j}\omega t} + X_{22}e^{\mathrm{j}2\omega t} + X_{32}e^{\mathrm{j}3\omega t}\right]. \tag{4.7}$$

In order to simplify the HB equation, we eliminate X_{12}, X_{22}, and X_{32} by the relations $\mathrm{j}\omega X_{11} = X_{12}$, $\mathrm{j}2\omega X_{21} = X_{22}$, and $\mathrm{j}3\omega X_{31} = X_{32}$. Further, we transform the variables X_{11}, X_{21}, and X_{31} into $x_{\mathrm{r}1}, x_{\mathrm{s}1}, x_{\mathrm{r}2}, x_{\mathrm{s}2}, x_{\mathrm{r}3}$, and $x_{\mathrm{s}3}$ based on the relations

$$\begin{aligned} X_{11} &= x_{\mathrm{r}1} + \mathrm{j}x_{\mathrm{s}1}, \\ X_{21} &= x_{\mathrm{r}2} + \mathrm{j}x_{\mathrm{s}2}, \\ X_{31} &= x_{\mathrm{r}3} + \mathrm{j}x_{\mathrm{s}3}. \end{aligned} \tag{4.8}$$

We consider the case of $m = 3$ with $\omega_s = m\omega$, i.e., the target oscillation is the 1/3 sub-harmonic oscillation. The HB equation is written by

$$\begin{aligned} \boldsymbol{f}(\boldsymbol{x}) &= \boldsymbol{f}(\boldsymbol{x}; \omega, \boldsymbol{\lambda}, E) \\ &= (f_{\mathrm{r}1}, f_{\mathrm{s}1}, f_{\mathrm{r}2}, f_{\mathrm{s}2}, f_{\mathrm{r}3}, f_{\mathrm{s}3})^{\mathrm{T}} = \boldsymbol{0}, \end{aligned} \tag{4.9}$$

where $\boldsymbol{x} \equiv (x_{\mathrm{r}1}, x_{\mathrm{s}1}, x_{\mathrm{r}2}, x_{\mathrm{s}2}, x_{\mathrm{r}3}, x_{\mathrm{s}3})^{\mathrm{T}}$.

Symmetry of System

In order to obtain the fundamental invariants, let us consider the symmetry. The HB equation $\boldsymbol{f}(\boldsymbol{x}) = \boldsymbol{0}$ has the symmetries Γ_{odd} and $\Gamma_{2\pi/3}$. The corresponding linear representations $\boldsymbol{\theta}_{\mathrm{odd}}$ and $\boldsymbol{\theta}_{2\pi/3}$ are

$$\boldsymbol{\theta}_{\mathrm{odd}} = \begin{bmatrix} 1 & & & & 0 & \\ & 1 & & & & \\ & & -1 & & & \\ & & & -1 & & \\ & & & & 1 & \\ 0 & & & & & 1 \end{bmatrix}, \tag{4.10}$$

$$\boldsymbol{\theta}_{2\pi/3} = \begin{bmatrix} -\frac{1}{2} & \frac{\sqrt{3}}{2} & & & 0 & \\ -\frac{\sqrt{3}}{2} & -\frac{1}{2} & & & & \\ & & -\frac{1}{2} & -\frac{\sqrt{3}}{2} & & \\ & & \frac{\sqrt{3}}{2} & -\frac{1}{2} & & \\ & & & & 1 & \\ 0 & & & & & 1 \end{bmatrix}. \tag{4.11}$$

The numbers of the different but equivalent solutions with respect to $\Gamma_{\rm odd}$ and $\Gamma_{2\pi/3}$ are 2 and 3, respectively. Thus, the number of the different but equivalent solutions with respect to both $\Gamma_{\rm odd}$ and $\Gamma_{2\pi/3}$ is 6.

Invariants with Respect to Symmetry

Using $\boldsymbol{\theta}_{2\pi/3}$ and $\boldsymbol{\theta}_{\rm odd}$, the fundamental invariants with respect to the symmetries $\Gamma_{2\pi/3}$ and $\Gamma_{\rm odd}$ are

$$\boldsymbol{g}_{\rm F}(\boldsymbol{x}) = \begin{bmatrix} g_{\rm F1} \\ g_{\rm F2} \\ g_{\rm F3} \\ g_{\rm F4} \\ g_{\rm F5} \\ g_{\rm F6} \\ g_{\rm F7} \\ g_{\rm F8} \\ g_{\rm F9} \\ g_{\rm F10} \\ g_{\rm F11} \\ g_{\rm F12} \\ g_{\rm F13} \\ g_{\rm F14} \end{bmatrix} = \begin{bmatrix} x_{\rm r3} \\ x_{\rm s3} \\ x_{\rm r2}^2 + x_{\rm s2}^2 \\ x_{\rm r1}^2 + x_{\rm s1}^2 \\ 3x_{\rm r1}^2 x_{\rm s1} - x_{\rm s1}^3 \\ x_{\rm r1}^3 - 3x_{\rm r1} x_{\rm s1}^2 \\ 3x_{\rm r2}^5 x_{\rm s2} - 10x_{\rm r2}^3 x_{\rm s2}^3 + 3x_{\rm r2} x_{\rm s2}^5 \\ 9x_{\rm r2}^6 + 45x_{\rm r2}^4 x_{\rm s2}^2 + 15x_{\rm r2}^2 x_{\rm s2}^4 + 11x_{\rm s2}^6 \\ x_{\rm s1} x_{\rm r2}^2 - 2x_{\rm r1} x_{\rm r2} x_{\rm s2} - x_{\rm s1} x_{\rm s2}^2 \\ x_{\rm r1} x_{\rm r2}^2 + 2x_{\rm s1} x_{\rm r2} x_{\rm s2} - x_{\rm r1} x_{\rm s2}^2 \\ x_{\rm r1} x_{\rm s1} x_{\rm r2}^2 + x_{\rm r1}^2 x_{\rm r2} x_{\rm s2} - x_{\rm s1}^2 x_{\rm r2} x_{\rm s2} - x_{\rm r1} x_{\rm s1} x_{\rm s2}^2 \\ x_{\rm r1}^2 x_{\rm r2}^2 - x_{\rm s1}^2 x_{\rm r2}^2 - 4x_{\rm r1} x_{\rm s1} x_{\rm r2} x_{\rm s2} - x_{\rm r1}^2 x_{\rm s2}^2 + x_{\rm s1}^2 x_{\rm s2}^2 \\ 3x_{\rm s1} x_{\rm r2}^4 - 6x_{\rm s1} x_{\rm r2}^2 x_{\rm s2}^2 - 8x_{\rm r1} x_{\rm r2} x_{\rm s2}^3 - x_{\rm s1} x_{\rm s2}^4 \\ 3x_{\rm r1} x_{\rm r2}^4 - 6x_{\rm r1} x_{\rm r2}^2 x_{\rm s2}^2 + 8x_{\rm s1} x_{\rm r2} x_{\rm s2}^3 - x_{\rm r1} x_{\rm s2}^4 \end{bmatrix}. \tag{4.12}$$

The fundamental invariants generate the all invariants which enable to transform the equivalent 6 solutions with respect to $\Gamma_{\rm odd}$ and $\Gamma_{2\pi/3}$ into a unique solution. The $g_{\rm F4}(\boldsymbol{x})$ and $g_{\rm F3}(\boldsymbol{x})$ is the squared amplitudes of 1/3 and 2/3 subharmonic frequency components, respectively.

We write the squared amplitude $\boldsymbol{A} = \boldsymbol{g}_A(\boldsymbol{x})$ which is generated by $\boldsymbol{g}_{\rm F}(\boldsymbol{x})$ as follows:

$$\boldsymbol{A} \equiv \begin{bmatrix} A_1 \\ A_2 \\ A_3 \end{bmatrix} \equiv \begin{bmatrix} {x_{\rm r1}}^2 + {x_{\rm s1}}^2 \\ {x_{\rm r2}}^2 + {x_{\rm s2}}^2 \\ {x_{\rm r3}}^2 + {x_{\rm s3}}^2 \end{bmatrix} = \begin{bmatrix} g_{\rm F4}(\boldsymbol{x}) \\ g_{\rm F3}(\boldsymbol{x}) \\ g_{\rm F1}^2(\boldsymbol{x}) + g_{\rm F2}^2(\boldsymbol{x}) \end{bmatrix} \equiv \boldsymbol{g}_A(\boldsymbol{x}). \tag{4.13}$$

The $\sqrt{A_1}$, $\sqrt{A_2}$, and $\sqrt{A_3}$ corresponds to the amplitude of each frequency component, respectively.

Bifurcation Diagram of Squared Amplitude

Let us calculate the bifurcation diagram of the squared amplitude. First, we obtain $\boldsymbol{f}_A(\boldsymbol{A}; \omega, \mu, E) = \boldsymbol{0}$ by using Gröbner base of the block order $\boldsymbol{x} \succ_{\rm block} \boldsymbol{A}$ to the ideal $\langle \boldsymbol{f}(\boldsymbol{x}) \rangle + \langle \boldsymbol{A} - \boldsymbol{g}_A(\boldsymbol{x}) \rangle$. Next, we obtain the bifurcation diagram of the squared amplitude A_3 from the ideal $\langle \boldsymbol{f}_A(\boldsymbol{A}; \omega, \mu, E) \rangle$

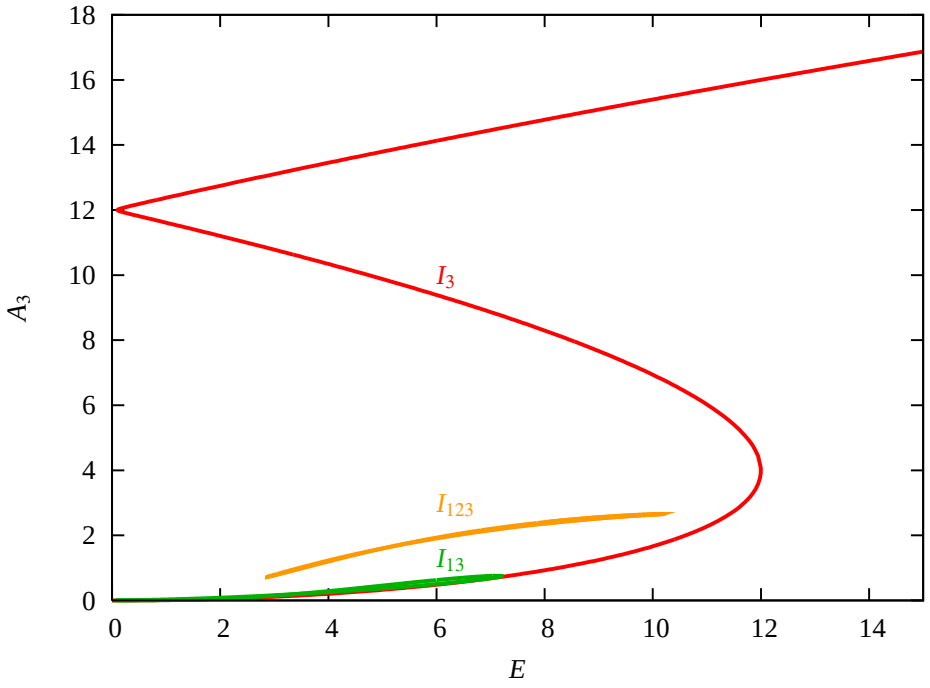

Figure 4.1: Bifurcation diagram of squared amplitude (E - A_3), the parameter E versus the squared amplitude A_3 ($\omega = 1, \mu = 0.01$, I_3 corresponds to asymmetric solutions, I_{13} corresponds to solutions based on symmetry Γ_{odd}, and I_{123} corresponds to solutions based on symmetries $\Gamma_{2\pi/3}$ and Γ_{odd}).

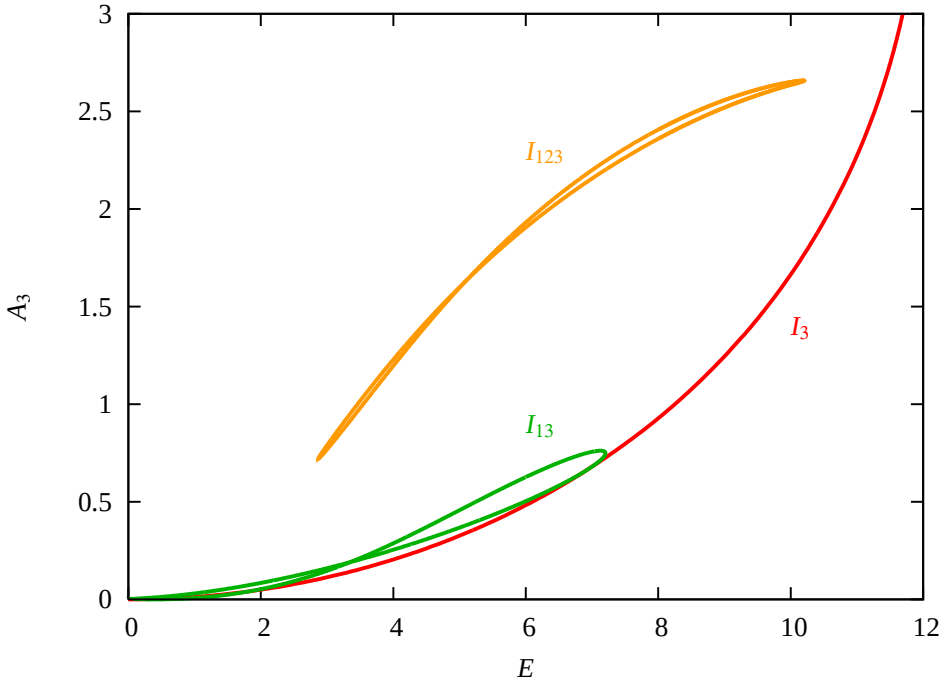

Figure 4.2: Bifurcation diagram (enlargement of Figure 4.1).

Table 4.1: Complexity of bifurcation diagrams ($\omega = 1, \mu = 0.01$)

Method	Max degree	Number of terms
Original method	18	64
Proposed method	6	12

Calculated by a PC with Xeon 3.06GHz CPU.

Table 4.2: Computational cost of obtaining bifurcation diagrams ($\omega = 1$)

Method	μ; symbolically		$\mu = 0.01$	
	Computational time [s]	Required memory[MB]	Computational time [s]	Required memory [MB]
Original method	50643.5	533.8	612.4	133.5
Proposed method	0.112	2.9	0.099	1.8

Calculated by a PC with Xeon 3.06GHz CPU.

using Gröbner base of the block order $(A_1, A_3) \succ_{\text{block}} A_3$. The bifurcation diagram of the squared amplitude consists of three sub-diagrams which correspond to asymmetric solutions $\boldsymbol{V}(I_3)$, symmetric solutions $\boldsymbol{V}(I_{13})$ with respect to Γ_{odd} and symmetric solutions $\boldsymbol{V}(I_{123})$ with respect to both Γ_{odd} and $\Gamma_{2\pi/3}$ as shown in Figures 4.1 and 4.2. Namely, the bifurcation diagram can be also decomposed by the ideal decomposition, like Figures 3.3 and 3.4.

Computational Efficiency

In order to confirm the reduction of the bifurcation diagram by the squared amplitude, we consider a simpler problem. Namely, we set $x_{\text{r2}} = x_{\text{s2}} = 0$, i.e., we consider the HB method with 2 frequency components; 1/3 subharmonic and fundamental harmonic components. In this case, the number of the different but equivalent solutions with respect to $\Gamma_{2\pi/3}$ is 3. Then we obtain the bifurcation diagram which corresponds to the asymmetric solutions with respect to $\Gamma_{2\pi/3}$ using the ideal decomposition in Chapter 3. The bifurcation diagrams (E - x_{r1}) and (E - A_1) are calculated with the original method in Chapter 3 and the proposed method, respectively. As a result, we obtain the equations of the bifurcation diagrams shown in Appendix D. We show the bifurcation diagrams in Figure 4.3, and show its complexity in Table 4.1. Finally, the computational costs are shown in Table 4.2.

In Table 4.1, the number of the solutions of Eq.(D.1) is 18 in the original method, whereas the

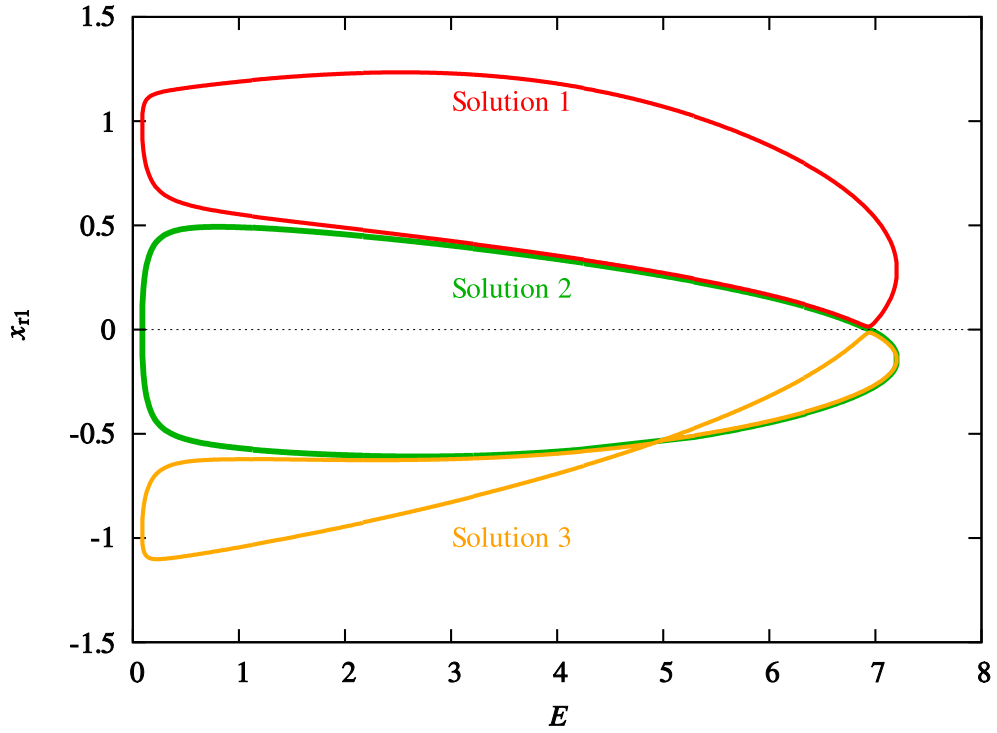

(a) E - x_{r1}

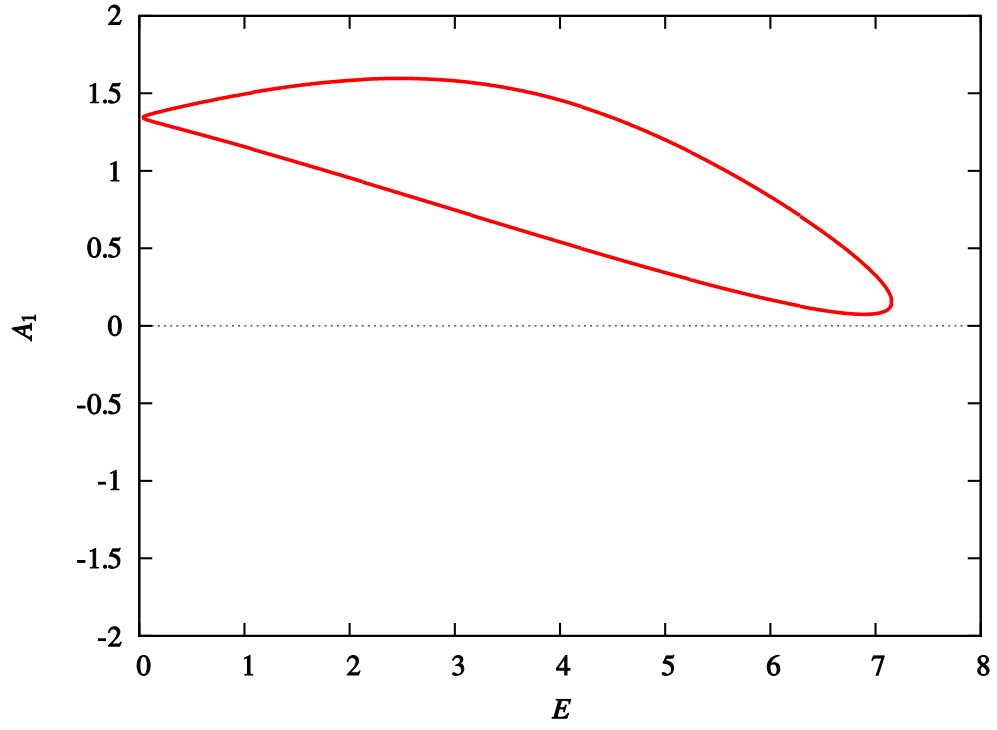

(b) E - A_1

Figure 4.3: Comparison of bifurcation diagrams (E - x_{r1}) and (E - A_1) ($\omega = 1, \mu = 0.01$).

number of the solutions of Eq.(D.2) is 6 in the proposed method. We can confirm that the squared amplitude A_1 transforms the equivalent 3 solutions into a unique solution. It is also confirmed by Figure 4.3, i.e., the number of the set of solutions x_{r1} in (a) is 3, and the number of the set of solutions A_1 in (b) is 1. Thus, the bifurcation diagram is reduced by the invariants.

By Table 4.2, the number of the terms in the proposed method is considerably smaller than the number of the terms in the original method. Further, the computational costs of obtaining the bifurcation diagram are reduced dramatically by invariants. Thus, we can confirm the efficiency of the proposed method.

4.4 Derivation of Intrinsic Algebraic Relations Using Invariants

4.4.1 Amplitude Relations Based on Squared Amplitude

Using the invariants such as the squared amplitude $\boldsymbol{A}$, we can reduce the degree of the HB equation. The reduction makes it possible to find out intrinsic algebraic relations. In particular, the invariant $\boldsymbol{A}$ gives the relations among the squared amplitudes at each frequency component by eliminating the phase information from the HB equation. We call the relations the amplitude relations. In particular, we can obtain the amplitude relations of the periodically forced system only by the polynomials which do not contain the forcing terms in HB equation. Moreover, the computational cost for obtaining the amplitude relations of the periodically forced system is remarkably less than that for bifurcation diagram of the squared amplitude.

Autonomous System

In the case of the autonomous system, we can obtain the amplitude relations because the phase information are removed by $\boldsymbol{A}$. The algorithm is as follows;

S1. We give invariants $\boldsymbol{A} = \boldsymbol{g}_A(\boldsymbol{x})$.

S2. We obtain the amplitude relations $\boldsymbol{a}(\boldsymbol{A}; \omega, \boldsymbol{\lambda}) = \boldsymbol{0}$ by eliminating $\boldsymbol{x}$ from the ideal $\langle \boldsymbol{f}(\boldsymbol{x}) \rangle + \langle \boldsymbol{A} - \boldsymbol{g}_A(\boldsymbol{x}) \rangle$ using Gröbner base of the block order $\boldsymbol{x} \succ_{\mathrm{block}} \boldsymbol{A}$.

Periodically Forced System

The HB equation of the system periodically forced by the frequency $\omega = \omega_s/m$ contains the terms corresponding to the sinusoidal forcing functions only in $\boldsymbol{f}_m$. The other equations $\boldsymbol{f}_0, \ldots, \boldsymbol{f}_{m-1}$, $\boldsymbol{f}_{m+1}, \ldots, \boldsymbol{f}_p$ do not contain the terms corresponding to the sinusoidal forcing functions. That is, the following HB equation $K_m\boldsymbol{f}(\boldsymbol{x}) = \boldsymbol{0}$ is identical with the HB equation of the autonomous system which is generated by removing the terms corresponding to the sinusoidal forcing functions from the original Eq.(2.1);

$$K_m\boldsymbol{f}(\boldsymbol{x}) \equiv \begin{bmatrix} \boldsymbol{f}_0 \\ \vdots \\ \boldsymbol{f}_{m-1} \\ \boldsymbol{f}_{m+1} \\ \vdots \\ \boldsymbol{f}_p \end{bmatrix} = \boldsymbol{0}, \tag{4.14}$$

where K_m is an operator which removes the mth frequency $\boldsymbol{f}_m$. Because $K_m\boldsymbol{f}(\boldsymbol{x}) = \boldsymbol{0}$ does not contain the terms corresponding to the sinusoidal forcing functions, $K_m\boldsymbol{f}(\boldsymbol{x}) = \boldsymbol{0}$ has the symmetry $\Gamma_{\text{arbitrary}}$ and has infinite equivalent solutions based on $\Gamma_{\text{arbitrary}}$. We can obtain the amplitude relation $\boldsymbol{a}(\boldsymbol{A}; \omega, \boldsymbol{\lambda}) = \boldsymbol{0}$ by eliminating $\boldsymbol{x}$ from the ideal $\langle K_m\boldsymbol{f}(\boldsymbol{x})\rangle + \langle \boldsymbol{A} - \boldsymbol{g}_A(\boldsymbol{x})\rangle$ using Gröbner base of the block order $\boldsymbol{x} \succ_{\text{block}} \boldsymbol{A}$.

It is noted that the obtained amplitude relations do not depend on the sinusoidal forcing function because the amplitude relations are calculated by the HB equation $K_m\boldsymbol{f}(\boldsymbol{x}) = \boldsymbol{0}$ which does not depend on the terms corresponding to the sinusoidal forcing functions.

4.4.2 Example

In order to obtain the amplitude relations, we consider the example in previous section. The HB equation $K_3\boldsymbol{f}(\boldsymbol{x}) = \boldsymbol{0}$ is represented by

$$K_3\boldsymbol{f}(\boldsymbol{x}) = (f_{\mathrm{r}1}, f_{\mathrm{s}1}, f_{\mathrm{r}2}, f_{\mathrm{s}2})^{\mathrm{T}}. \tag{4.15}$$

Then, we write the squared amplitude $\boldsymbol{A} = \boldsymbol{g}_A(\boldsymbol{x})$;

$$\boldsymbol{A} \equiv \begin{bmatrix} A_1 \\ A_2 \\ A_3 \end{bmatrix} \equiv \begin{bmatrix} {x_{\mathrm{r}1}}^2 + {x_{\mathrm{s}1}}^2 \\ {x_{\mathrm{r}2}}^2 + {x_{\mathrm{s}2}}^2 \\ {x_{\mathrm{r}3}}^2 + {x_{\mathrm{s}3}}^2 \end{bmatrix} \equiv \boldsymbol{g}_A(\boldsymbol{x}). \tag{4.16}$$

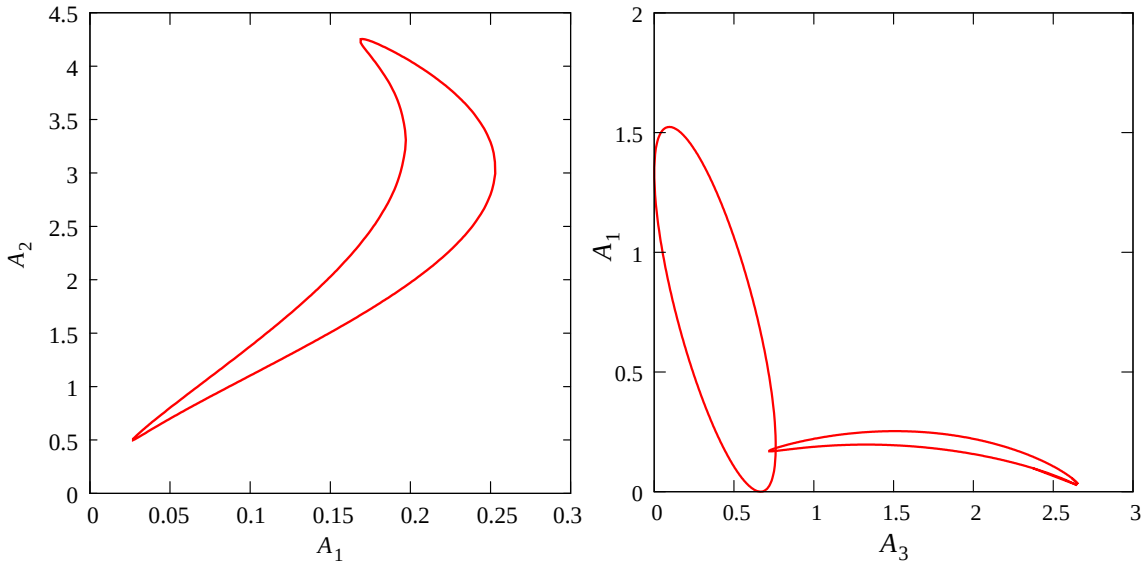

(a) A_3 - A_1

(b) A_3 - A_2

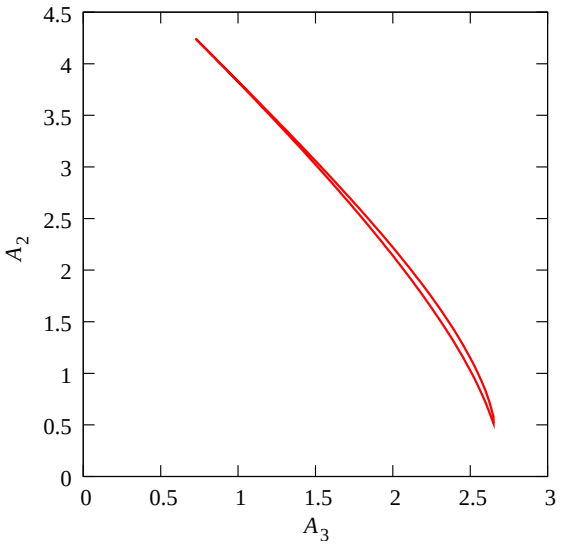

(c) A_1 - A_2

Figure 4.4: Amplitude relations ($\omega = 1, \mu = 0.01$).

We obtain the amplitude relations $\boldsymbol{a}(\boldsymbol{A};\omega,\boldsymbol{\lambda}) = \boldsymbol{0}$ by eliminating $\boldsymbol{x}$ from the ideal $\langle K_3\boldsymbol{f}(\boldsymbol{x})\rangle + \langle \boldsymbol{A} - \boldsymbol{g}(\boldsymbol{x})\rangle$ using Gröbner base of the block order $\boldsymbol{x} \succ_{\text{block}} \boldsymbol{A}$. Then, we obtain the amplitude relations (A_3 - A_1), (A_3 - A_2) and (A_1 - A_2) shown in Figure 4.4 by Gröbner base of the block order $A_2 \succ_{\text{block}} (A_3, A_1)$, $A_1 \succ_{\text{block}} (A_3, A_2)$, and $A_3 \succ_{\text{block}} (A_1, A_2)$, respectively. It is noted that the relation does not depend on the value of the sinusoidal forcing functions. Although the Figure 4.4 is not the bifurcation diagram, the amplitude relations give some information of bifurcations.

In order to confirm the efficiency of the method, we compare the computational cost of obtaining the bifurcation diagram of the squared amplitude and the amplitude relations for $\boldsymbol{f}(\boldsymbol{x}) = (f_{\text{r1}}, f_{\text{s1}}, f_{\text{r2}}, f_{\text{s2}}, f_{\text{r3}}, f_{\text{s3}})^{\text{T}}$. The result is shown in Table 4.3. Thus, computational cost of obtaining the amplitude relations is considerably less than that of the bifurcation diagram of the invariant.

Table 4.3: Computational cost of obtaining bifurcation diagram of squared amplitude and amplitude relations ($\omega = 1$ and $\mu = 0.01$)

	Computational time [s]	Required memory [MB]
Bifurcation diagrams of the invariant		
E - A_1	4598.23	304.0
E - A_2	3768.17	363.2
E - A_3	4548.63	256.7
Amplitude relations		
A_3 - A_1	17.83	12.1
A_3 - A_2	17.52	12.1
A_1 - A_2	17.40	12.1

Calculated by a PC with Xeon 3.06GHz CPU.

4.5 Method for Determining Design Parameters Using Amplitude Relations

4.5.1 Algorithm for Determining Design Parameters

The amplitude relations obtained in the previous section contain the squared amplitude $\boldsymbol{A}$ and the circuit parameters explicitly. In the amplitude relations $\boldsymbol{a}(\boldsymbol{A};\omega,\boldsymbol{\lambda})$, let us view the amplitudes as parameters and view the parameters as variables, i.e., we consider $\boldsymbol{a}(\omega,\boldsymbol{\lambda};\boldsymbol{A}) = \boldsymbol{0}$. That is, if we give the amplitudes, we can obtain the corresponding parameters. In this case, we put ω together in the amplitudes, i.e., $\boldsymbol{a}(\boldsymbol{\lambda};\boldsymbol{A},\omega)$.

Giving the amplitudes $\boldsymbol{A}$ and the frequency ω in the amplitude relations $\boldsymbol{a}(\boldsymbol{\lambda}; \boldsymbol{A}, \omega)$, we propose a method for determining the design parameters in which oscillations with the required $\boldsymbol{A}$ and ω are generated. The algorithm is as follows:

S1. We give the squared amplitude $\boldsymbol{A} = \boldsymbol{g}_A(\boldsymbol{x})$.

S2. We obtain the amplitude relations $\boldsymbol{a}(\boldsymbol{A}; \omega, \boldsymbol{\lambda}) = \boldsymbol{0}$.

S3. We give $\boldsymbol{A}$ and ω in the amplitude relations $\boldsymbol{a}(\boldsymbol{\lambda}; \boldsymbol{A}, \omega) = \boldsymbol{0}$.

S4. The relation among the parameters $\boldsymbol{p}(\boldsymbol{\lambda}) = \boldsymbol{0}$ is obtained from the ideal $\langle \boldsymbol{a}(\boldsymbol{\lambda}; \boldsymbol{A}, \omega) \rangle$ by Gröbner base of the lexicographic order $\lambda_1 \succ_{\text{lex}} \cdots \succ_{\text{lex}} \lambda_l$.

4.5.2 Example

Circuit Equation and HB Equation

We consider the oscillator with Esaki diode [57] shown in Figure 4.5 because the system is a damped simple oscillator. The circuit equation is written by

$$C\frac{\mathrm{d}^2 v}{\mathrm{d}t^2} + \left\{\frac{1}{R} + f'(v + E_0)\right\}\frac{\mathrm{d}v}{\mathrm{d}t} + \frac{1}{L}v = 0, \tag{4.17}$$

$$f'(V) = -\frac{1}{\rho}\left\{1 - \frac{(V - E_0)^2}{K^2}\right\}, \tag{4.18}$$

where $f(V) = \frac{V-E_0}{\rho}\left\{-1 + \frac{(V-E_0)^2}{3K^2}\right\} + I_0$ is characteristics of the Esaki diode, E_0 and I_0 are the operating voltage and current of the Esaki diode, $f'(V)$ denotes the derivative of $f(V)$ with respect to V, and ρ denotes a negative resistance. We can obtain the scaled circuit equation as follows;

$$\frac{\mathrm{d}^2 v}{\mathrm{d}t^2} - \alpha\left\{1 - \beta v^2\right\}\frac{\mathrm{d}v}{\mathrm{d}t} + \varepsilon v = 0, \tag{4.19}$$

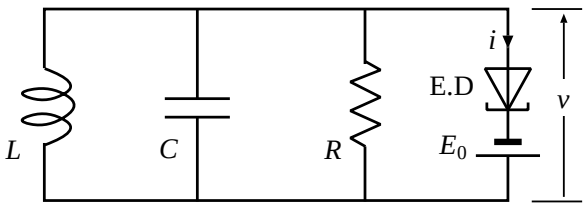

Figure 4.5: Oscillator with Esaki diode.

where

$$\alpha = \frac{1}{C}\left\{\frac{1}{\rho} - \frac{1}{R}\right\},\ \beta = \frac{R^2}{(R-\rho)K^2},\ \varepsilon = \frac{1}{LC}.$$

It is well known that the scaled circuit equation (4.19) is called van der Pol equation [2–4].

The Eq.(4.19) is represented by

$$\frac{\mathrm{d}}{\mathrm{d}t}\begin{bmatrix} u_1 \\ u_2 \end{bmatrix} = \begin{bmatrix} u_2 \\ \alpha\left\{1 - \beta {u_1}^2\right\} u_2 - \varepsilon u_1 \end{bmatrix}, \tag{4.20}$$

$$u_1 = v,\ u_2 = \frac{\mathrm{d}v}{\mathrm{d}t}.$$

We apply the HB method with 2 frequency components, i.e., the $u_1(t)$ and $u_2(t)$ are respectively approximated by

$$u_1^*(t) = \Re\left[X_{11}e^{\mathrm{j}\omega t} + X_{31}e^{\mathrm{j}3\omega t}\right], \tag{4.21}$$

$$u_2^*(t) = \Re\left[X_{12}e^{\mathrm{j}\omega t} + X_{32}e^{\mathrm{j}3\omega t}\right]. \tag{4.22}$$

In order to simplify the HB equation, we eliminate X_{12} and X_{32} by the relation $\mathrm{j}\omega X_{11} = X_{12}$ and $\mathrm{j}3\omega X_{31} = X_{32}$. Further, we transform the variables X_{11} and X_{31} into $x_{\mathrm{r}1}, x_{\mathrm{s}1}, x_{\mathrm{r}3}$, and $x_{\mathrm{s}3}$ based on the relations

$$\begin{aligned} X_{11} &= x_{\mathrm{r}1} + \mathrm{j}x_{\mathrm{s}1}, \\ X_{31} &= x_{\mathrm{r}3} + \mathrm{j}x_{\mathrm{s}3}. \end{aligned} \tag{4.23}$$

The HB equation is written by $\boldsymbol{f}(\boldsymbol{x}, \omega; \boldsymbol{\delta}) \equiv (f_{\mathrm{r}1}, f_{\mathrm{s}1}, f_{\mathrm{r}3}, f_{\mathrm{s}3})^{\mathrm{T}} = \boldsymbol{0}$, where $\boldsymbol{x} \equiv (x_{\mathrm{r}1}, x_{\mathrm{s}1}, x_{\mathrm{r}3}, x_{\mathrm{s}3})^{\mathrm{T}}$ and $\boldsymbol{\delta} \equiv (\alpha, \beta, \gamma)$.

Amplitude Relation

In order to obtain the amplitude relations, let us consider the symmetry $\Gamma_{\mathrm{arbitrary}}$. The corresponding linear representation $\boldsymbol{\theta}_{\mathrm{arbitrary}}(\phi)$ is written by

$$\boldsymbol{\theta}_{\mathrm{arbitrary}}(\phi) = \begin{bmatrix} \cos\phi & \sin\phi & & \\ -\sin\phi & \cos\phi & & \\ & & \cos 3\phi & \sin 3\phi \\ & & -\sin 3\phi & \cos 3\phi \end{bmatrix}. \tag{4.24}$$

Thus, the squared amplitude $\boldsymbol{A} = \boldsymbol{g}_A(\boldsymbol{x})$ is written by

$$\boldsymbol{A} \equiv \begin{bmatrix} A_1 \\ A_3 \end{bmatrix} \equiv \begin{bmatrix} {x_{\mathrm{r}1}}^2 + {x_{\mathrm{s}1}}^2 \\ {x_{\mathrm{r}3}}^2 + {x_{\mathrm{s}3}}^2 \end{bmatrix} \equiv \boldsymbol{g}_A(\boldsymbol{x}). \tag{4.25}$$

The $\sqrt{A_1}$ and $\sqrt{A_3}$ correspond to the amplitudes of the fundamental and the 3rd harmonic oscillation, respectively. The amplitude relations $\boldsymbol{a}_\delta(\boldsymbol{A};\omega,\boldsymbol{\delta}) = \boldsymbol{0}$ is obtained by eliminating $\boldsymbol{x}$ from the ideal $\langle \boldsymbol{f}(\boldsymbol{x})\rangle + \langle \boldsymbol{A} - \boldsymbol{g}(\boldsymbol{x})\rangle$ using Gröbner base of the block order $\boldsymbol{x} \succ_{\text{block}} \boldsymbol{A}$.

Determining Design Parameters

Because the $\boldsymbol{a}_\delta(\boldsymbol{A};\omega,\boldsymbol{\delta})$ is represented by the scaled parameters $\boldsymbol{\delta} = (\alpha,\beta,\gamma)$, let us transpose $\boldsymbol{a}_\delta(\boldsymbol{A};\omega,\boldsymbol{\delta}) = \boldsymbol{0}$ to equation with real circuit parameters. We define polynomial $\boldsymbol{l}$ of the real circuit parameters as follows;

$$\boldsymbol{l}(\boldsymbol{\lambda},\boldsymbol{\delta}) = \begin{bmatrix} \alpha CR\rho - (R-\rho) \\ \beta(R-\rho)K^2 - R \\ \gamma LC - 1 \end{bmatrix} = \boldsymbol{0}, \tag{4.26}$$

where $\boldsymbol{\lambda} = (R, L, C, K, \rho)$.

We can obtain the amplitude relations $\boldsymbol{a}_\lambda(\boldsymbol{A};\omega,\boldsymbol{\lambda}) = \boldsymbol{0}$ with the real circuit parameters by eliminating $\boldsymbol{\delta}$ from the ideal $\langle \boldsymbol{a}_\delta(\boldsymbol{A};\omega,\boldsymbol{\delta})\rangle + \langle \boldsymbol{l}(\boldsymbol{\lambda},\boldsymbol{\delta})\rangle$ using Gröbner base of the block order $\boldsymbol{\delta} \succ_{\text{block}} \boldsymbol{\lambda}$. Then, we fix the squared amplitude A_1 and frequency ω of the fundamental oscillation. For example, let us fix $A_1 = 1$ and $\omega = 2\pi$. The relation $\boldsymbol{p}(\boldsymbol{\lambda};A_3) = \boldsymbol{0}$ among the circuit parameters $\boldsymbol{\lambda}$ can be obtained from the ideal $\langle \boldsymbol{a}_\lambda(\boldsymbol{\lambda};A_3)\rangle$ using Gröbner base. The relations among the circuit parameters are shown in Figure 4.6, where $K = 0.6218$ and $\rho = 0.3448$ are determined by the characteristics of the Esaki diode [57]. Further, the relations between A_3 and R, L, C are shown in Figure 4.7. If we fix $A_3 = 0.01$, we can obtain the circuit parameters $R = 0.957,\ L = 0.0654$ and $C = 0.359$ by the relation $\boldsymbol{p}(\boldsymbol{\lambda};A_3) = \boldsymbol{0}$.

Figure 4.8 shows the voltage waveform and spectrum calculated by Runge-Kutta method on the above condition. The squared amplitude of the fundamental and 3rd harmonic oscillation, and frequency of the fundamental oscillation are $A_1 = 1.04$, $A_3 = 0.0095$, and $\omega \simeq 2\pi$, respectively. Thus, we can confirm that the amplitudes and frequency of the generated oscillation are close to the given values $A_1 = 1,\ A_3 = 0.01$, and $\omega = 2\pi$.

Although we use the simple system in this section, we can extend the proposed method to more complex system because the amplitude relations is obtained relatively easily such as the previous section.

4.6 Concluding Remarks

We proposed the reduction of the HB equation using invariants based on the symmetry of the system. The invariants enable to reduce the degree of the bifurcation diagram because the different but equivalent solutions are transformed into a unique solution. We confirmed that the proposed method dramatically reduces the computational cost by the bifurcation diagram represented by the invariant. Next we proposed a method to obtain relations of amplitudes at each frequency component by eliminating the information of phase. Further, we proposed a method for determining the design parameters of oscillators using the relations of the amplitudes, and confirmed the efficiency by an example with van der Pol oscillator.

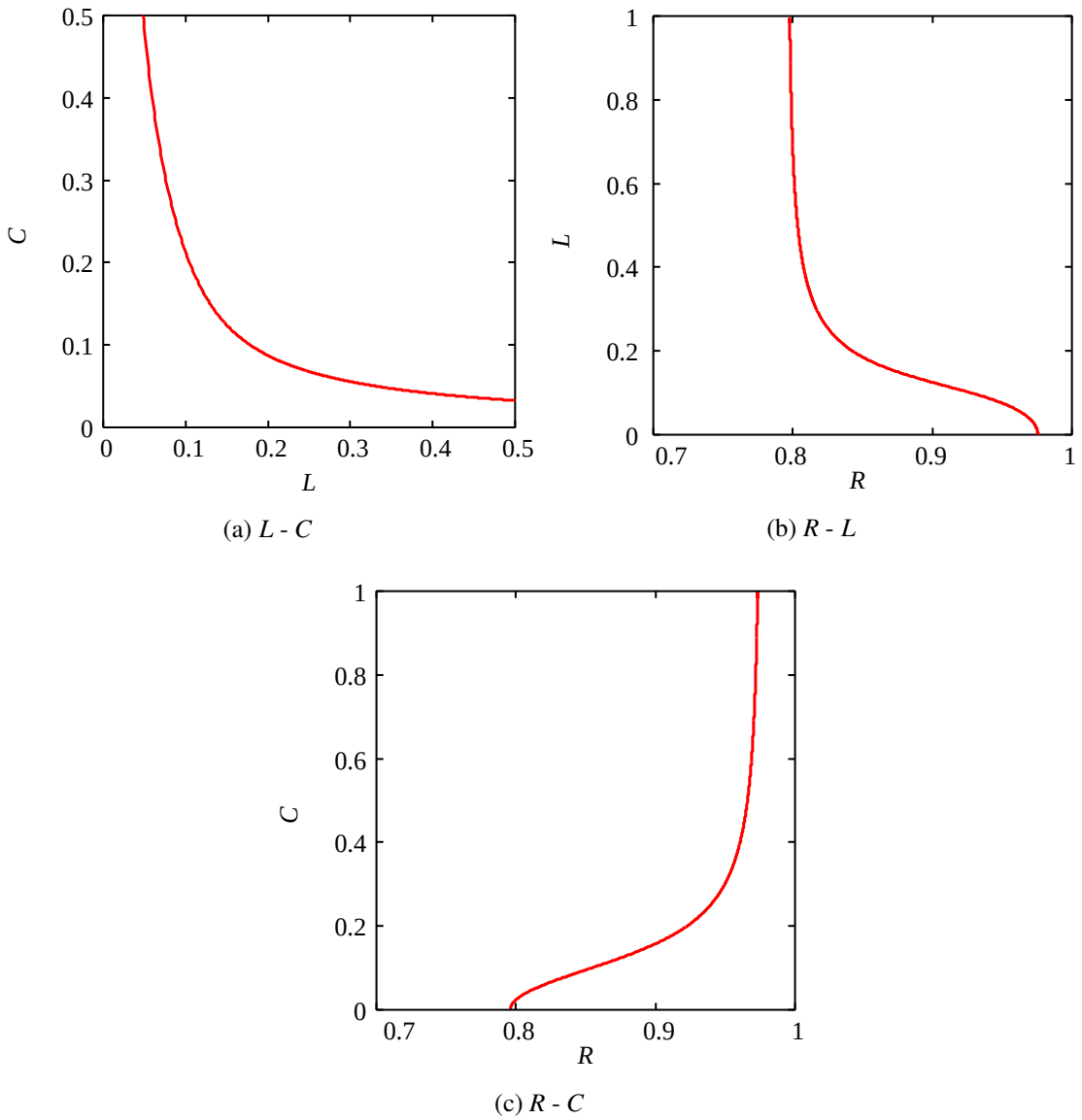

(a) L - C

(b) R - L

(c) R - C

Figure 4.6: Relations between the circuit parameters R, L, and C of the van der Pol oscillator ($A_1 = 1,\ \omega = 2\pi,\ \rho = 0.3448,\ K = 0.6218$).

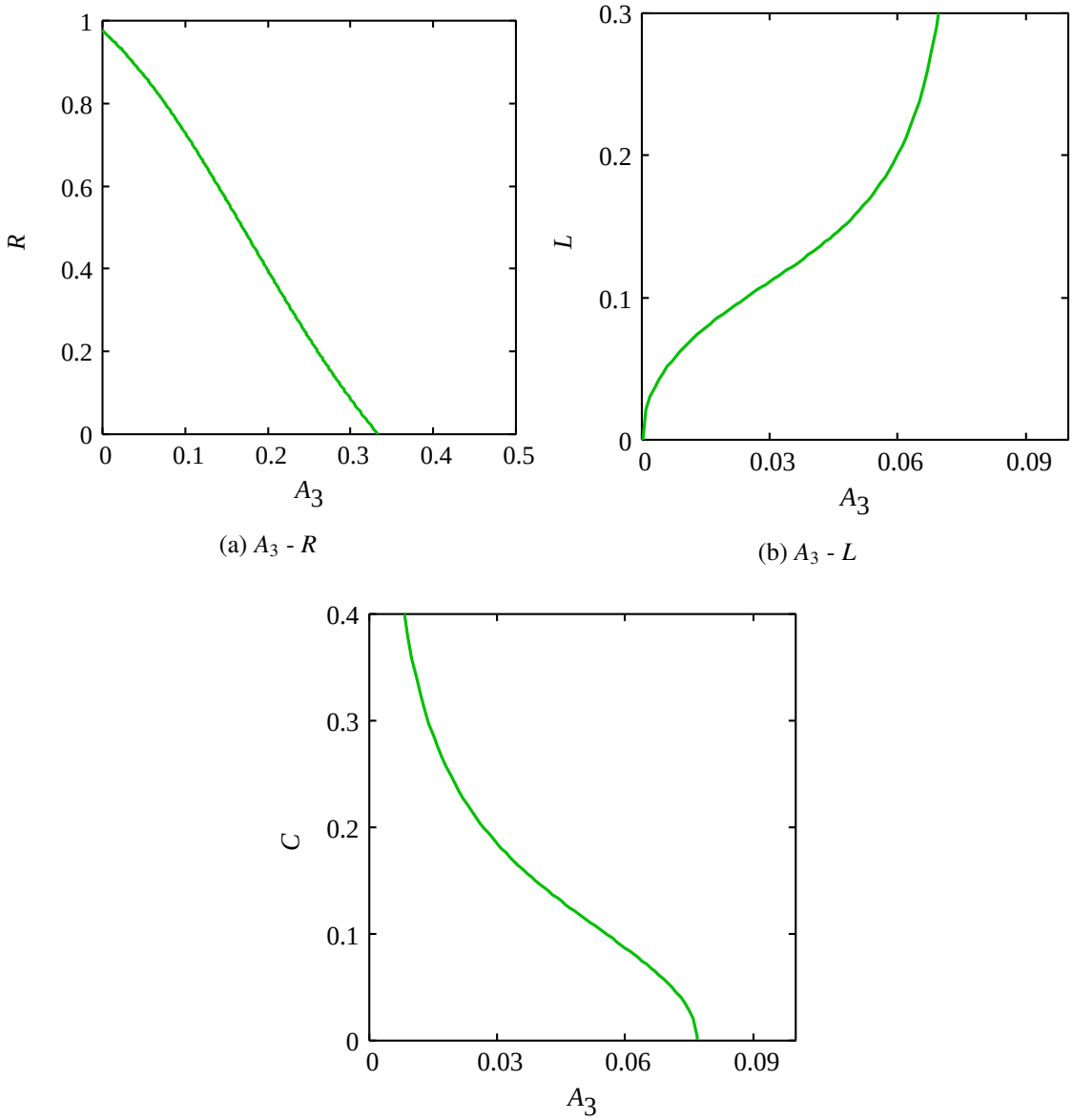

(a) A_3 - R

(b) A_3 - L

(c) A_3 - C

Figure 4.7: Relations between the invariant A_3 and the circuit parameters R, L, and C of the van der Pol oscillator ($A_1 = 1,\ \omega = 2\pi,\ \rho = 0.3448,\ K = 0.6218$).

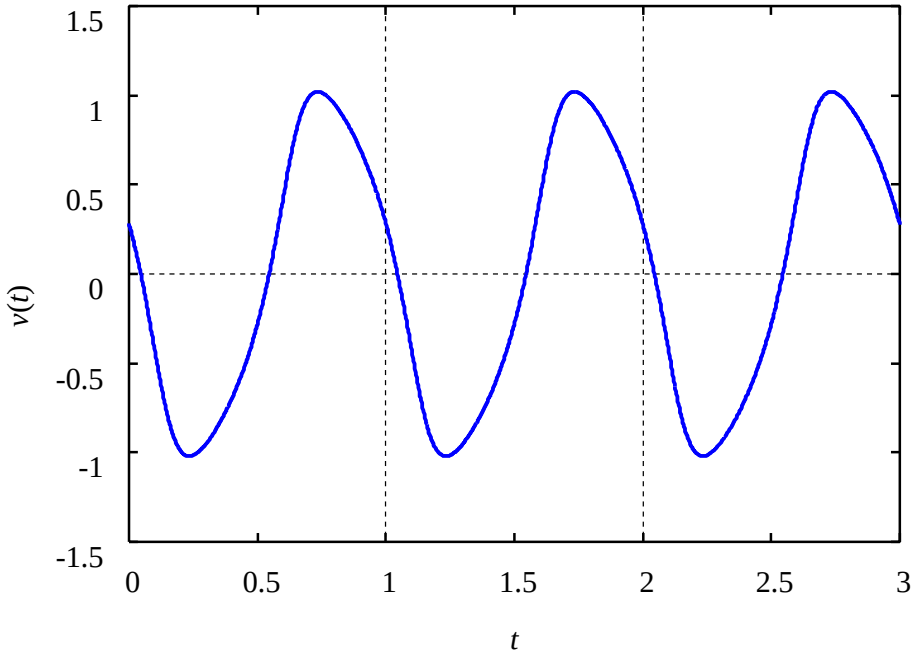

(a) Voltage waveform

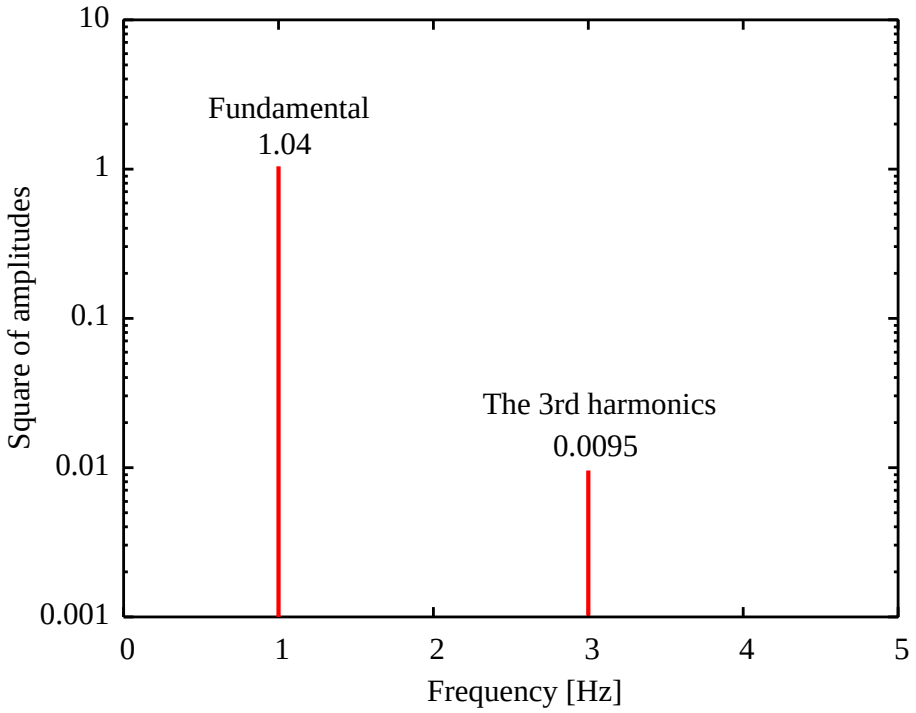

(b) Spectrum

Figure 4.8: Confirmation of the method for determining the circuit parameters by Runge-Kutta method (R = 0.957, L = 0.0654 and C = 0.359).

Chapter 5

Algebraic Representation of Error Bound

5.1 Introduction

Because the HB method has a truncation error, an approximated periodic solution have been guaranteed by the error bound, which is a region containing the approximated solution and the exact solution [13–15]. In particular, Swern presented a method to obtain the error bound for a feedback system with a polynomial-type nonlinear element [15]. However, if we need to obtain guaranteed bifurcation diagrams evaluated by the error bound, the numerical computation is very time-consuming because we must express the error bound as a set of numerical values. In order to overcome the limitation of the numerical approaches, in this chapter, we propose an algebraic representation of the error bound using Gröbner base. The representation is described by a single algebraic equation with system parameters. The proposed method does not depend on the number of specific frequency components. Further, linear elements of the system are contained as parameters. Thus, when we fix the nonlinear elements, the algebraic representation can be uniquely obtained.

In order to visualize the error bound, we project the error bound to a complex plane of a target frequency component using the algebraic representation. However, the computation of its projection is time-consuming. Thus, we propose an approximated error bound using the algebraic representation. The approximation of the error bound decreases the computational cost of the projection considerably.

When we set the values of the system parameters close to bifurcation values, there exist multiple error bounds in the neighborhood. In such cases, the error bounds are broken by a collision of them. Hence, we cannot guarantee the solutions near the bifurcation point. We present a

method to obtain the accurate break point of the error bound using the algebraic representation of the error bound.

5.2 Redefinition of HB Equation and Error Bound

5.2.1 Redefinition of HB Method

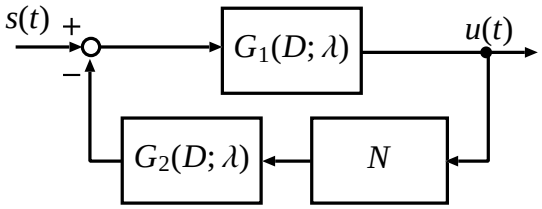

Figure 5.1: Nonlinear feedback system.

Because the proposed method in this chapter is based on the method reported by Swern [15], let us consider transformation of the system in Chapter 2 into the nonlinear feedback system which consists of one scalar state variable and one scalar input shown in Figure 5.1. The system equation is described by

$$u(t) \quad = \quad G_1(D;\boldsymbol{\lambda})\left\{s(t) - G_2(D;\boldsymbol{\lambda})N[u(t)]\right\}, \tag{5.1}$$

where $D = \mathrm{d}/\mathrm{d}t$, $u(t)$ is the scalar state variable, $s(t)$ is the scalar input function with the period $2\pi/\omega_s$, $\boldsymbol{\lambda} = (\lambda_1, \ldots, \lambda_l)$ is a set of system parameters, $G_1(D;\boldsymbol{\lambda})$, $G_2(D;\boldsymbol{\lambda})$ denote linear operators, and $N[u]$ is a polynomial-type nonlinear element. Now, we assume that $N[u]$ is represented by

$$N[u] \quad = \quad \sum_{i=0}^{q} c_{2i+1}u^{2i+1}, \quad c_{2i+1} \geq 0, \quad i = 0, \ldots q, \tag{5.2}$$

and $G_1(D;\boldsymbol{\lambda})$, $G_2(D;\boldsymbol{\lambda})$ must satisfy the following condition;

$$\sup_{0<k<\infty}\left|kG_1(\mathrm{j}k\omega;\boldsymbol{\lambda})\right| < \infty, \quad \sup_{0<k<\infty}\left|kG_1(\mathrm{j}k\omega;\boldsymbol{\lambda})G_2(\mathrm{j}k\omega;\boldsymbol{\lambda})\right| < \infty. \tag{5.3}$$

Let us apply the HB method to the equation (5.1). We assume that Eq.(5.1) has a periodic solution with the period $2\pi/\omega$ with $\omega_s = m\omega$. Thus, the solution $u(t)$ is given by

$$u(t) \quad \equiv \quad \sum_{k=0}^{\infty}\Re\left[X_k e^{\mathrm{j}k\omega t}\right] = \sum_{k=0}^{\infty}\Re\left[(x_{\mathrm{r}k} + \mathrm{j}x_{\mathrm{s}k})e^{\mathrm{j}k\omega t}\right], \tag{5.4}$$

where $X_k \in \mathbb{C}$ and $x_{s0} = 0$. Now, assuming that a projection operator K_L corresponds to the operator K^* in Chapter 2, the above solution is approximated by

$$u_L(t) \equiv K_L u(t) \equiv \sum_{k=0}^{p} \Re\left[X_k e^{jk\omega t}\right] = \sum_{k=0}^{p} \Re\left[(x_{rk} + jx_{sk})e^{jk\omega t}\right]. \tag{5.5}$$

Using the operator K_L and approximated solution (5.5), we can rewrite Eq.(5.1) to

$$\sum_{k=0}^{p} \Re\left[\left(X_k - G_1(j\omega k; \boldsymbol{\lambda})\left\{E_k - G_2(j\omega k; \boldsymbol{\lambda})Y_k\right\}\right) e^{jk\omega t}\right] = 0, \tag{5.6}$$

due to $D^n e^{j\omega t} = (j\omega k)^n e^{j\omega t}$, where

$$\begin{aligned} K_L s(t) &= \sum_{k=0}^{p} E_k e^{jk\omega t}, \quad E_k \in \mathbb{C}, \\ K_L N[u_L(t)] &= \sum_{k=0}^{p} Y_k e^{jk\omega t}, \quad Y_k \in \mathbb{C}. \end{aligned}$$

By this relation, HB equation is redefined by

$$\begin{aligned} \boldsymbol{f}(\boldsymbol{x}) &= \boldsymbol{f}(\boldsymbol{x}; \omega, \boldsymbol{\lambda}, \boldsymbol{e}) \\ &\equiv \left(f_{r0}, f_{r1}, f_{s1}, \ldots, f_{rp}, f_{sp}\right)^T = \boldsymbol{0} \in \mathbb{R}^N, \\ f_{r0} &\equiv \Re\left[X_0 - G_1(0; \boldsymbol{\lambda})\left\{E_0 - G_2(0; \boldsymbol{\lambda})Y_0\right\}\right], \\ f_{s0} &= 0, \\ f_{rk} &\equiv \Re\left[X_k - G_1(j\omega k; \boldsymbol{\lambda})\left\{E_k - G_2(j\omega k; \boldsymbol{\lambda})Y_k\right\}\right], \\ f_{sk} &\equiv \Im\left[X_k - G_1(j\omega k; \boldsymbol{\lambda})\left\{E_k - G_2(j\omega k; \boldsymbol{\lambda})Y_k\right\}\right], \\ \boldsymbol{x} &\equiv (x_{r0}, x_{r1}, x_{s1}, \ldots, x_{rp}, x_{sp})^T \in \mathbb{R}^N, \\ \boldsymbol{e} &\equiv (e_{r0}, e_{r1}, e_{s1}, \ldots, e_{rp}, e_{sp})^T \in \mathbb{R}^N, \\ E_k &= e_{rk} + je_{sk}, \quad E_0 = e_{r0}, \\ k &= 1, \ldots, p, \end{aligned} \tag{5.7}$$

and $N = 2p + 1$ is the number of unknowns of the HB equation $\boldsymbol{f}(\boldsymbol{x}) = \boldsymbol{0}$.

5.2.2 Error Bound for HB Method

Because the HB method has a truncation error, we consider the error bound which gives a bounded region in which the solution of the HB equation and the exact solution exist. In order to find the error bound of the HB equation $\boldsymbol{f}(\boldsymbol{x}) = \boldsymbol{0}$, we extend the method reported in [15]

to the periodically forced system (cf. Appendix.E). Although the error bound is determined by Eqs.(E.26) and (E.35), its numerical computation is very time-consuming compared with solving the HB equation because the error bound is $N-1$ dimensional surface in N dimensional space.

5.3 Algebraic Representation of Error Bound

5.3.1 Error Bound by Gröbner Base

To overcome the difficulty of the numerical method, we try to represent the error bound algebraically using Gröbner base. In order to apply Gröbner techniques, we transform Eqs.(E.26) and (E.35) into polynomial equations. Multiplying the both sides of Eq.(E.26) by $i(1-\xi\eta)^{2q}$, we rewrite Eq.(E.26) to the following polynomial equation of the variable ξ;

$$f_{\mathrm{EB1}}(\xi, \boldsymbol{x}; \boldsymbol{\lambda}, \boldsymbol{e}) \equiv \xi(1-\xi\eta)^{2q} - \sum_{i=0}^{q}(2i+1)c_{2i+1}(1-\xi\eta)^{2(q-i)}\left(\sum_{k=0}^{p}\sqrt{x_{kr}^2 + x_{ks}^2}\right)^{2i} = 0, \quad (5.8)$$

where

$$\begin{aligned} \eta(\boldsymbol{\lambda}) &\equiv \sup_{|k|>p}\left|G(\mathrm{j}\omega k; \boldsymbol{\lambda})\right| \in \mathbb{R}, \quad (5.9)\\ \|F\|_\infty &\equiv \xi\eta, \\ G(D; \boldsymbol{\lambda}) &= G_1(D; \boldsymbol{\lambda})G_2(D; \boldsymbol{\lambda}). \end{aligned}$$

Moreover, multiplying the both sides of Eq.(E.35) by $(1-\xi\eta)$ and squaring it, we obtain

$$f_{\mathrm{EB2}}(\xi, \boldsymbol{x}; \omega, \boldsymbol{\lambda}, \boldsymbol{e}) \equiv \xi^4\eta^2\sum_{k=0}^{p}\left(x_{\mathrm{r}k}^2 + x_{\mathrm{s}k}^2\right) - (1-\xi\eta)^2\sum_{k=0}^{p}\left(f_{\mathrm{r}k}^2 + f_{\mathrm{s}k}^2\right) = 0. \quad (5.10)$$

The equation (5.10) is the polynomial equation with respect to ξ. Thus, the error bound is given by removing the variable ξ from the Eqs.(5.8) and (5.10).

Because Gröbner base of the block order $\xi \succ_{\mathrm{block}} \boldsymbol{x}$ enables to eliminate ξ from Eqs.(5.8) and (5.10), we can obtain the following algebraic representation of the error bound;

$$g_{\mathrm{EB}}(\boldsymbol{x}; \omega, \boldsymbol{\lambda}, \boldsymbol{e}) = 0. \quad (5.11)$$

However, the computational cost of Gröbner base is highly dependent on the complexity of Eqs.(5.8) and (5.10). In particular, the computational cost increases exponentially according to the expansion of the number p because we have to deal with $N+1$ variables. Thus, the algebraic representation (5.11) can not be calculated by the naive method if we consider more than 2 frequency components.

5.3.2 Efficient Method to Obtain Algebraic Representation

In order to resolve the problem of Gröbner base, we propose an efficient method to obtain the algebraic representation of the error bound using transformations of variables. Because the number p of the specific frequency components complicates only the norms in Eqs.(5.8) and (5.10), we transform the norms into new variables;

$$z_1(\boldsymbol{x}) \equiv \|u_{\mathrm{L}}(t)\|_1 = \sum_{k=0}^{p} \sqrt{x_{\mathrm{r}k}^2 + x_{\mathrm{s}k}^2}, \tag{5.12}$$

$$z_2(\boldsymbol{x}) \equiv \|u_{\mathrm{L}}(t)\|_2{}^2 = \sum_{k=0}^{p} \left(x_{\mathrm{r}k}^2 + x_{\mathrm{r}k}^2\right), \tag{5.13}$$

$$z_3(\boldsymbol{x};\omega,\boldsymbol{\lambda},\boldsymbol{e}) \equiv \|\mathrm{FH}(u_{\mathrm{L}})\|_2{}^2 = \sum_{k=0}^{p} \left(f_{\mathrm{r}k}^2(\boldsymbol{x};\omega,\boldsymbol{\lambda},\boldsymbol{e}) + f_{\mathrm{s}k}^2(\boldsymbol{x};\omega,\boldsymbol{\lambda},\boldsymbol{e})\right), \tag{5.14}$$

$$\boldsymbol{z} \equiv (z_1, z_2, z_3)^{\mathrm{T}}. \tag{5.15}$$

Thus, using the transformation of the variable $\boldsymbol{x}$ into $\boldsymbol{z}$, we rewrite Eqs.(5.8) and (5.10) by

$$f_{\mathrm{EB1}}(\xi, z_1; \eta) = \xi(1-\xi\eta)^{2q} - \sum_{i=0}^{q}(2i+1)c_{2i+1}\,(1-\xi\eta)^{2(q-i)}\,z_1{}^{2i} = 0, \tag{5.16}$$

$$f_{\mathrm{EB2}}(\xi, z_2, z_3; \eta) = \xi^4\eta^2 z_2 - (1-\xi\eta)^2 z_3 = 0. \tag{5.17}$$

Because the representations (5.16) and (5.17) have only 4 variables ξ, z_1, z_2, z_3 instead of $N+1$ variables in Eqs.(5.8) and (5.10), the difficulty of Gröbner base can be removed.

Then, $g_{\mathrm{EB}}(\boldsymbol{z};\eta)$ is obtained by the elimination of ξ using Gröbner base from Eqs.(5.16) and (5.17). Since the expression of Eqs.(5.16) and (5.17) are far simpler than those of Eqs.(5.8) and (5.10), the computational cost of obtaining $g_{\mathrm{EB}}(\boldsymbol{z};\eta)$ is remarkably less than the cost of Eq.(5.11) by the naive method. After we calculate $g_{\mathrm{EB}}(\boldsymbol{z};\eta)$, the algebraic representation (5.11) is obtained by the substitutions of $\boldsymbol{z}$, η into $g_{\mathrm{EB}}(\boldsymbol{z};\eta)$. Thus, the algorithm is given by

S1. We give the polynomial equations $f_{\mathrm{EB1}}(\xi, z_1; \eta) = 0$ and $f_{\mathrm{EB2}}(\xi, z_2, z_3; \eta) = 0$.

S2. We obtain $g_{\mathrm{EB}}(\boldsymbol{z};\eta)$ by the elimination of ξ using Gröbner base of order $\xi \succ_{\mathrm{block}} \boldsymbol{z}$ from f_{EB1} and f_{EB2}.

S3. We obtain the algebraic representation (5.11) of the error bound by the substitution of $\boldsymbol{z}$ and η into the $g_{\mathrm{EB}}(\boldsymbol{z};\eta)$.

As is easily seen from this algorithm, we can obtain the algebraic representation (5.11) of the error bound even if we consider many frequency components. Moreover, the representation $g_{\mathrm{EB}}(\boldsymbol{z};\eta)$ is uniquely determined only by the nonlinear element $N[u]$ because the linear operators G_1 and G_2 are contained only in the variable $\boldsymbol{z}$ and the parameter η in $g_{\mathrm{EB}}(\boldsymbol{z};\eta)$ symbolically.

5.3.3 Example

We apply the proposed method to the fundamental harmonic oscillations ($m = 1$) in Duffing equation [1];

$$\frac{\mathrm{d}^2u(t)}{\mathrm{d}t^2} + \mu\frac{\mathrm{d}u(t)}{\mathrm{d}t} + u^3 = E\cos\omega t, \tag{5.18}$$

which corresponds to Eq.(2.11). This equation can be rewritten as Eq.(5.19);

$$\begin{aligned} u(t) &= G_1(D;\mu)\left\{s(t) - G_2(D;\mu)N[u(t)]\right\}, \\ & s(t) = E\cos\omega t, \quad N[u(t)] = u^3, \\ & G_1(D;\mu) = \frac{1}{D^2+\mu D}, \quad G_2 = 1, \quad G = G_1. \end{aligned} \tag{5.19}$$

The equations f_{EB1} and f_{EB2} is written by

$$f_{\mathrm{EB1}}(\xi, z_1;\eta) = \xi(1-\xi\eta)^2 - 3{z_1}^2 = 0, \tag{5.20}$$

$$f_{\mathrm{EB2}}(\xi, z_2, z_3;\eta) = \xi^4\eta^2 z_2 - (1-\xi\eta)^2 z_3 = 0. \tag{5.21}$$

Thus, we obtain the following algebraic representation $g_{\mathrm{EB}}(\boldsymbol{z};\eta)$ of the error bound by the elimination of ξ using Gröbner base of the block order $\xi \succ_{\mathrm{block}} \boldsymbol{z}$;

$$\begin{aligned} g_{\mathrm{EB}}(\boldsymbol{z};\eta) &= 9{z_1}^4\eta^6{z_3}^3 - 135{z_1}^4 z_2\eta^4{z_3}^2 - 6{z_1}^2 z_2\eta^3{z_3}^2 - 270{z_1}^6{z_2}^2\eta^3 z_3 \\ &\quad +225{z_1}^4{z_2}^2\eta^2 z_3 - 30{z_1}^2{z_2}^2\eta z_3 + {z_2}^2 z_3 - 81{z_1}^8{z_2}^3\eta^2 = 0. \end{aligned} \tag{5.22}$$

Let us compare the proposed method using Gröbner base of the block order $\xi \succ_{\mathrm{block}} \boldsymbol{z}$ with the naive method of the block order $\xi \succ_{\mathrm{block}} \boldsymbol{x}$. The computational cost of both methods is shown in Table 5.1 where $p = 1$. From this table, we can confirm the efficiency of the proposed method.

Further, Eq.(5.22) does not contain the linear operator $G(D;\mu)$ and the number of the specific frequency components explicitly. Thus, when we fix the nonlinear element $N[u]$, we can obtain the algebraic representation (5.11) from $g_{\mathrm{EB}}(\boldsymbol{z};\eta)$ even if we consider many frequency components.

Table 5.1: Comparison of computational cost between proposed method and naive method ($p = 1$)

Method	Order of variables	Computation time [s]	Required memory [MB]
Naive method	$\xi \succ_{\text{block}} \boldsymbol{x}$	7425	956
Proposed method	$\xi \succ_{\text{block}} \boldsymbol{z}$	0.007	1.09

Calculated by a PC with Xeon 3.06GHz CPU.

5.4 Fast Computation of Approximated Error Bound

5.4.1 Quadratic Approximation of Error Bound

In this section, we propose an application of the algebraic representation of the error bound. If we need to obtain a guaranteed bifurcation diagram of the HB equation by the error bound, its numerical computation is huge time-consuming because we must calculate the projection of the error bound to a target frequency component for all specified parameters one by one. In order to reduce the computational cost of the projection, we propose an approximated error bound using the algebraic representation of the error bound. Although we cannot guarantee solutions of the HB equation by the proposed error bound, the computational cost of the projection is dramatically reduced. The proposed approximation utilizes the fact that the error bound is in the neighborhood of the solution of the HB equation, and resembles an ellipsoidal body in general. Namely, we approximate the error bound to the quadratic form using variations of the solution.

Let us consider the projection of the error bound to a complex plane $(x_{\mathrm{r}l}, x_{\mathrm{s}l})$ for $l \in 1, \ldots, p$. Then we rewrite the vector of the variable

$$\begin{aligned} \boldsymbol{x} &= (x_{\mathrm{r}l}, x_{\mathrm{s}l}, x_{\mathrm{r}0}, \ldots, x_{\mathrm{r}l-1}, x_{\mathrm{s}l-1} x_{\mathrm{r}l+1}, x_{\mathrm{s}l+1} \ldots, x_{\mathrm{r}p}, x_{\mathrm{s}p})^{\mathrm{T}} \\ &\equiv (x_1, x_2, \ldots, x_N)^{\mathrm{T}}. \end{aligned} \tag{5.23}$$

Further, we consider that the variable $\boldsymbol{x}$ is described by

$$\boldsymbol{x} = \tilde{\boldsymbol{x}} + \Delta \boldsymbol{x}, \tag{5.24}$$

where, $\tilde{\boldsymbol{x}} \equiv (\tilde{x}_1, \ldots, \tilde{x}_N)^{\mathrm{T}}$ is a vector of the solution of the HB equation and $\Delta \boldsymbol{x} \equiv (\Delta x_1, \ldots, \Delta x_N)^{\mathrm{T}}$ is a vector of its variations.

Using $\Delta\boldsymbol{x}$ and Taylor expansion, we obtain the quadratic approximation $g_{\Delta\mathrm{EB}}(\Delta\boldsymbol{x};\omega,\boldsymbol{\lambda},\boldsymbol{e})$ of the error bound as follows;

$$\begin{aligned} g_{\mathrm{EB}}(\boldsymbol{x};\omega,\boldsymbol{\lambda},\boldsymbol{e}) &\approx g_{\Delta\mathrm{EB}}(\Delta\boldsymbol{x};\omega,\boldsymbol{\lambda},\boldsymbol{e}) \\ &= \sum_{i=1}^{N} a_{ii}\Delta x_i^2 + 2\sum_{i=1}^{N}\sum_{j=i+1}^{N} a_{ij}\Delta x_i\Delta x_j + 2\sum_{i=1}^{N} a_{0i}\Delta x_i + a_{00}. \end{aligned} \tag{5.25}$$

Then, the approximated error bound is rewritten by

$$g_{\Delta\mathrm{EB}}(\Delta\boldsymbol{x};\omega,\boldsymbol{\lambda},\boldsymbol{e}) = (1,\Delta\boldsymbol{x}^{\mathrm{T}})\boldsymbol{A}\begin{bmatrix} 1 \\ \Delta\boldsymbol{x} \end{bmatrix} = 0, \tag{5.26}$$

where

$$\boldsymbol{A} \equiv \boldsymbol{A}(\tilde{\boldsymbol{x}},\omega,\boldsymbol{\lambda},\boldsymbol{e}) \equiv \begin{bmatrix} a_{00} & a_{01} & \cdots & a_{0N} \\ a_{01} & a_{11} & \cdots & a_{1N} \\ \vdots & \vdots & \ddots & \vdots \\ a_{0N} & a_{1N} & \cdots & a_{NN} \end{bmatrix} \in \mathbb{R}^{(N+1)\times(N+1)}.$$

In order to obtain the projection of the approximated error bound $g_{\Delta\mathrm{EB}}(\Delta\boldsymbol{x};\omega,\boldsymbol{\lambda},\boldsymbol{e})$, we decompose $\boldsymbol{A}(\tilde{\boldsymbol{x}},\omega,\boldsymbol{\lambda},\boldsymbol{e})$ and $\Delta\boldsymbol{x}$ into

$$\boldsymbol{A} \equiv \begin{bmatrix} \boldsymbol{A}_1 & \boldsymbol{A}_2 \\ \boldsymbol{A}_2^{\mathrm{T}} & \boldsymbol{A}_3 \end{bmatrix},\ \begin{bmatrix} 1 \\ \Delta\boldsymbol{x} \end{bmatrix} \equiv \begin{bmatrix} \Delta\boldsymbol{x}_1 \\ \Delta\boldsymbol{x}_2 \end{bmatrix},\ \Delta\boldsymbol{x}_1 = \begin{bmatrix} 1 \\ \Delta x_1 \\ \Delta x_2 \end{bmatrix},\ \Delta\boldsymbol{x}_2 = \begin{bmatrix} \Delta x_3 \\ \vdots \\ \Delta x_N \end{bmatrix}, \tag{5.27}$$

where partial matrices of $\boldsymbol{A}$ denote $\boldsymbol{A}_1 \in \mathbb{R}^{3\times3}$, $\boldsymbol{A}_2 \in \mathbb{R}^{(N-2)\times3}$ and $\boldsymbol{A}_3 \in \mathbb{R}^{(N-2)\times(N-2)}$, respectively. Now let

$$\nabla g_{\Delta\mathrm{EB}} = \left(\frac{\partial g_{\Delta\mathrm{EB}}}{\partial\Delta x_1},\ldots\frac{\partial g_{\Delta\mathrm{EB}}}{\partial\Delta x_N}\right)^{\mathrm{T}} \in \mathbb{R}^N \tag{5.28}$$

be a gradient vector of $g_{\Delta\mathrm{EB}}$. Then, the boundary of the projected error bound to (x_1, x_2) plane satisfies that $\nabla g_{\Delta\mathrm{EB}}$ is orthogonal to the following unit vectors which are parallel to the $x_3,\ldots,x_N$ axes.

$$\begin{array}{llllll} (0, & 0, & 0, & 1, & 0, & \ldots,\ 0)^{\mathrm{T}}, \\ (0, & 0, & 0, & 0, & 1, & \ldots,\ 0)^{\mathrm{T}}, \\ & & & \vdots & & \\ (0, & 0, & 0, & 0, & 0, & \ldots,\ 1)^{\mathrm{T}}. \end{array} \tag{5.29}$$

Namely, the projection of $g_{\Delta\mathrm{EB}}(\Delta\boldsymbol{x})$ satisfies

$$\frac{\partial g_{\Delta\mathrm{EB}}(\Delta\boldsymbol{x})}{\partial \Delta x_k} = 0, \quad k = 3, \ldots, N. \tag{5.30}$$

Thus, applying this relation to Eq.(5.26), we obtain a constraint for the projection;

$$\boldsymbol{A}_2^{\mathrm{T}}\Delta\boldsymbol{x}_1 + \boldsymbol{A}_3\Delta\boldsymbol{x}_2 = \boldsymbol{0}. \tag{5.31}$$

As a result, the projection of the approximated error bound is represented by

$$\begin{aligned}
(1, \Delta\boldsymbol{x}^{\mathrm{T}})\boldsymbol{A}\begin{bmatrix} 1 \\ \Delta\boldsymbol{x} \end{bmatrix} &= \left(\Delta\boldsymbol{x}_1^{\mathrm{T}}, \Delta\boldsymbol{x}_2^{\mathrm{T}}\right)\begin{bmatrix} \boldsymbol{A}_1\Delta\boldsymbol{x}_1 + \boldsymbol{A}_2\Delta\boldsymbol{x}_2 \\ \boldsymbol{0} \end{bmatrix} \\
&= \Delta\boldsymbol{x}_1^{\mathrm{T}}\boldsymbol{A}_1\Delta\boldsymbol{x}_1 + \Delta\boldsymbol{x}_1^{\mathrm{T}}\boldsymbol{A}_2\Delta\boldsymbol{x}_2 \\
&= \Delta\boldsymbol{x}_1^{\mathrm{T}}\left(\boldsymbol{A}_1 - \boldsymbol{A}_2\boldsymbol{A}_3^{-1}\boldsymbol{A}_2^{\mathrm{T}}\right)\Delta\boldsymbol{x}_1 = 0.
\end{aligned} \tag{5.32}$$

Finally, the substitution of $\Delta x_1 = x_1 - \tilde{x}_1$, $\Delta x_2 = x_2 - \tilde{x}_2$ into Eq.(5.32) gives the projection of the approximated error bound.

The quadratic approximation algorithm is written by

S1. We calculate the algebraic representation (5.11) of the error bound using Gröbner base.

S2. We set the target complex plane (x_1, x_2) and other variables $x_3, \ldots, x_N$.

S3. We obtain algebraic representations of the elements $a_{ij}(\tilde{\boldsymbol{x}}, \omega, \boldsymbol{\lambda}, \boldsymbol{e})$, $(i, j = 0, \ldots, N, i \leq j)$ of the matrix $\boldsymbol{A}$ with the solution $\tilde{\boldsymbol{x}}$ of the HB equation and the system parameters ω, $\boldsymbol{\lambda}$, $\boldsymbol{e}$.

S4. We determine a_{ij} by the substitution of the given solution $\tilde{\boldsymbol{x}}$ and parameters ω, $\boldsymbol{\lambda}$, $\boldsymbol{e}$ into $a_{ij}(\tilde{\boldsymbol{x}}, \omega, \boldsymbol{\lambda}, \boldsymbol{e})$, $(i, j = 0, \ldots, N, i \leq j)$.

S5. We obtain the projection of the approximated error bound by $\boldsymbol{A}_1 - \boldsymbol{A}_2\boldsymbol{A}_3^{-1}\boldsymbol{A}_2^{\mathrm{T}}$ and the substitution of $\Delta x_1 = x_1 - \tilde{x}_1$, $\Delta x_2 = x_2 - \tilde{x}_2$ into Eq.(5.32).

Using this algorithm, the projection of the error bound can be plotted easily on a two-dimensional space. Thus, we can reduce the computational cost of the guaranteed bifurcation diagram of the HB equation using the approximated error bound though the proposed method approximately guarantees solutions of the HB equation,

5.4.2 Example

We apply the quadratic approximation of the error bound to Duffing equation (5.18), where we assume that zero frequency component is zero for simplicity because it complicates the projection of the error bound. We consider the approximated projection to fundamental frequency component, namely, $x_1 = x_{\mathrm{r}1}, x_2 = x_{\mathrm{s}1}, x_3 = x_{\mathrm{r}2}, \ldots, x_{N-1} = x_{\mathrm{r}p}, x_N = x_{\mathrm{s}p}$, and $f_1 = f_{\mathrm{r}1}, f_2 = f_{\mathrm{s}1}, f_3 = f_{\mathrm{r}2}, \ldots, f_{N-1} = f_{\mathrm{r}p}, f_N = f_{\mathrm{s}p}$, where $N = 2p$. Let a solution of the HB equation $\boldsymbol{f}(\boldsymbol{x}; \omega, \mu, E) = \boldsymbol{0}$ be $\tilde{\boldsymbol{x}} = (\tilde{x}_1, \ldots, \tilde{x}_N)^{\mathrm{T}}$. Then the matrix $\boldsymbol{A}$ of the approximated error bound is represented by the elements

$$
\begin{aligned}
a_{00} &= -81\eta^2\tilde{z}_1^8\tilde{z}_2, && (5.33)\\
a_{0i} &= -81\eta^2\tilde{z}_1^8\tilde{x}_i + 4\tilde{z}_1^7\tilde{z}_{1,i}\tilde{z}_2, && (5.34)\\
a_{ii} &= -81\eta^2\tilde{z}_1^6(16\tilde{z}_1\tilde{z}_{1,i}\tilde{x}_i + 8\tilde{z}_1\tilde{z}_{1,ii}\tilde{z}_2 + 28\tilde{z}_{1,i}^2\tilde{z}_2 + \tilde{z}_1^2),\\
&\quad (225\tilde{z}_1^4\eta^2 - 30\tilde{z}_1^4\eta - 270\tilde{z}_1^6\eta^3 + 1)\sum_{k=1}^{N}\left(\frac{\partial f_k(\tilde{\boldsymbol{x}}; \omega, \mu, E)}{\partial \tilde{x}_i}\right)^2 && (5.35)\\
a_{ij} &= -81\eta^2\tilde{z}_1^6(8\tilde{z}_1\tilde{z}_{1,i}\tilde{x}_j + 8\tilde{z}_1\tilde{z}_{1,j}\tilde{x}_i + 28\tilde{z}_{1,i}\tilde{z}_{1,j}\tilde{z}_2 + 4\tilde{z}_1\tilde{z}_{1,ij}\tilde{z}_2)\\
&\quad +(225\tilde{z}_1^4\eta^2 - 30\tilde{z}_1^4\eta - 270\tilde{z}_1^6\eta^3 + 1)\sum_{k=1}^{N}\left(\frac{\partial f_k(\tilde{\boldsymbol{x}}; \omega, \mu, E)}{\partial \tilde{x}_j}\frac{\partial f_k(\tilde{\boldsymbol{x}}; \omega, \mu, E)}{\partial \tilde{x}_i}\right), && (5.36)
\end{aligned}
$$

where

$$
\tilde{z}_1 = \sum_{k=1}^{p}\sqrt{\tilde{x}_{2k}^2 + \tilde{x}_{2k+1}^2},\quad \tilde{z}_{1,i} = \frac{\tilde{x}_i}{\Delta_{\tilde{z},i}},\quad \tilde{z}_{1,ij} = \begin{cases} \dfrac{\tilde{x}_i}{2\Delta_{\tilde{z},i}} - \dfrac{\tilde{x}_i^2}{2\Delta_{\tilde{z},i}^3} & i = j \\ -\dfrac{\tilde{x}_i\tilde{x}_j}{2\Delta_{\tilde{z},i}} & |i-j| = 1 \\ 0 & |i-j| \neq 1 \end{cases},
$$

$$
\Delta_{\tilde{z},i} = \begin{cases} \sqrt{\tilde{x}_i^2 + \tilde{x}_{i+1}^2} & i = 1 \bmod 2 \\ \sqrt{\tilde{x}_{i-1}^2 + \tilde{x}_i^2} & i = 0 \bmod 2 \end{cases},
$$

$$
\tilde{z}_2 = \sum_{k=1}^{N}\tilde{x}_k^2,
$$

$$
i = 1, \ldots, N,\ j = 1, \ldots, N,
$$

$$
\eta = \frac{1}{(p+1)\sqrt{(p+1)^2 + \mu^2}}.
$$

In order to confirm the validity of the approximation, the projections by the proposed method and the method in [15] are shown in Figure 5.2 where $\omega = 1,\ \mu = 0.1,\ E = 0.35,\ p = 4, 6, 8$.

We can see that the projection of the approximated error bound is very close to the projection in [15].

Moreover, the projection of the approximated error bound with the parameter E varying from 0.1 to 0.4 is shown in Figure5.3 where $\omega = 1$, $\mu = 0.1$ and $p = 4$. Because the elements (5.33), (5.34), (5.35) and (5.36) contain the system parameters symbolically, the approximated error bound can be easily obtained even if we change the system parameters as shown in Figure 5.3.

Further, the computational time of the proposed method and the method in [15] for $p = 4, 6, 8, 20$ is shown in Table 5.2 when we vary the parameters μ from 0.1 to 1.0, E from 0.1 to 0.4. Additionally, we also show the solving time of the HB equation in Table 5.2. Although the proposed method in Table 5.2 does not contain the computational cost of $g_{\mathrm{EB}}(\boldsymbol{x}; \omega, \mu, E)$, $g_{\mathrm{EB}}(\boldsymbol{x}; \omega, \mu, E)$ is calculated only once and the computational cost is very low as shown in Table 5.1. Thus, we can confirm that the proposed method reduces the computational cost of the error bound dramatically. Although the conventional method is very time-consuming compared with solving the HB equation, the proposed method approximately guarantees the solutions as fast as solving the HB equation.

Table 5.2: Computational time of obtaining projection of error bound [s] (μ varied from 0.1 to 1.0 and E varied from 0.1 to 0.4, using Newton method with $90 \times 300 \times 32$ points)

Method	$p = 4$	$p = 6$	$p = 8$	$p = 20$
HB method	1.50	2.23	3.47	16.63
Method in [15]	237.02	303.73	390.45	1172.47
Proposed method	7.52	8.70	10.29	26.22

Calculated by a PC with Xeon 3.06GHz CPU.

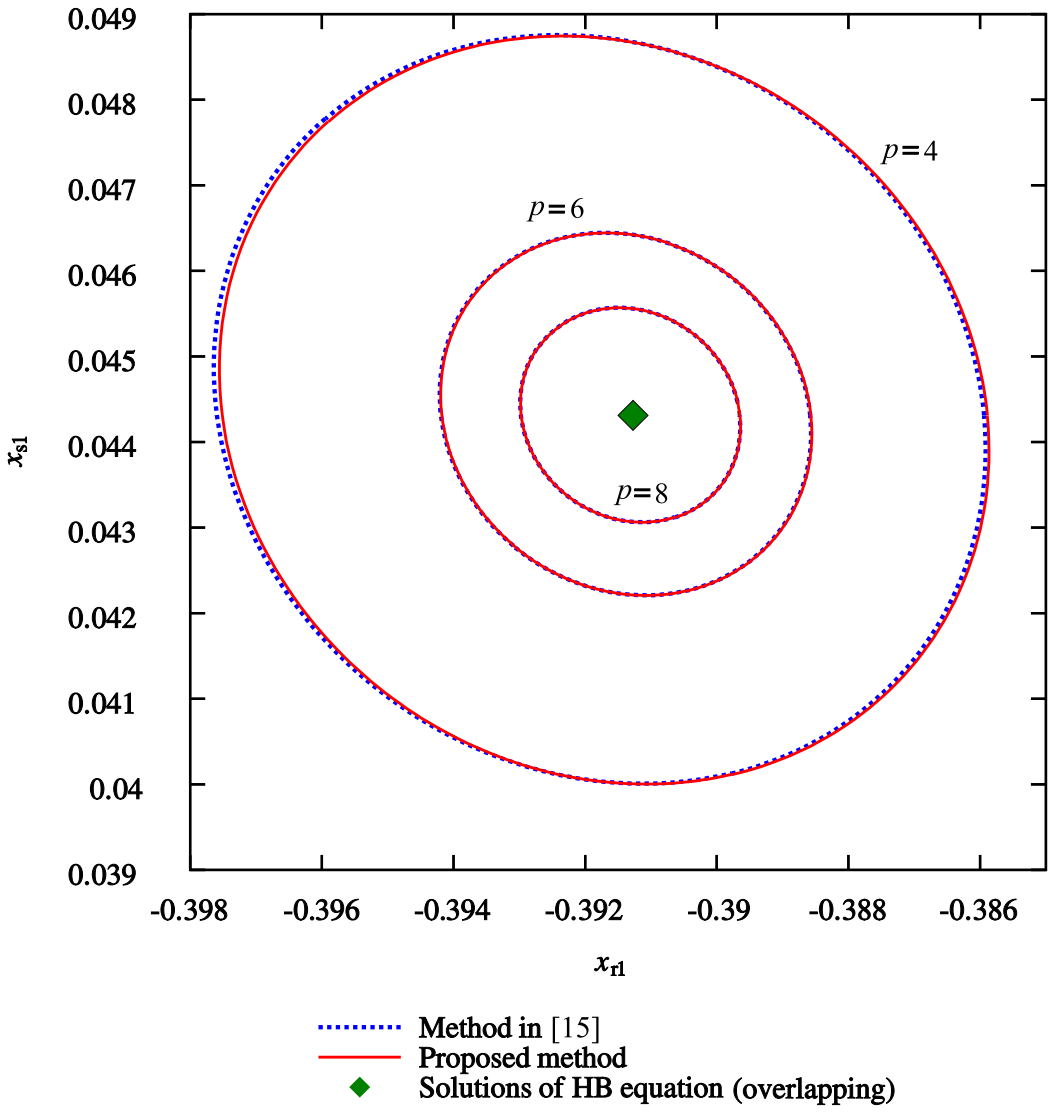

Figure 5.2: Projections of error bound for HB method on the (x_{r1}, x_{s1}) plane ($\omega = 1, \mu = 0.1$, $E = 0.35$ and $p = 4, 6, 8$).

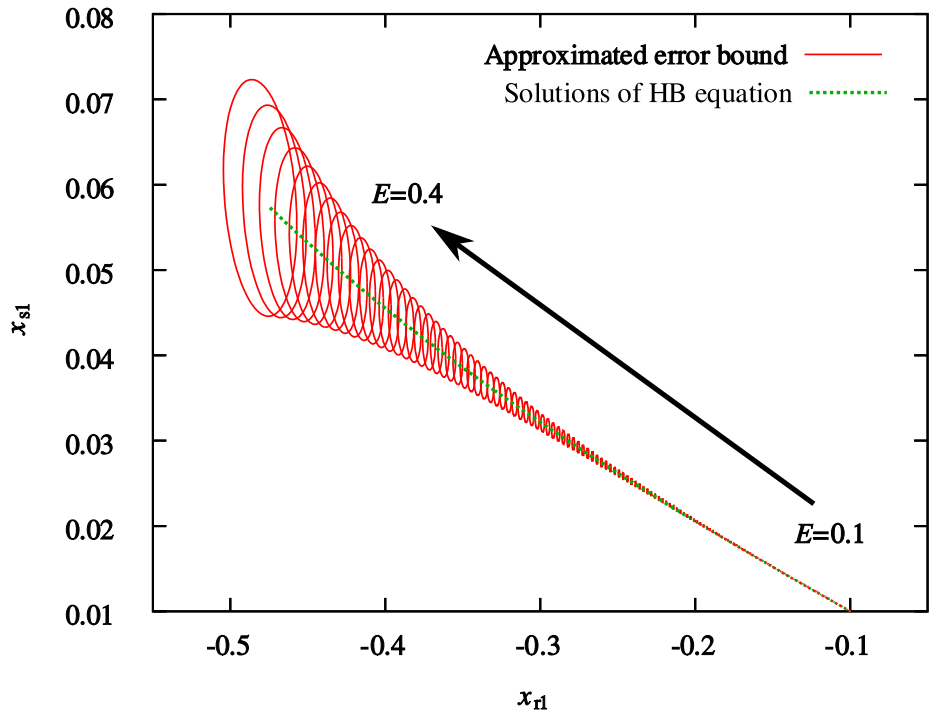

Figure 5.3: Projection of approximated error bound with parameter E varying from 0.1 to 0.4 ($\omega = 1, \mu = 0.1$ and $p = 4$).

5.5 Break Point of Error Bound

5.5.1 Break Point and Singular Point of Error Bound

In this section, we propose another application of the algebraic representation of the error bound. When we set the system parameters close to bifurcation values, there exist two solutions of the HB equation in the neighborhood. In such cases, we can not guarantee these solutions by the error bound because the error bound containing only a single solution of the HB equation can guarantee the solution (cf.Appendix.E). Namely, two error bounds containing the solutions of the HB equation are broken by a collision of each other near the bifurcation point. We call this collision point a break point of the error bound. Although the break point is important for the guaranteed bifurcation diagram by the error bound, it is difficult to obtain the break point using numerical computations. We propose a method to obtain the accurate break point using the algebraic representation of the error bound. We assume that the approximated bifurcation diagram has already calculated.

Because a gradient vector of singular points equals zero in general [21, 22], the break point of the error bound satisfies the following relations based on the algebraic representation (5.11)

$$\begin{cases} g_{\mathrm{EB}}(\boldsymbol{x};\omega,\boldsymbol{\lambda},\boldsymbol{e}) = 0 \\ \nabla g_{\mathrm{EB}}(\boldsymbol{x};\omega,\boldsymbol{\lambda},\boldsymbol{e}) = \boldsymbol{0} \end{cases}, \tag{5.37}$$

where a gradient vector $\nabla g_{\mathrm{EB}}(\boldsymbol{x};\omega,\boldsymbol{\lambda},\boldsymbol{e})$ is written by

$$\nabla g_{\mathrm{EB}} = \left(\frac{\partial g_{\mathrm{EB}}}{\partial x_{\mathrm{r}0}}, \frac{\partial g_{\mathrm{EB}}}{\partial x_{\mathrm{r}1}}, \frac{\partial g_{\mathrm{EB}}}{\partial x_{\mathrm{s}1}}, \ldots \frac{\partial g_{\mathrm{EB}}}{\partial x_{\mathrm{r}p}}, \frac{\partial g_{\mathrm{EB}}}{\partial x_{\mathrm{s}p}}\right)^{\mathrm{T}} \in \mathbb{R}^N. \tag{5.38}$$

Thus, if we view one system parameter $\varepsilon \in \{\omega, \boldsymbol{\lambda}, \boldsymbol{e}\}$ as the variable, the simultaneous equation (5.37) gives the break point $(\boldsymbol{x}, \varepsilon)$. We obtain the break point of the error bound by numerical method using an initial point $((\tilde{\boldsymbol{x}}_1 + \tilde{\boldsymbol{x}}_2)/2, \tilde{\varepsilon})$, where $\tilde{\varepsilon}$ is the parameter value close to the bifurcation parameters, and $\tilde{\boldsymbol{x}}_1, \tilde{\boldsymbol{x}}_2$ denote two close numerical solutions of the HB equation $\boldsymbol{f}(\boldsymbol{x};\tilde{\varepsilon}) = \boldsymbol{0}$.

The algorithm to obtain the break point of the error bound is described by

S1. We calculate the algebraic representation (5.11) of the error bound using Gröbner base.

S2. We select the parameter ε in the system parameters $\omega, \boldsymbol{\lambda}, \boldsymbol{e}$.

S3. Using the initial value $((\tilde{\boldsymbol{x}}_1 + \tilde{\boldsymbol{x}}_2)/2, \tilde{\varepsilon})$, we obtain the break point of the error bound by solving Eq.(5.37).

5.5.2 Example

We obtain the break points of the error bound for Duffing equation (5.18), where we assume that zero frequency component is neglected for simplicity. Let us select the parameter $\varepsilon = E$ and let $\omega = 1, \mu = 0.1,\ p = 30$. Then the bifurcation diagram (E - $x_{\mathrm{r}1}$) is shown in Figure 5.4. Additionally, we also show the guaranteed bifurcation diagram by the approximated error bound in Figure 5.4. Namely, we can guarantee the solutions of the HB equation in a orange region. Thus, the bifurcation points in Figure 5.4 lie close to $E = 0.45$ and $E = 0.12$.

Using the proposed method, we can calculate the parameters $E_{\mathrm{B}1} = 0.445168$ and $E_{\mathrm{B}2} = 0.135366$ of the break points. We show the projection of the error bound at $E_{\mathrm{B}1}$ and $E_{\mathrm{B}2}$ in Figure 5.5 and Figure 5.6, respectively. The Solution A, B, C and D in Figure 5.5 and Figure 5.6 correspond to the Solution A, B, C and D in Figure 5.4. Thus, we can confirm that the proposed method enables to obtain the accurate break points of the error bound by the collisions, and that the calculation of the break points and the approximated error bound clarify the guaranteed bifurcation diagram.

5.6 Concluding Remarks

In this chapter, we proposed an algebraic representation of an error bound for HB method using Gröbner base. Further, we proposed the efficient method to calculate the algebraic representation using transformations of variables. The proposed method does not depend on linear elements of the system and the number of specific frequency components. Next, we proposed a fast computational method of an approximated error bound by a quadratic approximation using the algebraic representation. We confirmed that the quadratic approximation guarantees approximately the solutions as fast as solving the HB equation. Moreover, we proposed a method to obtain accurate break points of the error bound near bifurcation points. In this way, the algebraic approach is very powerful for high dimensional varieties such as error bounds.

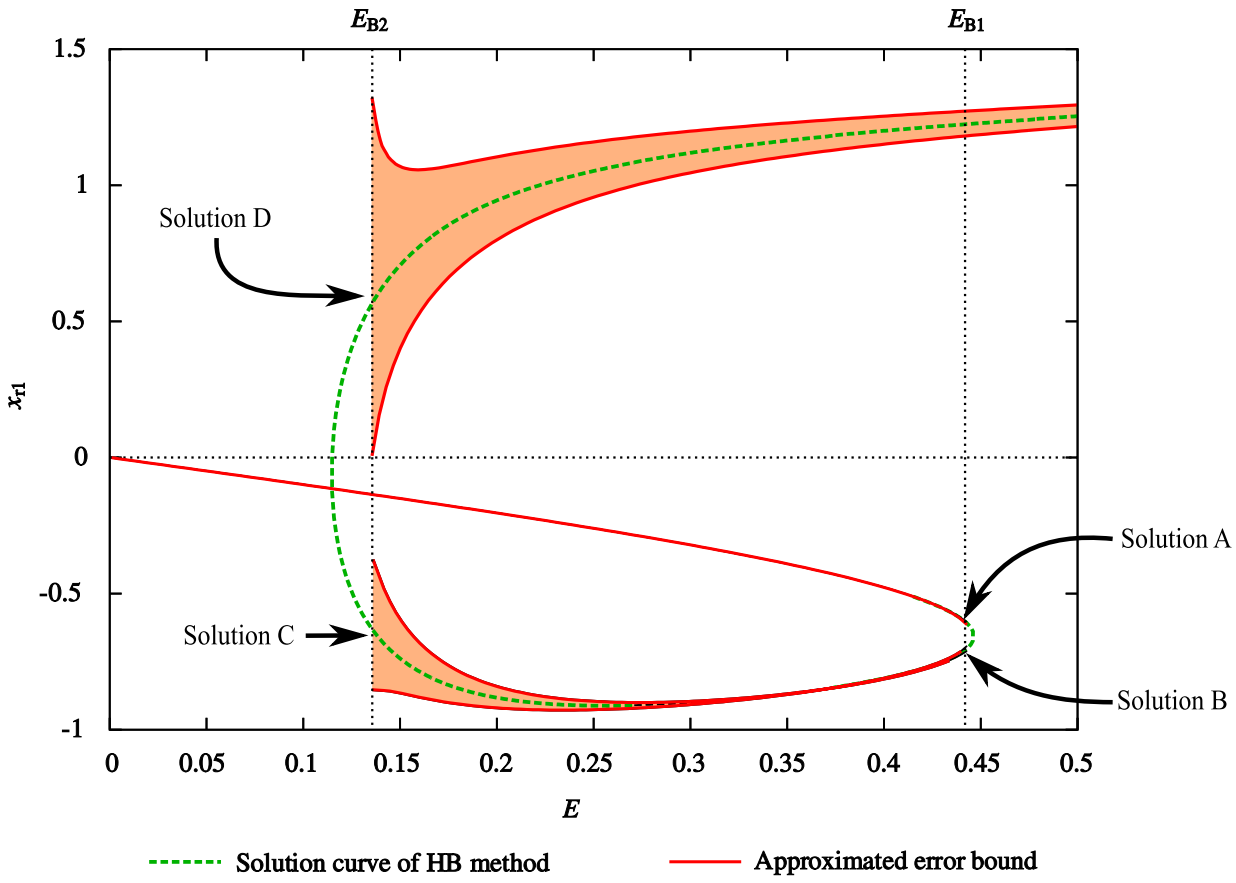

Figure 5.4: Guaranteed bifurcation diagram of the HB method by the approximated error bound and break points ($\omega = 1, \mu = 0.1$ and $p = 30$).

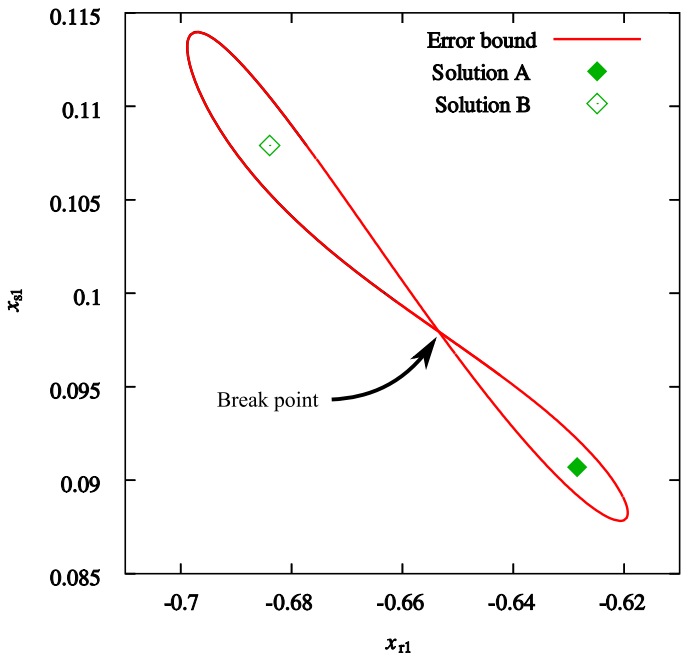

Figure 5.5: Projection (x_{r1}, x_{s1}) of the error bound at the parameter E_{B1} of the break point ($E_{B1} = 0.445168$, $\omega = 1, \mu = 0.1$ and $p = 30$).

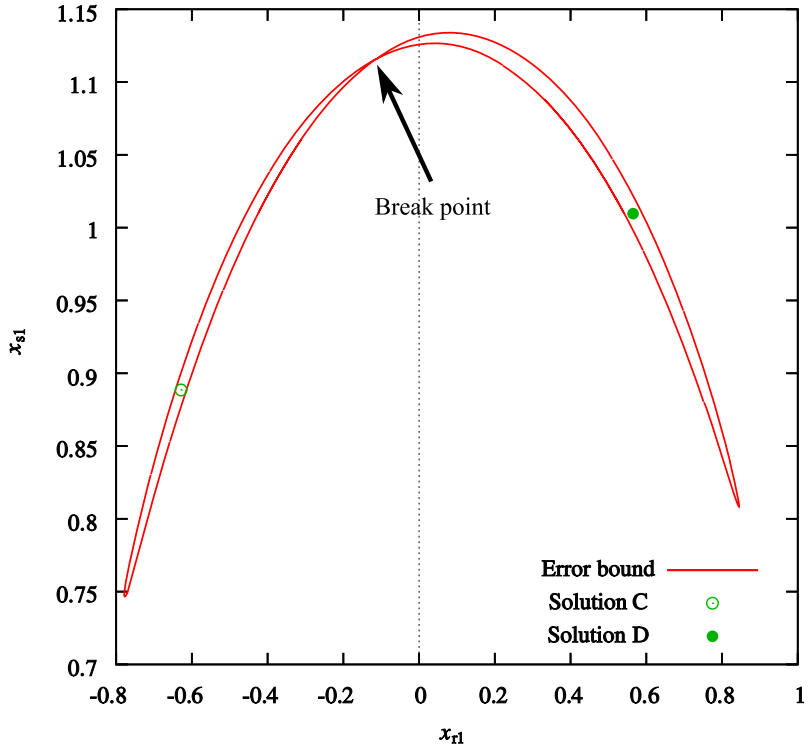

Figure 5.6: Projection (x_{r1}, x_{s1}) of the error bound at the parameter E_{B2} of the break point ($E_{B2} = 0.135366$, $\omega = 1, \mu = 0.1$ and $p = 30$).

Chapter 6

Conclusions

This thesis propose algebraic approaches to the analysis of periodic oscillations in nonlinear systems using computer algebra including Gröbner base. In order to overcome the difficulty of numerical approaches to the analysis in global parameter spaces, we introduced Gröbner base to decompositions of bifurcation diagrams, reductions of the system and determination of design parameters based on invariants, and an algebraic representation of error bounds for the harmonic balance (HB) method.

Chapter 2 serves as a preparation for the subsequent chapters. We formulated the polynomial determining equation of periodic oscillations using the HB method. Then, introducing the fundamentals of the ideal and Gröbner base, we reviewed an application of Gröbner base to bifurcation analysis in the global parameter spaces.

In Chapter 3, we proposed an algebraic approach to decompose bifurcation diagrams of periodic oscillations. In order to realize the decomposition, we proposed an efficient method using partial ideal quotient based on symmetries of the system. We confirmed that the bifurcation diagram of the HB equation is decomposed into sub-diagrams efficiently and that the pitchfork bifurcation points of the bifurcation diagram are expressed as intersection points of the sub-diagrams. This decomposition revealed algebraic aspects of local bifurcations. Further, we clarified the symmetries of nonhomogeneous HB equations based on the break of the symmetries of the corresponding homogeneous HB equation. Using the symmetries, we proposed a systematic procedure to decompose the bifurcation diagrams of the nonhomogeneous HB equations.

In Chapter 4, we proposed an algebraic approach to reduce the degree of the HB equation using the invariants which enable to transform a set of different but equivalent solutions into a unique solution. Using the fact that squared amplitude of each frequency component is invariant,

we confirmed that the computational cost of obtaining the bifurcation diagram of the squared amplitude is reduced dramatically. Moreover, using the property of the amplitudes, we proposed an efficient algorithm to obtain amplitude relation which represents the relation of each frequency component of oscillations. Further, using the amplitude relations, we presented a method for determining the design parameters of electric oscillators, and confirmed the efficiency by an example with van der Pol oscillator.

In Chapter 5, we proposed the algebraic representation of the error bound for the HB method and its efficient computational method. Further, we also proposed two applications of the algebraic representation of the error bound. First, we proposed a fast computational method of the approximated error bound using a quadratic approximation. We confirmed that proposed method guarantees the solutions as fast as solving the HB equation. Secondly, we presented a method to obtain accurate break points of the error bound near bifurcation points and showed the validity of the proposed method.

As noted above, this thesis proposed the algebraic approaches for the analysis of periodic oscillations in global parameter spaces. The proposed methods enable to clarify the algebraic structures of oscillations which is not given only by the numerical approaches. Because computer algebra will be further improved with the development of the computer technology, we can expect that the algebraic approaches such as the proposed methods based on the computer algebra will become widely used to advance the field of nonlinear oscillation.

Acknowledgments

First of all I wish to express my gratitude to Professor Osami Wada at Kyoto University for his excellent supervision of this work. He has been leading interesting seminars for his invaluable advices.

I would like to thank Associate Professor Takashi Hisakado at Kyoto University which has encouraged me in my work and has patiently helped me with all the problems that I have encountered along the way.

I would also like to thank Professor of Kyoto University Takashi Hikihara for his helpful comments.

I also benefited very much from discussions with Professor Tomomichi Hagiwara at Kyoto University.

I am also thankful to Emeritus Professor of Kyoto University Kohshi Okumura for his precious comments and encouragement.

Special thanks are due to the members of my laboratory for their support.

Bibliography

[1] G. Duffing, "Erzwungene Schwingungen bei veränderlicher Eigenfrequenz und ihre technische Bedeutung," Sammlung Vieweg, Braunschweig, 1918.

[2] B. van der Pol, "On relaxation oscillations", Phil. Mag., vol.2, pp.978–992, 1926.

[3] B. van der Pol, "Forced oscillations in a circuit with non-linear resistance (Reception with reactive triode)," Phil. Mag., vol.3, no.13, pp.65–80, Jan. 1927.

[4] B. van der Pol and M. J. O. Strutt, "On the stability of the solutions of Mathieu's equation," Phil. Mag., vol.5, no.27, pp.18-38, Jan. 1928.

[5] C. Hayashi, "Nonlinear Oscillations in Physical Systems," McGraw-Hill, New York, 1964.

[6] A.I. Mees, "Dynamics of Feedback Systems," Wiley-Interscience, New York, 1981.

[7] D.D. Siljak, "Nonlinear Systems: The Parameter Analysis and Design," Wiley, New York, 1969.

[8] D.P. Atherton, "Nonlinear Control Engineering," Van Nostrand Reinhold, London, 1975.

[9] M. Basso, R. Genesio, and A. Tesi, "A frequency method for predicting limit cycle bifurcations," Nonlinear Dynamics, vol.13, no.4, pp.339–360, Aug. 1997.

[10] C. Piccardi, "Bifurcations of limit cycles in periodically forced nonlinear systems: The harmonic balance approach," IEEE Trans. Circuits & Syst. -I, vol.41, no.4, pp.315–320, April 1994.

[11] J.L. Moiola, and G. Chen, "Hopf bifurcation analysis: A frequency domain approach," Series on Nonlinear Science, Series A, vol.21, World Scientific, Singapore, 1996.

[12] F. Bonani, and M. Gilli, "Analysis of stability and bifurcations of limit cycles in Chua's circuit through the harmonic balance approach," IEEE Trans. Circuits & Syst. -I, vol.46, no.8, pp.881–890, Aug. 1999.

[13] A.R. Bergen and R.L. Franks, "Justification of the describing function method," SIAM J. Contr. Optimiz., vol.9, no.4, pp.568–569, Nov. 1971.

[14] A.I. Mees and A.P. Bergen, "Describing functions revisited," IEEE Trans. Automat. Contr., vol.AC-20, no.4, pp.473-478, Aug. 1975.

[15] F.L. Swern, "Analysis of oscillations in systems with polynomial-type nonlinearities using describing functions," IEEE Trans. Automat. Contr., vol.AC-28, no.1, pp.31–41, Jan. 1983.

[16] H. Hironaka, "Resolution of singularities of an algebraic variety over a field of characteristic zero: I," Ann. Math., vol.79, no.1, pp.109–203, Jan. 1964.

[17] H. Hironaka, "Resolution of singularities of an algebraic variety over a field of characteristic zero: II," Ann. Math., vol.79, no.2, pp.205–326, March 1964.

[18] B. Buchberger, "Ein Algorithmus zum Auffinden der Basiselemente des Restklasse-ringes nach einem nulldimensionalen Polynomideal," Ph.D. Thesis, University of Insbruck 1965.

[19] B. Buchberger, "Ein algorithmisches Kriterium für die Lösbarkeit eines algebraischen Gleichungssystems," Aequationes Mathematicae, vol.4, no.3, pp.374–383, Oct. 1970.

[20] B. Buchberger, "Gröbner bases: An algorithmic method in polynomial ideal theory," Recent Trends in Multidimensional Systems Theory, eds. N.K. Bose and D. Reidel, pp.184–232, 1985.

[21] D. Cox, J. Little, and D. O'shea, "Ideals, Varieties, and Algorithms," Springer-Verlag, New York, 1992.

[22] D. Cox, J. Little, and D. O'shea, "Using Algebraic Geometry," Springer-Verlag, New York, 1998.

[23] J. Baillieul, D.P. Martin, R.W. Brockett, and B.R. Donald, "Robotics," AMS Proc. Symposia in Applied Mathematics American Mathematical Society, vol.41, pp.49–89, 1990.

[24] J.C. Faugère, F.M. de Saint Martin, and F. Rouillier, "Design of regular nonseparable bidimensional wavelets using Gröbner basis techniques," IEEE Trans. Signal. Process., vol.46, no.4, pp.845–856, April 1998.

[25] I.W. Selesnick, "Balanced multiwavelet bases based on symmetric FIR filters," IEEE Trans. Signal. Process., vol.48, no.1, pp.184–191, Jan. 2000.

[26] J. Lebrun and M. Vetterli, "High order balanced multiwavelets: Theory, factorization and design," IEEE Trans. Signal. Process., vol.49, no.9, pp.1918–1930, Sept. 2001.

[27] L.S. Kotsireas and K. Karamanos, "Exact computation of the bifurcation point B-4 of the logistic map and the Bailey-Broadhurst conjectures," Int. J. Bif. & Chaos, vol.14, no.7, pp.2417–2423, July 2004.

[28] M.A.M. Alwash, "Periodic solutions of a quartic differential equation and Groebner bases," J. Comput. Appl. Math., vol 75, no.1, pp.67–76, Nov. 1996.

[29] K. Gatermann, and R. Lauterbach, "Automatic classification of normal forms," Nonlinear Analysis, vol.34, pp.157–190, Oct. 1998.

[30] I. Stewart, and A.P.S. Dias, "Toric geometry and equivariant bifurcations," Physica D, vol.143, pp.235–261, Sept. 2000.

[31] K. Okumura, "Classifying nonlinear circuits by Gröbner base," Proc. Workshop on Nonlinear Dynamics in Electronic Systems (NDES98), pp.267–270, July 1998.

[32] P. Conti and C. Traverso, "Buchberger algorithm and integer programming," Lecture Notes in Computer Science 539, pp.130–139, Springer-Verlag, New York, 1991.

[33] B. Sturmfels and R.R. Thomas, "Variation of cost functions in integer programming," Mathematical Programming, vol.77, no.3, pp.357–387, June 1997.

[34] R.R. Thomas, "A geometric Buchberger algorithm for integer programming," Mathematics of Operations Research, vol.20, no.4, pp.864–884, Nov. 1995.

[35] T. Hisakado and K. Okumura, "Mode decomposition of global bifurcation diagram with Gröbner bases," Physics Letters A, vol.292, pp.263–268, Jan. 2002.

[36] T. Hisakado and K. Okumura, "Algebraic representation of bifurcations in global parameter space with Gröbner bases," Proc. IEEE International Symposium on Circuits and Systems (ISCAS2001), vol.2 pp.747–750, May 2001.

[37] K. Forsman and S.T. Glad, "Constructive algebraic geometry in nonlinear control," Proc. IEEE 29th Conference on Decision and Control (CDC), vol 5, pp.2825–2827, Honolulu, Hawaii, 1990.

[38] H. Fortell, "Algebraic approaches to normal forms and zero dynamics," PhD. thesis, Dept. of Electrical Engineering, Linköping Univ., Sweden, 1995.

[39] M. Jirstrand, "Algebraic methods for modeling and design in control," PhD. thesis, Dept. of Electrical Engineering, Linköping Univ., Sweden, 1996.

[40] G.L. Calandrini, E.E. Paolini and J.L. Moiola, "Groebner bases for designing dynamical systems," Latin American Applied Research, vol.33, no.4, pp.427–434, Oct. 2003.

[41] P. Diaconis and B. Sturmfels, "Algebraic algorithms for sampling from conditional distributions," Ann. Statist., vol.26, no.1, pp.363–397, Feb. 1998.

[42] A. Takemura and S. Aoki, "Some characterizations of minimal Markov basis for sampling from discrete conditional distributions," Ann. Inst. Statist. Math., vol.56, no.1, pp.1–17, March 2004.

[43] S. Sakata "Finding a minimal set of linear recurring relations capable of generating a given finite two-dimensional array," J. Symb. Comput., vol.5, no.3, pp.321–337, June 1988.

[44] S. Sakata "Extension of the Berlekamp-Massey algorithm to N-dimensions," Inf. & Comp., vol.84, no.2, pp.207–239, Feb. 1990.

[45] S. Sakata, H.E. Jensen and T. Hoholdt, "Generalized Berlekamp-Massey decoding of algebraic-geometric codes up to half the Feng-Rao bound," IEEE Trans. Inf. Theory, vol.41, no.6, pp.1762–1768, Nov. 1995.

[46] J.C. Faugère, "A new efficient algorithm for computing Gröbner bases (F4)," J. Pure Appl. Algebra 139, pp.61–88, 1999.

[47] J.C. Faugère, "A new efficient algorithm for computing Gröbner bases without reduction to zeros (F5)," Proc. the 2002 International Symposium on Symbolic and Algebraic Computation, ACM, pp.75–83, New York, 2002.

[48] S. Collart, M. Kalkbrener, and D. Mall, "Converting bases with the Gröbner walk," J. Symb. Comput., vol.24, no.3-4, pp.465–469, Sep-Oct. 1997.

[49] K. Fukada, N. Jensen, N. Lauritzen and R. Thomas, "The generic Gröbner walk," J. Symb. Comput., no.3, vol.42, pp.298–312, March. 2007.

[50] W. Boege, R. Gebauer, and H. Kredel, "Some examples for solving systems of algebraic equations by calculating Gröbner bases," J. Symb. Comput., vol.2, no.1, pp.83–98, March 1986.

[51] S.N. Chow and J.K. Hale, "Methods of Bifurcation Theory," Springer-Verlag, NewYork, 1982.

[52] S. Wiggins, "Introduction to Applied Nonlinear Dynamical Systems and Chaos," Springer-Verlag, NewYork, 1990.

[53] M. Golubitsky, I. Stewart, and D.G. Schaeffer, "Singularities and Groups in Bifurcation Theory, vol.II," Springer-Verlag, NewYork, 1988.

[54] B. Sturmfels, "Algorithms in Invariant Theory," Springer-Verlag, New York, 1993.

[55] G.M. Greuel and G. Pfister, "A Singular Introduction to Commutative Algebra," Springer-Verlag, Berlin Heidelberg, 2002.

[56] B. Mishra, "Algorithmic Algebra," Springer-Verlag, NewYork, 1993.

[57] L.O. Chua and A. Ushida, "A switching-parameter algorithm for finding multiple solutions of nonlinear resistive circuits," Int. J. Circuit Theory Appl, vol.4, pp.215–239, July 1976.

[58] J.M. Ortega and W.C. Rheinboldt, "Iterative Solution of Nonlinear Equations in Several Variables," Academic Press, New York, 1970.

[59] C.B. Garcia, "Computation of solutions to nonlinear equations under homotopy invariance," Mathematics of Operations Research, vol.2, no.1, pp.25–29, Feb. 1977.

[60] M.H. Shih, “Bolzano’s theorem in several complex variables,” Proc. Amcr. Math. Soc., vol. 79, no.1, pp.32–34. May 1980.

Publications

Journal Publications

[A] M. Yagi and T. Hisakado, "Efficient applications of invariants to harmonic balance equation using Gröbner base," IEICE Trans. Fundamentals, vol. E90-A, no. 10, pp. 2178–2186, Oct. 2007.

[B] M. Yagi, T. Hisakado, and K. Okumura, "Decomposition of bifurcation diagram on harmonic balance equation for periodic oscillation using ideal quotient by computer algebra," IET Proc.-Circuits Devices Syst., (Submitted).

[C] M. Yagi, T. Hisakado, and K. Okumura, "An algebraic approach to guarantee harmonic balance method using Gröbner base," IEICE Trans. Fundamentals, (Conditionally Accepted).

Conference Publications

[D] M. Yagi, T. Hisakado, and K. Okumura, "Algebraic representation of error bounds for describing function using Groebner base," IEEE International Symposium on Circuits and Systems (ISCAS2005), pp.2831–2834, 2005.

[E] M. Yagi, T. Hisakado, and K. Okumura, "Decomposition of bifurcation diagram for periodic oscillation using ideal quotient," International Symposium on Nonlinear Theory and its Applications (NOLTA2005), pp.34–37, 2005.

[F] M. Yagi and T. Hisakado, "Reduced bifurcation diagram for harmonic balance method using invariant," International Symposium on Nonlinear Theory and its Applications (NOLTA2006), pp.1003–1006, 2006.

[G] M. Yagi and T. Hisakado, “Fast computation of approximated error bound for harmonic balance method using algebraic representation,” International Symposium on Nonlinear Theory and its Applications (NOLTA2007), pp.250–253, 2007.

[H] M. Yagi, T. Hisakado, and K. Okumura, “Verification of describing function using Groebner base,” IEICE General Conference, no.A-2-22, 2004. Japanese.

[I] M. Yagi, T. Hisakado, and K. Okumura, “Algebraic expression of verification region for describing function using Groebner base,” IEICE Technical Report, no.CAS2004-38,NLP2004-50, pp.61–66, 2004. Japanese.

[J] M. Yagi, T. Hisakado, and K. Okumura, “Decomposition of bifurcation diagram on resonance circuit using ideal quotient,” IEICE General Conference, no.A-1-38, 2005. Japanese.

[K] M. Yagi, T. Hisakado, and K. Okumura, “Bifurcation and ideal decomposition of harmonic balance equations for periodic oscillation using ideal quotient,” IEICE Technical Report, no.CAS2005-35,NLP2005-48, pp.8–12, 2005.

[L] M. Yagi, T. Hisakado, and K. Okumura, “Systematical ideal decomposition of bifurcation diagram for periodic oscillation,” Record of the Kansai-section Joint Convention of Institutes of Electrical Engineering, no.G1-8, p.G8, 2005.

[M] M. Yagi and T. Hisakado, “Gröbner base for harmonic balance method using invariant equation,” IEICE General Conference, no.A-2-28, p.64, 2006. Japanese.

[N] M. Yagi and T. Hisakado, “Determination of circuit parameters for oscillator using invariant,” IEICE Technical Report, no.CAS2006-21,NLP2006-44, pp.1–6, 2006.

[O] M. Yagi and T. Hisakado, Record of the Kansai-section Joint Convention of Institutes of Electrical Engineering, no.G1-32, p.G32, 2006. Japanese.

[P] M. Yagi and T. Hisakado, “Algebraic expression of solutions for harmonic balance method,” IEICE Technical Report, no.NLP2006-95, pp.33–38, 2006.

[Q] M. Yagi and T. Hisakado, “Algebraic expression of error bound for harmonic balance method,” IEICE General Conference, no.A-2-43, p.90, 2007.

[R] T. Hisakado and M.Yagi “An approach on oscillator circuit design using Groebner base,” The Papers of Thechnical Meeting on Electronic Circuits, IEE Japan, no.ECT-07-100, 2007. Japanese.

Appendix A

Ideal Operations and Correspondence to Variety

We review ideal operations and correspondences between ideals and varieties [21, 22].

A.1 Sums of Ideals

Definition 2 (Sums of ideals)**.** *Let I, J be ideals in $\mathbb{Q}(\boldsymbol{\lambda})[\boldsymbol{x}]$. Then the sum of I and J, defined $I + J$, is the set*

$$I + J = \{f + g \mid f \in I, g \in J\}. \tag{A.1}$$

If $I = \langle \boldsymbol{f}(\boldsymbol{x}) \rangle = \langle f_1, \ldots, f_s \rangle$ and $J = \langle \boldsymbol{g}(\boldsymbol{x}) \rangle = \langle g_1, \ldots, g_r \rangle$ are ideals in $\mathbb{Q}(\boldsymbol{\lambda})[\boldsymbol{x}]$ where $\boldsymbol{f}(\boldsymbol{x}) = (f_1, \ldots, f_s)^{\mathrm{T}}$ and $\boldsymbol{g}(\boldsymbol{x}) = (g_1, \ldots, g_r)^{\mathrm{T}}$, then $I + J = \langle \boldsymbol{f}(\boldsymbol{x}), \boldsymbol{g}(\boldsymbol{x}) \rangle = \langle f_1, \ldots, f_s, g_1, \ldots, g_r \rangle$ is held. Thus, the sum of ideals $I + J$ corresponds geometrically to taking intersections of varieties as follows;

$$\boldsymbol{V}(I + J) = \boldsymbol{V}(I) \cap \boldsymbol{V}(J). \tag{A.2}$$

A.2 Products of Ideals

Definition 3 (Products of Ideals)**.** *Let I, J be two ideals in $\mathbb{Q}(\boldsymbol{\lambda})[\boldsymbol{x}]$. Then their product $I \cdot J$ is defined to be the ideal generated by all polynomials $f \cdot g$ where $f \in I$ and $g \in J$.*

Thus, the product $I \cdot J$ is the set

$$I \cdot J = \{f_1 g_1 + \cdots + f_s g_s \mid f_1, \ldots, f_s \in I,\ g_1, \ldots, g_s \in J,\ s \in \mathbb{Z}_{>0}\}. \tag{A.3}$$

Then the product of ideals $I \cdot J$ corresponds geometrically to the operation of taking the union of varieties as follows;

$$\boldsymbol{V}(I \cdot J) = \boldsymbol{V}(I) \cup \boldsymbol{V}(J). \tag{A.4}$$

A.3 Intersections of Ideals

Definition 4 (Intersections of Ideals)**.** *The intersection $I \cap J$ of two ideals I and J in $\mathbb{Q}(\boldsymbol{\lambda})[\boldsymbol{x}]$ is the set of polynomials which belong to both I and J.*

We always have $I \cdot J \subset I \cap J$ since elements of $I \cdot J$ are sums of polynomials of the form $f \cdot g$ with $f \in I$ and $g \in J$. Note that $I \cdot J = I \cap J$ if I and J are coprime [21,22,56]. Now, we describe the definition of coprime ideals;

Definition 5 (Coprime Ideals)**.** *Let I and J be ideals in $\mathbb{Q}(\boldsymbol{\lambda})[\boldsymbol{x}]$. The ideal I and J are said to be coprime if $I + J = \mathbb{Q}(\boldsymbol{\lambda})[\boldsymbol{x}]$.*

Then intersection of ideals $I \cap J$ corresponds geometrically to

$$\boldsymbol{V}(I \cap J) = \boldsymbol{V}(I) \cup \boldsymbol{V}(J). \tag{A.5}$$

Thus, the intersection of two ideals corresponds to the same variety as the product.

A.4 Ideal Quotient

Definition 6 (Ideal Quoitent)**.** *Let I, J be ideals in $\mathbb{Q}(\boldsymbol{\lambda})[\boldsymbol{x}]$. Then, $I : J$ is the set*

$$I : J = \{f \in \mathbb{Q}(\boldsymbol{\lambda})[\boldsymbol{x}] \mid fg \in I,\ \forall g \in J\}, \tag{A.6}$$

and is called the ideal quotient of I by J.

The ideal quotient is indeed the algebraic analogue of the Zariski closure of a difference of varieties. Namely,

$$\boldsymbol{V}(I : J) \supset \overline{\boldsymbol{V}(I) - \boldsymbol{V}(J)}. \tag{A.7}$$

In particular, if I is a radical ideal, then

$$\boldsymbol{V}(I : J) = \overline{\boldsymbol{V}(I) - \boldsymbol{V}(J)}. \tag{A.8}$$

The relation $\overline{\boldsymbol{V}(I) - \boldsymbol{V}(J)}$ denotes the remove of $\boldsymbol{V}(J)$ from $\boldsymbol{V}(I)$.

Now, we describe the definition of the radical ideal;

Definition 7 (Radical Ideal)**.** *Let I be an ideal in $\mathbb{Q}(\boldsymbol{\lambda})[\boldsymbol{x}]$. The radical of I is defined by the set*

$$\sqrt{I} = \{f \in \mathbb{Q}(\boldsymbol{\lambda})[\boldsymbol{x}] \mid f^a \in I \text{ for some } a \geq 1\}. \tag{A.9}$$

An ideal I is said to be a radical ideal if $\sqrt{I} = I$.

Using the radical ideal, we prove the following proposition.

Proposition 1. *Let I, J, and K be ideals in $\mathbb{Q}(\boldsymbol{\lambda})[\boldsymbol{x}]$, and let K be $K = I : J$. If I is a radical ideal, and has the relation $I \subset J$, then $I = J \cap K$ is satisfied.*

Proof. If let f be a polynomial in I, then $f \in J$ due to the assumption. Because the relation $I \subseteq I : J = K$ is satisfied, we have $f \in K$. Thus, $f \in J \cap K$ gives $I \subseteq J \cap K$.

Conversely, if let f be a polynomial in $J \cap K$, then $f \in J$ and $f \in K$ are satisfied. Because the relation $K = I : J$ gives $f \in I : J$, we have $f^2 \in I$. Since I is the radical ideal, the polynomial f belongs to I. That is, we get $I \supseteq J \cap K$. Thus, $I = J \cap K$ holds. □

A.5 Propositions for Ideal Quotient

We write propositions of ideal quotient used in Section 3.4.2.

Proposition 2. *Let I and J_i be ideals in $\mathbb{Q}(\boldsymbol{\lambda})[\boldsymbol{x}]$ for $i = 1, \ldots, s$. Then;*

$$I : \left(\sum_{i=1}^{s} J_i \right) = \bigcap_{i=1}^{s} (I : J_i). \tag{A.10}$$

Proof. If let f be a polynomial in $I : (\sum_{i=1}^{s} J_i)$ and let g_i be a polynomial in J_i for $i = 1, \ldots, s$, then $f(g_1 + \cdots + g_s) \in I$ is satisfied. Since we have $f \cdot g_i \in I$, the polynomial f belongs to $I : J_i$ for $i = 1, \ldots, s$. Thus, $f \in \cap_{i=1}^{s} (I : J_i)$ gives $I : (\sum_{i=1}^{s} J_i) \subseteq \cap_{i=1}^{s} (I : J_i)$.

Conversely, let f be a polynomial in $\cap_{i=1}^{s} (I : J_i)$ and let g_i be a polynomial in J_i for $i = 1, \ldots, s$. Since $f \in I : J_i$ is satisfied, we have $f \cdot g_i \in I$. The relations $f \cdot g_1 + \cdots + f \cdot g_s \in I$ and $g_1 + \cdots + g_s \in \sum_{i=1}^{s} J_i$ give $I : (\sum_{i=1}^{s} J_i) \supseteq \cap_{i=1}^{s} (I : J_i)$. Thus, the proposition (A.10) holds. □

Proposition 3. *Let J, I_i, and $K_i = I_i : J$ be ideals in $\mathbb{Q}(\boldsymbol{\lambda})[\boldsymbol{x}]$ for $i = 1, \ldots, r$. If let $I = \sum_{i=1}^{r} I_i$ and I_i be radical ideals which satisfy $I, I_i \subset J$, and if let J be coprime to K_i for $i = 1, \ldots, r$, then*

$$\left(\sum_{i=1}^{r} I_i \right) : J = \sum_{i=1}^{r} (I_i : J) \,. \tag{A.11}$$

Proof. Because I_i is the radical ideal where $I_i \subset J$, we have $I_i = K_i \cap J$ due to $K_i = I_i : J$. Moreover $I_i = K_i \cdot J$ is satisfied since J is coprime to K_i. Now, if we define $K = \sum_{i=1}^{r} K_i$, then K is coprime to J. Thus, $\sum_{i=1}^{r} I_i = \sum_{i=1}^{r} (K_i \cdot J) = K \cdot J$ gives $K = (\sum_{i=1}^{r} I_i) : J$. Thus, the proposition (A.11) holds. □

A.6 Summary

Table A.1 summarizes the results of the correspondences between ideals and varieties. In this table, it is supposed that all ideals are radical.

Table A.1: Correspondences between ideal and affine variety

Algebra		**Geometry**
ideals		varieties
I	$\rightarrow$	$\boldsymbol{V}(I)$
addition of ideals		intersection of varieties
$I + J$	$\rightarrow$	$\boldsymbol{V}(I) \cap \boldsymbol{V}(J)$
product of ideals		union of varieties
$I \cdot J$	$\rightarrow$	$\boldsymbol{V}(I) \cup \boldsymbol{V}(J)$
intersection of ideals		union of varieties
$I \cap J$	$\rightarrow$	$\boldsymbol{V}(I) \cup \boldsymbol{V}(J)$
quotient of ideals		difference of varieties
$I : J$	$\rightarrow$	$\overline{\boldsymbol{V}(I) - \boldsymbol{V}(J)}$

Appendix B

HB Equation Containing Symmetric Solutions

In this appendix, let us demonstrate the following relations used in Section 3.4.2;

$$\sum_{k\in\kappa}\langle \boldsymbol{f}_k(\boldsymbol{x})\rangle \subset \sum_{k\in\kappa}\langle \boldsymbol{x}_k\rangle, \tag{B.1}$$

$$\sum_{k\notin\kappa}\langle \boldsymbol{f}_k(\boldsymbol{x})\rangle \not\subset \sum_{k\in\kappa}\langle \boldsymbol{x}_k\rangle. \tag{B.2}$$

If the HB equation has a symmetry $\Gamma \in \{\Gamma_{\mathrm{odd}}, \Gamma_{2\pi/m}\}$, namely, $\boldsymbol{f}(\boldsymbol{\theta x}) = \boldsymbol{\theta f}(\boldsymbol{x})$ is satisfied where $\boldsymbol{\theta} \in \{\boldsymbol{\theta}_{\mathrm{odd}}, \boldsymbol{\theta}_{2\pi/m}\}$, symmetric solutions with respect to Γ satisfy $\boldsymbol{x} = \boldsymbol{\theta x}$. Using κ determined by Eq.(3.29), we rewrite $\boldsymbol{x} = \boldsymbol{\theta x}$ to

$$\boldsymbol{x}_k = \boldsymbol{0} \ \text{ for } \ k \in \kappa. \tag{B.3}$$

Thus, the ideal $\sum_{k\in\kappa}\langle \boldsymbol{x}_k\rangle$ corresponds to the symmetric solutions.

When we consider the symmetric solutions $\boldsymbol{x} = \boldsymbol{\theta x}$, the HB equation have the following relation;

$$\boldsymbol{f}(\boldsymbol{x}) = \boldsymbol{\theta f}(\boldsymbol{x}). \tag{B.4}$$

According to the discussion of Eq.(B.3), we can obtain

$$\boldsymbol{f}_k(\boldsymbol{x}) = \boldsymbol{0} \ \text{ for } \ k \in \kappa, \tag{B.5}$$

when $\boldsymbol{x}_k = \boldsymbol{0}$ for $k \in \kappa$. That is, the equation tells that the symmetric solutions $\boldsymbol{x}_k = \boldsymbol{0}$ are solutions of $\boldsymbol{f}_k(\boldsymbol{x})$ for $k \in \kappa$. Thus, the relation (B.1) is held.

By same reason, the relation

$$\sum_{k \notin \kappa} \langle \boldsymbol{f}_k(\boldsymbol{x}) \rangle \subset \sum_{k \in \kappa} \langle \boldsymbol{x}_k \rangle \tag{B.6}$$

is held if the polynomial equation in the HB equation

$$\boldsymbol{f}_k(\boldsymbol{x}) = \boldsymbol{0} \tag{B.7}$$

is satisfied for all $k \notin \kappa$ when $\boldsymbol{x}_i = \boldsymbol{0},\ \forall \boldsymbol{x}_j,\ i \in \kappa, j \notin \kappa$. However, the set κ in Eq.(3.29) does not contain m, that is, the set of $\boldsymbol{f}_k(\boldsymbol{x})$ for $k \notin \kappa$ contains $\boldsymbol{f}_m(\boldsymbol{x})$ which has the forcing terms. Because the forcing terms in $\boldsymbol{f}_m$ are constant terms, the HB equation dose not satisfy the relation (B.7) when $\boldsymbol{x}_k = \boldsymbol{0}$. Thus, we get the relation (B.2).

Appendix C

Elimination Theorem and Gröbner Base

In this appendix, we review the elimination theorem based on Gröbner base and elimination order of Gröbner base [21, 22].

C.1 Elimination Theorem Based on Gröbner Base

In order to recall the elimination theorem, we define the elimination ideal as follows;

Definition 8 (Elimination Ideal)**.** *Let $X = \{x_1, \ldots, x_N\}$, and let $I = \langle f_1, \ldots, f_s \rangle$ be an ideal in $\mathbb{Q}(\boldsymbol{\lambda})[X]$. If*

$$I_Y = I \cap \mathbb{Q}(\boldsymbol{\lambda})[Y],\ Y \subset X, \tag{C.1}$$

then we call I_Y an elimination ideal of I.

The elimination ideal I_Y is generated by the elimination of the variables not in Y from the polynomial equations $f_1 = \cdots = f_s = 0$, and is calculated by Gröbner base of the following elimination order.

Definition 9 (Elimination Order)**.** *Let $X = \{x_1, \ldots, x_N\}$, $Y \subset X$. and let $t_1, t_2 \in \mathbb{Q}(\boldsymbol{\lambda})[X]$ be monomials. If a monomial order $t_1 \succ t_2$ is satisfied*

$$t_1 \notin \mathbb{Q}(\boldsymbol{\lambda})[Y],\ t_2 \in \mathbb{Q}(\boldsymbol{\lambda})[Y], \tag{C.2}$$

we say an elimination order with respect to (X, Y).

Theorem 1 (Elimination Theorem)**.** *Let $X = \{x_1, \ldots, x_N\}$, $Y \subset X$, and let $I = \langle f_1, \ldots, f_s \rangle \in \mathbb{Q}(\boldsymbol{\lambda})[X]$ be an ideal, If let G be a Gröbner base of the elimination order with respect to (X, Y) of I, then*

$$G_Y \quad = \quad G \cap \mathbb{Q}(\boldsymbol{\lambda})[Y]. \tag{C.3}$$

is the Gröbner base of the elimination ideal $I_Y = I \cap \mathbb{Q}(\boldsymbol{\lambda})[Y]$. Then $I_Y = \langle G_Y \rangle$ is satisfied.

C.2 Lexicographic Order and Block Order

We consider the elimination order which is used in this thesis. First, let us review lexicographic order.

Definition 10 (Lexicographic Order)**.** *Let $x_1^{\alpha_1} x_2^{\alpha_2} \cdots x_N^{\alpha_N}$ and $x_1^{\beta_1} x_2^{\beta_2} \cdots x_N^{\beta_N}$ be monomials. If a monomial order $x_1^{\alpha_1} x_2^{\alpha_2} \cdots x_N^{\alpha_N} \succ x_1^{\beta_1} x_2^{\beta_2} \cdots x_N^{\beta_N}$ satisfies*

$$\alpha_l = \beta_l,\ \alpha_k > \beta_k,\ \ k < l \leq N,\ \exists k, \tag{C.4}$$

we say a lexicographic order $\succ_{\text{lex}}$.

If we consider the ideal $I = \langle f_1, \ldots, f_N \rangle \subset \mathbb{Q}(\boldsymbol{\lambda})[x_1, \ldots, x_N]$, then the elimination ideal with respect to the lexicographic order $x_1 \succ_{\text{lex}} \cdots \succ_{\text{lex}} x_N$ gives the triangular form. Namely, the lexicographic order $x_1, \succ_{\text{lex}} \cdots \succ_{\text{lex}} x_N$ denotes the elimination order with respect to $(\{x_1, \ldots, x_N\}, \{x_{i+1}, \ldots, x_N\})$ for some i.

Next, we review Gröbner base of block order.

Definition 11 (Block Order)**.** *Let $X = \{x_1, \ldots, x_N\}$, and let $Y \subset X$. Then let X be divided into $X = (X \backslash Y) \cap Y$. and let $t_1, s_1 \in \mathbb{Q}(\boldsymbol{\lambda})[X \backslash Y]$, $t_2, s_2 \in \mathbb{Q}(\boldsymbol{\lambda})[Y]$ be monomials. If*

$$t_1 t_2 \succ s_1 s_2 \Leftrightarrow t_1 \succ s_1 \ \text{ or } \ (t_1 = s_1 \text{ and } t_2 \succ s_2), \tag{C.5}$$

is satisfied, then we say that this order is a block order $\succ_{\text{block}}$ with respect to X.

The block order is the elimination order with respect to (X, Y). Using the block order, we can only eliminate target variables in polynomials. Hence, the computational cost of Gröbner base of the block order is less than Gröbner base of the lexicographic order in general. Thus, we usually use the block order of Gröbner base for the elimination of variables in this thesis.

Appendix D

Equations of Bifurcation Diagram Using Invariants

We show the equations of bifurcation diagrams (E - x_{r1}) and (E - A_1) in Section 4.3.2. The equation of the bifurcation diagrams (E - x_{r1}) is obtained by

$$
\begin{aligned}
&-369363860947265625000000000000000000000000E^6 x_{\mathrm{r1}}^{18} \\
&+759834228234375000000000000000000000000000E^6 x_{\mathrm{r1}}^{16} \\
&+(791493987744140625000000000000000000000000E^7 \\
&\quad +241217215312500000000000000000000000000E^5) x_{\mathrm{r1}}^{15} \\
&-662141843999774824218750000000000000000000E^6 x_{\mathrm{r1}}^{14} \\
&+(142468917793945312500000000000000000000000E^7 \\
&-373536241640988890625000000000000000000000E^5) x_{\mathrm{r1}}^{13} \\
&+(-490443595977172851562500000000000000000000E^8 \\
&\quad +300607128966070643554687500000000000000000000E^6 \\
&\quad -332157371085062899917187500000000000000000E^4) x_{\mathrm{r1}}^{12} \\
&+(-114366650774428520507812500000000000000000000E^7 \\
&\quad +209743797590710375781250000000000000000000E^5) x_{\mathrm{r1}}^{11} \\
&+(370467645079833984375000000000000000000000000E^8 \\
&\quad -800200752353241776916503906250000000000000000E^6 \\
&\quad +402371987433471658653750000000000000000000E^4) x_{\mathrm{r1}}^{10} \\
&+(-305559753771972656250000000000000000000000E^9
\end{aligned}
$$

$$
\begin{aligned}
&+28786161210951421142578125000000000000000000E^{7}\\
&-58189517315368840039324218750000000000000000E^{5}\\
&+11253975862082301224100000000000000000000E^{3})x_{\mathrm{r1}}^{9}\\
&+(-11317638238599825439453125000000000000000000E^{8}\\
&+13069426322307410018947265625000000000000000000E^{6}\\
&-13546903783894864604749749375000000000000000E^{4})x_{\mathrm{r1}}^{8}\\
&+(38074783666992187500000000000000000000000000E^{9}\\
&-25944583220469947640673828125000000000000000E^{7}\\
&+78572350076065866567914062500000000000000000E^{5}\\
&-49000245206682047654663910000000000000000E^{3})x_{\mathrm{r1}}^{7}\\
&+(-20306551289062500000000000000000000000000000E^{10}\\
&+18271644039740878417968750000000000000000000E^{8}\\
&-13015879231389043370398652856445312500000000000E^{6}\\
&+19066079898070358443919596406250000000000000E^{4}\\
&-78142857631053713756139269652750000000E^{2})x_{\mathrm{r1}}^{6}\\
&+(14875679854586865234375000000000000000000000E^{9}\\
&-60768308419453360195312500000000000000000000E^{7}\\
&-53205077565087916964777736328125000000000000E^{5}\\
&+79501778417558295760212956250000000000000E^{3})x_{\mathrm{r1}}^{5}\\
&+(67644550722656250000000000000000000000000000E^{10}\\
&-16972750918008278164160156250000000000000000E^{8}\\
&+74229921193857086365711171875000000000000000000E^{6}\\
&-13591757946114184741582729426171875000000000E^{4}\\
&+17433517993277425325750517849000000000000E^{2})x_{\mathrm{r1}}^{4}\\
&+(-65930361328125000000000000000000000000000000E^{11}\\
&-34608221968470117187500000000000000000000000E^{9}\\
&+20232422554352415807521030273437500000000000000E^{7}\\
&+25473158364685344085158247265625000000000000E^{5}
\end{aligned}
$$

$$
\begin{aligned}
&-660735784274514723269413214630625000000E^3 \\
&-10151528565306369169588391054400000E)x_{r1}^3 \\
&+(-904189470177656250000000000000000000000000E^{10} \\
&+87108390600336867234375000000000000000000000E^8 \\
&-20982707338441359977375314587890625000000000000E^6 \\
&+6324184903341590831033371140468750000000000E^4 \\
&-1281683263765410014125410876264187500000E^2)x_{r1}^2 \\
&+(-22604695312500000000000000000000000000000000E^{11} \\
&+21772133696982217500000000000000000000000000E^9 \\
&-52409235104946039342842578125000000000000000E^7 \\
&-98453633247761367967107921225000000000000E^5 \\
&+23022899835359304510156455669250000000E^3 \\
&-5829306243452976745046734139105100000E)x_{r1} \\
&+(-20093062500000000000000000000000000000000E^{12} \\
&+29033829464062500000000000000000000000000E^{10} \\
&-13985494550614663691301562500000000000000000E^8 \\
&+22461695986020306707058969656250000000000000E^6 \\
&-18908467536973157216034255512113500000000E^4 \\
&+28145381462620361354348644168711050000E^2 \\
&-7026681228671263612475845695437383 21) = 0,
\end{aligned}
\tag{D.1}
$$

where $\omega = 1, \mu = 0.01$.

On the other hand, the equation of the bifurcation diagrams (E - A_1) is obtained by

$$
\begin{aligned}
&844101562500A_1^6 - 23152500000000A_1^5 + 269010238875000A_1^4 \\
&+(2136093750000E^2 - 1618216692750000)A_1^3 \\
&+(-32602500000000E^2 + 5056637137100900)A_1^2 \\
&+(123750507000000E^2 - 6936243489452800)A_1 \\
&+1440000000000E^4 - 138723312000000E^2 + 3341259637044449 = 0,
\end{aligned}
\tag{D.2}
$$

where $\omega = 1, \mu = 0.01$.

Appendix E

Error Bound of HB Method for Periodic Input

In this appendix, we extend the method in [15] to the periodically forced system.

E.1 Definition for Error Bound

Let a projection operator K_{H} be

$$\begin{aligned} u_{\mathrm{H}}(t) &= K_{\mathrm{H}}u(t) = \sum_{k=p+1}^{\infty} \Re\left[(x_{\mathrm{r}k} + \mathrm{j}x_{\mathrm{s}k})e^{\mathrm{j}k\omega t}\right], \\ u(t) &= u_{\mathrm{L}}(t) + u_{\mathrm{H}}(t), \\ I &= K_{\mathrm{L}} + K_{\mathrm{H}}, \end{aligned} \tag{E.1}$$

where I is an identity operator. We define norms as follows;

$$l^{1}\text{norm}: \quad \|u(t)\|_1 \equiv \sum_{k=0}^{\infty} |X_k| = \sum_{k=0}^{\infty} \sqrt{x_{\mathrm{r}k}^2 + x_{\mathrm{s}k}^2}, \tag{E.2}$$

$$l^{2}\text{norm}: \quad \|u(t)\|_2 \equiv \sqrt{\sum_{k=0}^{\infty} |X_k|^2} = \sqrt{\sum_{k=0}^{\infty} \left(x_{\mathrm{r}k}^2 + x_{\mathrm{s}k}^2\right)}, \tag{E.3}$$

$$L^{\infty}\text{norm}: \quad \|u(t)\|_{\infty} \equiv \sup_{t\in[0,2\pi/\omega)} |u(t)|. \tag{E.4}$$

The norms satisfy the following relations;

$$\|u(t)\|_2{}^2 = \frac{\omega}{\pi}\int_0^{2\pi/\omega} |u(t)|^2 \,\mathrm{d}t, \tag{E.5}$$

$$\|u(t)\|_2 \leq \|u(t)\|_1, \tag{E.6}$$

$$\|u(t)\|_\infty \leq \|u(t)\|_1. \tag{E.7}$$

E.2 Estimation of High Frequency Components

In order to obtain the error bound, we consider the estimation of the high frequency components. Suppose that a periodic solution of Eq.(5.1) exists and $\|u\|_1 < \infty$. To see this, let ξ be any positive number satisfying

$$\xi \geq \left\| \frac{\mathrm{d}N[u]}{\mathrm{d}u} \right\|_\infty. \tag{E.8}$$

Using the mean-value theorem, we find

$$\frac{\omega}{\pi} \int_0^{2\pi/\omega} N[u(t)]^2 \mathrm{d}t \leq \frac{\omega}{\pi} \xi^2 \int_0^{2\pi/\omega} |u(t)|^2 \mathrm{d}t = \xi^2 \|u\|_2{}^2. \tag{E.9}$$

Because solutions with convergent Fourier series satisfy $\|u\|_2 < \infty$, $\|N[u]\|_2 < \infty$ is satisfied. Now we set

$$s(t) = \sum_{k=0}^{\infty} E_k e^{\mathrm{j}k\omega t}, \quad E_k \in \mathbb{C}, \tag{E.10}$$

$$N[u(t)] = \sum_{k=0}^{\infty} Y_k e^{\mathrm{j}k\omega t}, \quad Y_k \in \mathbb{C}. \tag{E.11}$$

From Eq.(5.1), we obtain

$$u(t) = \sum_{k=0}^{\infty} \Re\left[X_k e^{\mathrm{j}k\omega t}\right] = \sum_{k=0}^{\infty} \Re\left[G_1(\mathrm{j}k\omega;\boldsymbol{\lambda})\left\{E_k - G_2(\mathrm{j}k\omega;\boldsymbol{\lambda})Y_k\right\} e^{\mathrm{j}k\omega t}\right]. \tag{E.12}$$

Observe that

$$\sum_{k=0}^{\infty} |X_k| = \sum_{k=0}^{\infty} \left|G_1(\mathrm{j}k\omega;\boldsymbol{\lambda})\left\{E_k - G_2(\mathrm{j}k\omega;\boldsymbol{\lambda})Y_k\right\}\right|, \tag{E.13}$$

and, applying the Cauchy-Schwartz inequality, we obtain

$$\begin{aligned} \sum_{k=0}^{\infty} |X_k| &\leq \sum_{k=0}^{\infty} \left|G_1(\mathrm{j}k\omega;\boldsymbol{\lambda})E_k\right| + \sum_{k=0}^{\infty} \left|G(\mathrm{j}k\omega;\boldsymbol{\lambda})Y_k\right|, \\ &\leq \sqrt{\sum_{k=0}^{\infty} \left|G_1(\mathrm{j}k\omega;\boldsymbol{\lambda})\right|^2} \sqrt{\sum_{k=0}^{\infty} |E_k|^2} + \sqrt{\sum_{k=0}^{\infty} \left|G(\mathrm{j}k\omega;\boldsymbol{\lambda})\right|^2} \sqrt{\sum_{k=0}^{\infty} |Y_k|^2}, \end{aligned} \tag{E.14}$$

where $G(D;\boldsymbol{\lambda}) = G_1(D;\boldsymbol{\lambda})G_2(D;\boldsymbol{\lambda})$. It follows from Eq.(5.3) that

$$\sqrt{\sum_{k=0}^{\infty}\left|G_1(\mathrm{j}k\omega;\boldsymbol{\lambda})\right|^2} < \infty, \quad \sqrt{\sum_{k=0}^{\infty}|E_k|^2} < \infty, \quad \sqrt{\sum_{k=0}^{\infty}\left|G(\mathrm{j}k\omega;\boldsymbol{\lambda})\right|^2} < \infty. \tag{E.15}$$

Hence $\|u\|_1 < \infty$. We write $\|u\|_1 \le \upsilon$ with a certain υ.

Applying the operator K_{H} to Eq.(5.1), we can obtain the following relation;

$$u_{\mathrm{H}}(t) \;=\; -K_{\mathrm{H}}G(D;\boldsymbol{\lambda})N[u_{\mathrm{L}}(t) + u_{\mathrm{H}}(t)]. \tag{E.16}$$

In order to prove the existence of a unique u_{H}, we consider two points u'_{H} and u''_{H} with $\left\|u'_{\mathrm{H}} - u''_{\mathrm{H}}\right\|_2$. Using Eq.(E.16) and the mean-value theorem, we obtain

$$\begin{aligned}
&\left\|K_{\mathrm{H}}G(D;\boldsymbol{\lambda})N[u_{\mathrm{L}} + u'_{\mathrm{H}}] - K_{\mathrm{H}}G(D;\boldsymbol{\lambda})N[u_{\mathrm{L}} + u''_{\mathrm{H}}]\right\|_2 \\
&\quad\le \sup_{k>p}\left|G(\mathrm{j}k\omega;\boldsymbol{\lambda})\right| \sqrt{\frac{\omega}{\pi}\int_0^{2\pi/\omega}\left|K_{\mathrm{H}}\left\{N[u_{\mathrm{L}} + u'_{\mathrm{H}}] - N[u_{\mathrm{L}} + u''_{\mathrm{H}}]\right\}\right|^2 \mathrm{d}t} \\
&\quad\le \sup_{k>p}\left|G(\mathrm{j}k\omega;\boldsymbol{\lambda})\right| \xi \sqrt{\frac{\omega}{\pi}\int_0^{2\pi/\omega}\left|u'_{\mathrm{H}} - u''_{\mathrm{H}}\right|^2 \mathrm{d}t} \\
&\quad= \|F\|_\infty\left\|u'_{\mathrm{H}} - u''_{\mathrm{H}}\right\|_2,
\end{aligned} \tag{E.17}$$

where

$$\|F\|_\infty \equiv \xi \sup_{k>p}\left|G(\mathrm{j}k\omega;\boldsymbol{\lambda})\right|. \tag{E.18}$$

Thus, by the contraction mapping theorem, there exists a unique u_{H} when $\|F\|_\infty < 1$.

Now, if let u_{H0} be an arbitrary value, then

$$\begin{aligned}
\|u_{\mathrm{H}} - u_{\mathrm{H0}}\|_2 &= \|-K_{\mathrm{H}}G(D;\boldsymbol{\lambda})N[u_{\mathrm{L}} + u_{\mathrm{H}}] - u_{\mathrm{H0}}\|_2 \\
&\le \|-K_{\mathrm{H}}G(D;\boldsymbol{\lambda})N[u_{\mathrm{L}} + u_{\mathrm{H}}] + K_{\mathrm{H}}G(D;\boldsymbol{\lambda})N[u_{\mathrm{L}} + u_{\mathrm{H0}}]\|_2 \\
&\qquad + \|-K_{\mathrm{H}}G(D;\boldsymbol{\lambda})N[u_{\mathrm{L}} + u_{\mathrm{H0}}] - u_{\mathrm{H0}}\|_2 \\
&\le \|F\|_\infty\|u_{\mathrm{H}} - u_{\mathrm{H0}}\|_2 + \|-K_{\mathrm{H}}G(D;\boldsymbol{\lambda})N[u_{\mathrm{L}} + u_{\mathrm{H0}}] - u_{\mathrm{H0}}\|_2 .
\end{aligned} \tag{E.19}$$

Thus, we obtain the following relation;

$$\|u_{\mathrm{H}} - u_{\mathrm{H0}}\|_2 \;\le\; \frac{1}{1 - \|F\|_\infty}\|-K_{\mathrm{H}}G(D;\boldsymbol{\lambda})N[u_{\mathrm{L}} + u_{\mathrm{H0}}] - u_{\mathrm{H0}}\|_2 . \tag{E.20}$$

Substituting $u_{\mathrm{H}0} = 0$ into Eq.(E.20), we estimate the high frequency components u_{H} by the low frequency components u_{L} for l^2 norm as follows;

$$\begin{aligned} \|u_{\mathrm{H}}\|_2 &\leq \frac{1}{1-\|F\|_\infty} \|K_{\mathrm{H}} G(D;\boldsymbol{\lambda}) N[u_{\mathrm{L}}]\|_2 \\ &\leq \frac{\|F\|_\infty}{1-\|F\|_\infty} \|u_{\mathrm{L}}\|_2 . \end{aligned} \tag{E.21}$$

From Eq.(E.16), we obtain

$$\begin{aligned} \|u_{\mathrm{H}}\|_1 &= \|K_{\mathrm{L}} G(D;\boldsymbol{\lambda}) N[u_{\mathrm{L}} + u_{\mathrm{H}}]\|_1 \\ &\leq \sup_{k>p} \left|G(\mathrm{j}k\omega;\boldsymbol{\lambda})\right| \|N[u_{\mathrm{L}} + u_{\mathrm{H}}]\|_1 \\ &\leq \sup_{k>p} \left|G(\mathrm{j}k\omega;\boldsymbol{\lambda})\right| \xi \|u_{\mathrm{L}} + u_{\mathrm{H}}\|_1 \\ &\leq \|F\|_\infty \|u_{\mathrm{L}}\|_1 + \|F\|_\infty \|u_{\mathrm{H}}\|_1 . \end{aligned} \tag{E.22}$$

Thus, we can obtain the following inequality;

$$\|u_{\mathrm{H}}\|_1 \leq \frac{\|F\|_\infty}{1-\|F\|_\infty} \|u_{\mathrm{L}}\|_1 . \tag{E.23}$$

This inequality estimates the high frequency components for l^1 norm.

E.3 Determination of ξ

When we set υ as follows;

$$\|u\|_1 \leq \|u_{\mathrm{L}}\|_1 + \|u_{\mathrm{H}}\|_1 \leq \left(1 + \frac{\|F\|_\infty}{1-\|F\|_\infty}\right) \|u_{\mathrm{L}}\|_1 \equiv \upsilon, \tag{E.24}$$

the inequality

$$\begin{aligned} \left\| \frac{\mathrm{d}N[u]}{\mathrm{d}u} \right\|_\infty \leq \left\| \frac{\mathrm{d}N[u]}{\mathrm{d}u} \right\|_1 &\leq \sum_{i=0}^{q} (2i+1) c_{2i+1} \upsilon^{2i} \\ &= \sum_{i=0}^{q} (2i+1) c_{2i+1} \left(1 + \frac{\|F\|_\infty}{1-\|F\|_\infty}\right)^{2i} \|u_{\mathrm{L}}\|_1{}^{2i} \end{aligned} \tag{E.25}$$

is satisfied because $c_{2i+1} \geq 0$ for $i = 0, \ldots, q$. Thus, if we determine the variable ξ as

$$\xi = \sum_{i=0}^{q} (2i+1) c_{2i+1} \left(1 + \frac{\|F\|_\infty}{1-\|F\|_\infty}\right)^{2i} \|u_{\mathrm{L}}\|_1{}^{2i}. \tag{E.26}$$

then ξ satisfies Eq.(E.8).

E.4 Error Bound by Homotopy Invariance

Applying the operator K_{L} to Eq.(5.1), we obtain

$$\mathrm{FT}(u_{\mathrm{L}}) \equiv G^{-1}(D;\boldsymbol{\lambda})u_{\mathrm{L}} - \{G_2^{-1}(D;\boldsymbol{\lambda})s(t) - K_{\mathrm{L}}N[u_{\mathrm{L}} + u_{\mathrm{H}}]\} = 0. \tag{E.27}$$

The equation (E.27) corresponds to the low frequency components of Eq.(5.1), and u_{L} in Eq.(E.27) is the exact solution of Eq.(5.1). Now, if we set $u_{\mathrm{H}} = 0$ in Eq.(E.27), we obtain

$$\mathrm{FH}(u_{\mathrm{L}}) \equiv G^{-1}(D;\boldsymbol{\lambda})u_{\mathrm{L}} - \{G_2^{-1}(D;\boldsymbol{\lambda})s(t) - K_{\mathrm{L}}N[u_{\mathrm{L}}]\} = 0 \tag{E.28}$$

which corresponds to the HB equation (5.7). That is, u_{L} in Eq.(E.28) is an approximated solution by the HB equation (5.7).

In order to obtain the error bound from Eqs.(E.27) and (E.28), we use the following lemma of homotopy invariance theorem [58–60].

Theorem 2 (Homotopy Invariance Theorem)**.** *Let Ω be an open bounded set in $\mathbb{R}^n$ and $\boldsymbol{H} : \overline{\Omega} \times [0,1] \to \mathbb{R}^n$ be a continuous map where $\overline{\Omega}$ denotes the closure of the set Ω. Suppose that $\boldsymbol{y} \in \mathbb{R}^n$ satisfies $\boldsymbol{H}(z,t) \neq \boldsymbol{y}$ for all $(z,t) \in \partial\Omega \times [0,1]$ where $\partial\Omega$ is the boundary of the set Ω. Then $\deg(\boldsymbol{H}(\cdot,t),\Omega,\boldsymbol{y})$ is constant for $t \in [0,1]$ where we denote by $\deg(\boldsymbol{H}(\cdot,t),\Omega,\boldsymbol{y})$ the degree of $\boldsymbol{H}(\cdot,t)$ with respect to Ω at $\boldsymbol{y}$.*

Lemma 1. *Let Ω be an open bounded set in $\mathbb{R}^n$ and let $\boldsymbol{f}, \boldsymbol{g}{:}\overline{\Omega} \to \mathbb{R}^n$ be two continuous maps. Let $\boldsymbol{y} \in \mathbb{R}^n$ be a certain vector. Suppose further that α satisfies*

$$0 < \alpha = \min\{\|\boldsymbol{f}(z) - \boldsymbol{y}\| \mid z \in \partial\Omega\}. \tag{E.29}$$

If

$$\|\boldsymbol{f}(z) - \boldsymbol{g}(z)\| < \alpha \quad \forall z \in \partial\Omega, \tag{E.30}$$

then

$$\deg(\boldsymbol{f},\Omega,\boldsymbol{y}) = \deg(\boldsymbol{g},\Omega,\boldsymbol{y}). \tag{E.31}$$

Proof. Define $\boldsymbol{H} : \overline{\Omega} \times [0,1] \to \mathbb{R}^n$ by

$$\boldsymbol{H}(z,t) = (1-t)\boldsymbol{f}(z) + t\boldsymbol{g}(z) \quad \text{for } (z,t) \in \overline{\Omega} \times [0,1].$$

By hypothesis, it is easy to see that $\boldsymbol{H}(z,t) \neq \boldsymbol{y}$ for all $(z,t) \in \partial\Omega \times [0,1]$. By the homotopy invariance theorem, the result follows. □

If we set $\boldsymbol{f}(z) = \mathrm{FH}$, $\boldsymbol{g}(z) = \mathrm{FT}$, $z = \boldsymbol{x}$, $\boldsymbol{y} = 0$ in Eq.(E.30), then $\deg(\mathrm{FH}(u_\mathrm{L}), \Omega, 0) = \deg(\mathrm{FT}(u_\mathrm{L}), \Omega, 0)$ is satisfied. Namely, if there exists a region Ω containing a single solution of Eq.(E.28) on whose boundary

$$\|\mathrm{FT}(u_\mathrm{L}) - \mathrm{FH}(u_\mathrm{L})\| < \|\mathrm{FH}(u_\mathrm{L})\| \tag{E.32}$$

holds, then a solution of Eq.(E.27) exists belonging to Ω.

Using the mean-value theorem and the estimation of the high frequency components, we obtain the following relation from Eq.(E.32);

$$\begin{aligned} \|\mathrm{FT}(u_\mathrm{L}) - \mathrm{FH}(u_\mathrm{L})\|_2 &= \|K_\mathrm{L}N[u_\mathrm{L}(t)] - K_\mathrm{L}N[u_\mathrm{L}(t) + u_\mathrm{H}(t)]\|_2 \\ &\leq \xi\|u_\mathrm{H}(t)\|_2 \\ &\leq \frac{\xi\|F\|_\infty}{1 - \|F\|_\infty}\|u_\mathrm{L}(t)\|_2. \end{aligned} \tag{E.33}$$

Because an inequality

$$\frac{\xi\|F\|_\infty}{1 - \|F\|_\infty}\|u_\mathrm{L}\|_2 < \|\mathrm{FH}(u_\mathrm{L})\|_2 \tag{E.34}$$

satisfies Eq.(E.32), we can define the error bound for the HB method by

$$\frac{\xi\|F\|_\infty}{1 - \|F\|_\infty}\|u_\mathrm{L}\|_2 = \|\mathrm{FH}(u_\mathrm{L})\|_2. \tag{E.35}$$